GKSS
FORSCHUNGSZENTRUM
in der HELMHOLTZ-GEMEINSCHAFT

The spatial and temporal patterns of erodibility of an intertidal flat in the East Frisian Wadden Sea, Germany

(Von der Mathematisch-Naturwissenschaftlichen Fakultät der Christian-Albrechts-Universität zu Kiel als Dissertation angenommene Arbeit)

Author:

Mahatma Lanuru

GKSS 2004/14

GKSS 2004/14

The spatial and temporal patterns of erodibility of an intertidal flat in the East Frisian Wadden Sea, Germany

(Von der Mathematisch-Naturwissenschaftlichen Fakultät der Christian-Albrechts-Universität zu Kiel als Dissertation angenommene Arbeit)

Author:
Mahatma Lanuru
(Institute for Coastal Research)

GKSS-Forschungszentrum Geesthacht GmbH • Geesthacht • 2004

Die Berichte der GKSS werden kostenlos abgegeben.
The delivery of the GKSS reports is free of charge.

Anforderungen/Requests:

GKSS-Forschungszentrum Geesthacht GmbH
Bibliothek/Library
Postfach 11 60
D-21494 Geesthacht
Germany
Fax.: (49) 04152/871717

Als Manuskript vervielfältigt.

ISSN 0344-9629

GKSS-Forschungszentrum Geesthacht GmbH · Telefon (04152)87-0
Max-Planck-Straße · D-21502 Geesthacht / Postfach 11 60 · D-21494 Geesthacht

GKSS 2004/14

The spatial and temporal patterns of erodibility of an intertidal flat in the East Frisian Wadden Sea, Germany

(Von der Mathematisch-Naturwissenschaftlichen Fakultät der Christian-Albrechts-Universität zu Kiel als Dissertation angenommene Arbeit)

Mahatma Lanuru

138 pages with 52 figures and 10 tables

Summary

Erosion and physical and biological sediment parameters measurements were carried out at an intertidal flat in the East Frisian Wadden Sea, Germany, to examine the small-scale (meter) and large-scale (hundred of meters) spatial and temporal variation of sediment erodibility, and to identify the main processes that cause these variations. The erodibility was determined by means of lab and portable (in situ) EROMES erosion devices and quantified in terms of critical erosion shear stresses and erosion rates. The study showed that the small and large-scale variations of sediment erodibility were mainly governed by biological factors, especially microphytobenthos (dominated by benthic diatoms) and the presence of vagile worms. A strong spatial and temporal pattern of erodibility was observed. The sediments were more stable (i.e. higher critical erosion shear stresses and lower erosion rates) close to the salt marsh and and in middle tidal flat between mussel beds. By contrast, sediments were less stable at the site dominated by mud snail Hydrobia ulvae (station B) and this was probably due to surface tracking, pelletization of the bed material and grazing activities on benthic diatoms of the mud snails. The sediments were more stable in September 2002 compared to other sampling periods, and this attributed to be the results of bio-stabilization by benthic diatoms. By contrast, during June and October 2001 the sediments were easily eroded due to lower levels of bio-stabilising benthic diatoms.

Die räumlichen und zeitlichen Muster der Erodierbarkeit auf einem Wattrücken des Ostfriesischen Wattenmeers, Deutschland

Zusammenfassung

Die zeitliche und räumliche Variabilität der Erodierbarkeit von Sedimentoberflächen wurde auf einem Rückseitenwatt des ostfriesischen Wattenmeeres auf Skalen von Metern bis zu mehreren Hunderten von Metern untersucht. Zugleich wurden diejenigen Prozesse, die für die beobachteten Variabilitäten verantwortlich sind, identifiziert. Ziel war die Schaffung von Grundlagen zur großskaligen und flächendeckenden Abschätzung von Erosions-

parametern. Dazu wurden Erosionsmessungen durchgeführt sowie physikalische und biologische Sedimentparameter erfaßt. Die Erodierbarkeit wurde mit Hilfe von EROMES-Erosionsmessgeräten ermittelt, von denen sowohl die Laborversion als auch die in-situ-Variante eingesetzt wurde. Als Erosionsparameter wurden die kritische Schubspannung und die Erosionsrate bestimmt. Die Studie ergab, dass klein- und großskalige Variationen der Erodierbarkeit primär durch biologische Faktoren kontrolliert werden, insbesondere durch die Dichte benthischer Mikroalgen (Diatomeen) und die Dichte röhrenbauender Würmer. Die Erodierbarkeit wies signifikante räumliche und zeitliche Strukturen auf. Hohe Werte der kritischen Schubspannung und geringe Erosionsraten wurden auf der am Rand von Salzwiesen gelegenen Station weiter draußen zwischen Miesmuschelbänken beobachtet. Hier war das Sediment besonders stabil. Im Gegensatz dazu war das Sediment am wenigsten stabil in den Bereichen, die von der Wattschnecke Hydrobia ulvae dominiert wurden. Ursachen dafür sind vermutlich die Kriechspuren der Schnecke, deren Ausscheidungen und der Wegfraß der stabilisierenden benthischen Diatomeen. Als Folge der Bedeckung durch benthische Diatomeen war die Sedimentstabilität im September 2002 besonders hoch, während sie im Juni und Oktober 2001 auf Grund geringer Konzentrationen an Diatomeen wesentlich kleiner war.

Manuscript received / Manuskripteingang in TDB: 28. Oktober 2004

Acknowledgements

Many thanks to all those who have helped me throughout my Ph.D with advice, comments, and suggestions, especially to my supervisors, Prof. Dr. Franciscus Colijn, Prof. Dr. Roberto Mayerle, and Dr. Rolf Riethmüller. Special thanks go to Dr. Thorbjoen Joest Andersen for advice and suggestions and for working together on a part of the thesis. Thanks also to Carlo van Bernem for macrofauna and microphytobenthos analysis and for working together on a part of the thesis. Thanks also to Dr. Reiner Onken for English improvement and for the correction of the German version of the abstract of the thesis.

Special thanks also to Kerstin Heymann, Karin Wirth, Wolf Stille, Bernd Peters and Michael Janik for their full support of my field and laboratory works. I could not have done it without you! I will never forget the many beautiful, but sometimes also difficult days in the tidal flats. Thank you also to Maike Dibbern for helping with the field sampling and for the sediment carbohydrate analysis. I would like also to thank Dr. Ulrich Callies, for his expert help with the statistical analysis. Thanks also to Dr. Walter Puls, Dr. Dieter P. Eppel, Dr. Götz Flöser, and Dr. Clivia Häse for scientific advice and discussion.

I greatly appreciate the kind assistance, good cooperation, and social support that I received from Peter Perthun, Martina Heineke, Steffen Schmidt, Horst Garbe, Albert Werner, Bernd Vaessen and Heiko Rinck, during my work at the Institute for Coastal Research, GKSS Research Centre. I would like also to express my sincere gratitude to the Deutscher Akademischer Austauschdienst (DAAD) for its financial support and to Kiel University and GKSS Research Centre for providing me facilities and financial support.

Finally and especially, to my wife Ruhmi, my daughter Rina, my parents, my brothers and sisters and all of my family in Indonesia, a very special thank for all your love, patience, help and encouragement.

Abstract

Erosion and physical and biological sediment parameters measurements were carried out at an intertidal flat in the East Frisian Wadden Sea, Germany to examine the small-scale (a meter) and large-scale (hundred of meters) spatial and temporal variation of sediment erodibility, and to identify the main processes that cause these variations. Six stations along a cross-shore transect of 1.5 km length from immediately below the salt marsh to the middle of the tidal flat were visited during several field campaigns in 2001 and 2002. These stations differ in their sediment types, tidal emersion periods and benthic macrofauna assemblages. The erodibility was determined by means of Lab and portable (in situ) EROMES erosion devices and quantified in terms of critical erosion shear stress and erosion rate.

The study showed that the small and large-scale variations of sediment erodibility were mainly governed by biological factors, especially microphytobenthos (dominated by benthic diatoms). A strong spatial and temporal pattern of erodibility was observed. The sediments were more stable (i.e. higher critical erosion shearstresses and lower erosion rates) at station A (close to the salt marsh) and station F (middle tidal flat). The high stability at station A was attributed to be the results of physical process of drying and biostabilization by tube building worms. The high stability at station F was attributed mainly to be the results of biostabilization by benthic diatoms. By contrast, sediments were less stable at the site dominated by mud snail Hydrobia ulvae (station B) and this was probably due to surface tracking, pelletization of the bed material and grazing activities on benthic diatoms of the mud snails. The sediments were more stable in September 2002 compared to other sampling periods, and this attributed to be the results of biostabilization by benthic diatoms. By contrast, during June and October 2001 the sediments were easilyeroded due to lower level of bio-stabilization.

The results from study of erosion potential over bedforms showed that crests of the bedforms are generally more stable than troughs. In general, crests contained more chlorophyll-a, colloidal carbohydrate and EPS than troughs. The normalized water content and wet bulk density of the crests were not significantly different from those of the troughs except at the most landward station where crests had significantly lower normalized water content and higher wet bulk density than troughs. Two different processes were identified for the difference in erodibility between crests and troughs in this study: (1) At seawards stations (B–F), the higher benthic diatom biomass on the crests increases the amount of EPS, which is likely to stabilize the sediment surface of these features. (2) At most landward station (A), where benthic diatom biomass was low, physical processes (drying, compaction) are more important for sediment stability on the crests.

The measured critical erosion shear stresses fall above the abiotic non-cohesive sediment values, giving a biostabilization index of 4.2 to 11.6. Differences in critical erosion shear stress between natural and abiotic non-cohesive sediments are likely caused by the effect of biostabilization and by cohesive behaviour of naturalsediments.

Kurzfassung

Auf einer Wattfläche im ostfriesischen Wattenmeer wurde die zeitliche und räumliche Variabilität der Erodierbarkeit des Sediments kleinskalig im Bereich von Metern bis zu mehreren Hunderten von Metern (großskalig) untersucht. Dazu und um diejenigen Prozesse zu identifizieren, die für die Variabilität verantwortlich sind, wurden Erosionsmessungen durchgeführt sowie physikalische und biologische Sedimentparameter erfasst. Entlang einem ca. 1,5 km langen Schnitt, der sich von den Salzwiesen bis etwa zur Mitte der Wattfläche erstreckt, wurden im Rahmen mehrerer Messkampagnen in den Jahren 2001 und 2002 sechs Messstationen wiederholt beprobt. Diese Stationen weisen Unterschiede auf hinsichtlich des Sedimenttyps, der Gezeiten bedingten Trockenfall-Periode und des Bewuchses mit benthischer Makrofauna. Die Erodierbarkeit wurde mit Hilfe von EROMES-Erosionsmessgeräten ermittelt, von denen sowohl die Laborversion als auch die in-situ-Variante eingesetzt wurde. Als Parameter wurden die kritische Schubspannung und die Erosionsrate bestimmt.

Diese Studie zeigt, dass klein- und großskalige Variationen der Erodierbarkeit primär durch biologische Faktoren kontrolliert wurden, insbesondere durch das benthische Mikroalgen und hier vor allem durch benthische Diatomeen. Die Erodierbarkeit wies signifikante räumliche und zeitliche Strukturen auf. Hohe Werte der kritischen Schubspannung und geringe Erosionsraten wurden auf der in der Nähe der Salzwiesen gelegenen Station A und auf Station F in der Mitte der untersuchten Wattfläche beobachtet, d.h. hier war das Sediment war besonders stabil. Verantwortlich für die geringe Erodierbarkeit auf Station A war die Austrocknung des Sediments und die Biostabilisierung durch Röhren bildende Würmer. Auf Station F hingegen wurde Biostabilisierung durch benthische Diatomeen als ausschlaggebender Prozess identifiziert. Im Gegensatz dazu war das Sediment weniger stabil auf Stationen, die von der Wattschnecke Hydrobia ulvae dominiert wurden. Ursächlich dafür waren vermutlich die Kriechspuren der Schnecke, deren Ausscheidungen und der Wegfraß benthischer Diatomeen. Als Folge der Biostabilisierung durch benthische Diatomeen war die Sedimentstabilität im September 2002 besonders hoch, während im Juni und Oktober 2001 die Erodierbarkeit unter dem Einfluss geringerer Biostabilisierung wesentlich größere Werte aufwies.

Untersuchungen des Erosions-Potenzials in Abhängigkeit von der Morphologie haben gezeigt, dass höher gelegene Wattflächen (Kämme) stabiler als Rinnen waren. In vielen Fällen war auf den Kämmen der Gehalt an Chlorophyll-a, kolloidalen Kohlenhydraten und EPS höher als in den Rinnen. Im Gegensatz dazu waren die Unterschiede zwischen Kämmen und Rinnen hinsichtlich des normalisierten Wassergehalts und der Nassdichte nicht signifikant, mit Ausnahme der am weitesten landwärtig gelegenen Station, wo auf den Kämmen wesentlich geringere Werte des normalisierten Wassergehalts und höhere Nassdichten beeobachtet wurden. Als Ursache für die unterschiedliche Erodierbarkeit von Kämmen und Rinnen wurden zwei Prozesse identifiziert: Auf den seewärtigen Stationen B– F führt die größere Biomasse benthischer Diatomeen auf den Kämmen zu einer Erhöhung des EPS-Gehalts, wodurch die Oberfläche des Sediments stabilisiert wird. Auf der landnächsten Station A hingegen, mit der geringeren Biomasse benthischer Diatomeen, sind physikalische Prozesse wie Austrocknung und Kompaktierung auschlaggebend.

Die gemessenen Werte der kritischen Schubspannung liegen über den Werten des nichtkohäsiven Sediments und ergeben einen Biostabilisierungs-Index zwischen 4,2 und 11,6. Biostabilisierung und das kohäsive Verhalten natürlicher Sedimente sind wahrscheinliche Ursachen für Unterschiede der Schubspannungen bei natürlichen und nicht-kohäsiven Sedimenten.

CONTENTS

CHAPTER 1

INTRODUCTION AND LITERATURE REVIEW

1.1. Problem definition

In estuarine and coastal wetlands, sediment beds are formed under different hydrodynamic conditions, which results in mixtures or alternation of sand and mud, commonly expressed as cohesive sediments. The transports of the sediments are significantly influenced by interacting physical, chemical, and biological processes and cannot be parameterized by basic principles yet. Hence, quantitative predictions of coastal sediment transports have limited accuracy despite the ecological and economical importance of this issue in relation to various aspects of coastal zone management, such as shoreline protection, habitat stability, pollutant transport, aquaculture and coastal engineering. This is in contrast to the transport behaviour of non-cohesive coarse sediment (sand) that has been studied intensively in the past and much theoretical and empirical information has already become available concerning erosion and deposition of non-cohesive coarser sediments.

There are four key processes that govern fine-grained cohesive sediment transport in estuarine and coastal waters. These processes are erosion, transport, deposition, and consolidation. *Erosion* is the removal of sediment from the surface of the bed due to the stress of the moving water above the bed. *Transport* is the movement of the suspended mud and high concentration layers on or near the bed by the flow. *Deposition* involves the settling through the water column and on the bed of flocculated sediment. *Consolidation* of a deposit is the gradual expulsion of interstitial water by the self-weight of the sediment accompanied by an increase in both the density of the bed and its strength with time (Whitehouse et al. 2000a). A number of laboratory and field studies have been carried out to obtain a better understanding of each process. In the present study, only one of the key processes is addressed. The study focuses on the erosion process of intertidal flat sediment.

Erosive forces of bed material are generated by the action of tidal and wind driven currents and waves acting at different spatial and temporal scales.

Biological processes are also important in determining the erosion response of an intertidal flat. Flora and fauna inhabiting intertidal flats mediate sediment transport by either stabilizing or destabilizing the sediment surface (e.g. Paterson 1997). Erosion of sediment occurs whenever the shear stress exerted on the bed by waves or currents exceeds a threshold value, known as the critical erosion shear stress. The critical erosion shear stress or erosion threshold is one measure to quantify sediment surface erodibility, parameterizing the stability of the most upper sediment surface layer. As a second parameter the erosion rate is commonly used (Amos et al., 1992), which is defined as the amount of material eroded per time and area for a given bed shear stress. It describes the stability of surface sediments below the upper layer.

Erodibility is the term used here to describe the susceptibility of a surface sediment to erosion through interfacial fluid shear. Thus, a high erodibility corresponds to a less stable sediment with a lower critical erosion shear stress and greater erosion rate. It has been shown that a number of physical factors such as sediment grain-size, bulk density, water content, air exposure, rainfall and consolidation affect the erodibility of intertidal flat sediments (Anderson and Howell 1984, Amos et al. 1988, Paterson et al. 1990, Paterson et al. 2000, Williamson and Ockenden 1996).

Various studies have also shown that the erodibility can be substantially modified by biological factors such as biostabilization by microphytobenthos (Paterson 1989, Sutherland et al. 1998, Austen et al. 1999, Riethmüller et al. 2000) and biostabilization or destabilization by various benthic macrofauna species (Jumars and Nowel 1984, Blanchard et al. 1997, Widdows et al. 1998c, Andersen et al. 2002, Widdows and Brinsley 2002). Benthic diatoms have been considered as one of the major organisms groups contributing to stabilization. The stabilization occurs mainly through secretion of extracellular polymeric substance (EPS) by diatoms during locomotion (Holland et al. 1974, Grant et al. 1986). These EPS binds sediment particles together at the mud surface and smoothens the surface, hence reducing the susceptibility for erosion (Paterson 1989). Benthic macrofauna too may increase sediment stability by binding particles with secretions used to construct their tubes (Yingst and Rhoads 1978). In most cases, however, they destabilize sediment

through pellet productions, grazing, and burrowing activities (Gerdol and Hughes 1994, Widdows et al. 1998c, Andersen 2001a).

Previous sediment erosion studies concerned merely with the spatial variation in the erodibility in relation to sediment type, emersion period, and bed feature (Amos et al. 1988, Austen et al. 1999, Houwing 1999, Paterson et al. 1990, Paterson et al. 2000, Riethmüller et al. 2000). Few attempts have been made to examine the variation of erodibility of surface sediment in relation to lateral changes of benthic habitat on an intertidal flat. Moreover, few studies on sediment erodibility comprise both spatial and temporal dimensions (i.e. de Brouwer et al. 2000, Widdows et al. 2000a, Lelieveld et al. 2003).

1.2. Objectives and outline of the thesis

The main objective of this study is, to examine the small-scale (a meter) and large-scale (hundred of meters) spatial and temporal variation of sediment erodibility, and to identify and parameterize the main processes that cause these variations. A broad range of habitats with differences in emersion periods, sediment types, and benthic macrofauna assemblages is covered to disentangle the different contributions. The central hypothesis of this study is that intertidal flat erodibility is controlled over spatial and temporal scales by the influences of benthic organisms and sediment properties. Specific objectives of this study are:

- To quantify the spatial and temporal changes in sediment erodibility of intertidal flats and to relate these to spatial and temporal variations of benthic organisms, particularly the abundances of microphytobenthos.
- To compare critical erosion shear stress of natural sediments to the critical stress of abiotic sediment derived from threshold Shields parameter.
- To determine the small-scale spatial variation of the erodibility in different intertidal flat habitats.
- To examine and compare the erodibility of crests and troughs of the bedforms and to identify the processes governing differences in erodibility between crests and troughs.

- And to identify the potential proxy parameters that can be used to predict critical erosion shear stresses for the purpose of mapping of surface erosion parameters from small to large scales.

The thesis is set up in the following order:

This chapter, **chapter 1**, deals with the objectives of the thesis and a literature review on erosion characteristics of cohesive sediment, biological influence on sediment erosion, and instruments for determination of erodibility. **Chapter 2** deals with the description of the study site, field works and used methodologies. General feature of the data are presented and discussed in **Chapter 3**. **Chapter 4** deals with the erosion characteristics of the different habitat types studied. Specific attention is given to intertidal flats dominated by cockle *Cerastoderma edule* and polychaete worm *Heteromastus filiformis*, because these two species are abundant benthic animals at many tidal flats and no studies have specifically aimed at a determination of these species effect on sediment erodibility. The erosion characteristics for crests and troughs of bedforms in terms of critical erosion shear stress and erosion rate are also described in this chapter. **Chapter 5** describes the large-scale (hundreds of meters) spatial and temporal variation of erodibility in relation to abundance of microphytobenthos and benthic macrofauna, sediment type, and emersion period. **Chapter 6** describes various approaches or models that can be adopted to predict critical erosion shear stress from proxy parameters for purpose of large-scale mapping of sediment surface erosion parameters. The results of the erosion experiments and physical and biological sediment properties measurements in the previous chapters are used to generate the predictive models. In the concluding **chapter 7**, a synthesis and comprehensive assessment of all results is presented.

1.3. Erosion characteristics of cohesive sediment without biological influences

Natural cohesive sediments are a mixture of clay, fine silt, and sand. The clay particles are cohesive because electrochemical repulsive and attraction forces are acting between the particles. Sediment of this type is called cohesive because the sediment particles do not behave as individual discrete

particles but tend to stick together forming aggregates (mud flocs). The resulting inter-particle forces exceed considerably the pure gravitational forces, which alone counterbalance erosive forces in case of pure sand (Raudkivi 1998). Cohesion begins to be significant when sediment contains more than about 5–10 % of clay by weight (Dyer 1986).

Grain movement will occur when the fluid forces (lift and drag forces) on a grain are just larger than the resisting force related to the submerged grain weight and the friction coefficient (van Rijn 1993). The initiation of motion of non-cohesive sediment is resisted mainly by the submerge weight of the grains. For cohesive sediment, cohesive behavior contributes to erosion resistance (Dade et al. 1992). The strong binding forces that hold cohesive grains together once they have been deposited means the grains can not be eroded in the same way as can non-cohesive sediments. Cohesive grains are eroded as clumps or flocs, rather than individual grains, and if they have been partially consolidated (e.g. an exposed estuarine or tidal mud flat), erosion occurs following the mass failure of the sediment surface which is ripped off in large lumps. This process requires very high bed shear stress. Thus, once deposited, cohesive fine-grained sediment is not easily eroded despite their fine grain-size (Open university course team 1989).

Two main types of erosion have been noted since early in the description of cohesive sediment erosion: surface and mass erosion (Mehta et al. 1982). These have been recently described as Type I and Type II erosion and also as "benign" and " chronic" erosion (Amos 1995). Type I erosion takes place when we have an increase of critical erosion shear stress with sediment depth due to consolidation. Under Type I, erosion rates peak rapidly and then decrease with time. This mode of erosion is also often observed under natural field settings (see e.g. Amos et al. 1997). Under Type II, erosion may be rapid at first, as with Type I, but the bed continues to erode. Type II erosion tends to occur when the stress on the bed greatly exceeds the critical stress for erosion (Paterson and Black 1999).

If both the bed shear stress (τ_b) and the critical erosion shear stress (τ_{cr}) are known, the erosion rate can be calculated using an appropriate erosion formulation. The following equation is most often used for Type I erosion,

when τ_{cr} increases with depth into the sediments and limit the extent of erosion (Mehta 1988, Amos et al. 1992):

$$E = \varepsilon_f \exp(\alpha[\tau_b - \tau_{cr}(z)]^{\beta}) \quad (1)$$

where E is the erosion rate (kg m^{-2} s^{-1}), ε_f is the empirical floc erosion rate (kg m^{-2} s^{-1}), α and β are empirical constants, and z is the depth of erosion. Many researchers use a simple linear relationship between erosion rate and shear stress to calculate the erosion rate (e.g. Sanford and Halka 1993, Torfs et al. 2001). The linear erosion formulation is written as:

$$E = M(\tau_b - \tau_{cr}) \quad (2)$$

where M is the erosion rate constant (kg m^{-2} s^{-1}). Equation 2 is predominantly used to model Type II erosion, with a single constant value of τ_{cr} that does not change with depth in the sediments (Sanford and Maa 2001).

Laboratory and *in situ* erosion measurements have shown that a range of critical erosion shear stresses can be found for non-biostabilized natural cohesive sediments. Amos et al. (1997) found on the foreshore and upper foreslope of the Fraser River delta (Canada) critical erosion shear stress to vary between 0.11 and 0.50 N m^{-2} and seemed to be proportional to the sediment wet bulk density. On the Baltimore Harbor, Maryland (USA), Maa et al. (1998) found typical critical erosion shear stress of 0.05 and 0.1 N m^{-2} for sediment with high and minimal fluff layers, respectively. Additionally, Ziervogel and Bohling (2003) found a critical shear velocity of 0.62 cm s^{-1} (about 0.04 N m^{-2}) for muddy sediment covered by a well-developed fluffy surface layer in the south western Baltic Sea (Germany).

1.4. Biological influence on sediment erosion

Although during storms and floods physical forces (currents and waves) undoubtedly exceed most biological influence on sediment erosion, a wide range of biotic effects rise in importance during quiescent to moderate periods. These effects can broadly be classified as either contributing to sediment stability (bio-stabilization) or reducing stability (bio-destabilization) (Black et al. 2002).

Bio-stabilizer such as mussel beds, seagrass beds, macroalgal mats, microphytobenthos, and salt marsh macrophytes can modify their immediate

physical environment by reducing tidal currents, wave action, and sediment resuspension, thus reducing turbidity and increasing light penetration, as well as enhancing sediment cohesiveness and sedimentation processes (Widdows and Brinsley 2002). By contrast, the bio-destabilizers increase sediment erosion/resuspension and modify properties of surface sediments by increasing bed roughness, sediment water content, grazing on bio-stabilizers and producing fecal pellets (Widdows and Brinsley 2002).

In this section, the influences of microphytobenthos and benthic macro-fauna are emphasized, because microphytobenthos is the most important primary producer on intertidal mudflats and their significant role as sediment stabilizer has been well documented and quantified. Benthic macrofauna prevails everywhere and it is known to contribute both stabilization and destabilization. It is expected that microphytobenthos and benthic macrofauna are the most determinant parameters for sediment surface stability.

1.4.1. Microphytobenthos

The microphytobenthos comprises a number of photoautotrophic groups of microscopic algae but is dominated by diatoms, cyanobacteria, and euglenoids (Black et al. 2002). Benthic diatoms can be subdivided into epipsammic diatoms (immotile diatoms, living semi-permanently attached to sand grains) and epipelic diatoms (motile diatoms, moving freely through the sediment) (Vos et al. 1988). Epipsammic diatoms favour a sandy environment, whereas epipelic diatoms favour a fine-grained (silt/mud) environment, prevailing throughout the year at locations where wave and current energy are low (Augustinus 2002). These diatoms are mobile microorganisms that migrate up and down through the sediment in response to light and tidal conditions (Hay et al. 1993).

Benthic diatoms can stabilize sediment surface through their production of extracellular polymeric substance, EPS (Paterson 1989). The EPS creates bonds between the mixture of mineral and organic particles in the sediment and this results in a surface coating which may increase the erosion shear stress significantly (Figure 1.1). The production of EPS during diatom

locomotion may form a smooth and stable sediment surface when the density of the diatoms is high (Paterson 1997), and field evidence of this stabilization has been shown (e.g. Underwood and Paterson 1993b, Riethmüller et al. 1998, Austen et al. 1999, Andersen 2001a).

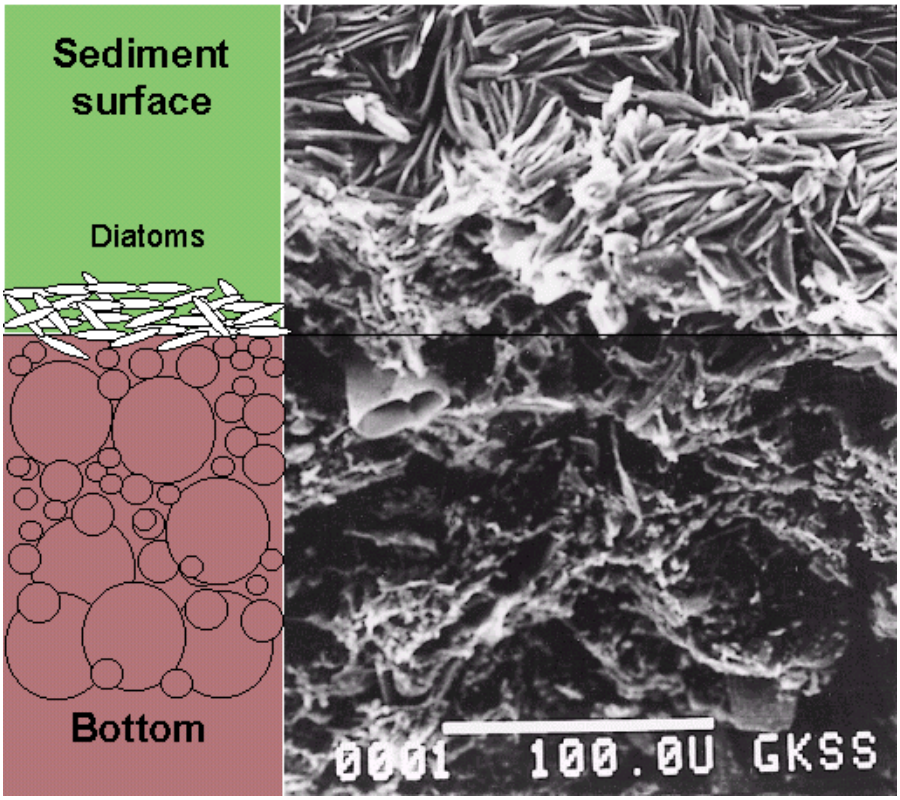

Figure 1.1. Scanning electron micrograph of the surface layer of an intertidal flat sediment showing benthic diatoms on the upper most sediment surface (Scale bar = 100 µm). Courtesy of GKSS Research Centre.

The critical erosion shear stress of soft fine-grained sediment in the intertidal zone is typically in the order of 0.2–0.5 N m^{-2} when diatom biofilms are absent (Andersen 2001b). However, when biofilms are present this critical shear stress may increase to more than 3 N m^{-2} (Riethmüller et al. 2000, Austen et al. 1999, Tolhurst et al. 1999).

The ratio between the critical erosion shear stress for sediments with and without biogenic stabilization has often been expressed as biostabilization index (Manzenrieder 1983). Tolhurst et al. (1999) reported an index of 6.2 for fine-grained sediments from Königshafen (German Wadden Sea), and the index may exceed 10 for the Kongsmark area (Danish Wadden Sea, Andersen 2001a). The seasonal variability of the biostabilization index was

reported by Grant et al. (1982) showing that the index approached unity in winter when biological activity was low and reached a maximum during the autumn growing season.

Benthic diatoms require light and are therefore restricted to the sediment-air and sediment-water interface of estuarine and intertidal sediments. Consequently, the biological influence of sediment erosion afforded by benthic diatoms is mainly a surface phenomenon and their influence is mostly upon critical erosion shear stress rather than erosion rates (Andersen 2001b). The critical erosion shear stresses of sediment with diatom biofilm are usually highest at the surface and do not increase with depth. Therefore, once erosion occurs, the sediment will continue to erode (i.e. mass erosion) because bed shear stresses are much higher than critical erosion shear stresses of sediment below the surface.

Chlorophyll-a concentration is an indicator of microphytobenthos biomass, while carbohydrate is a measure of EPS or mucopolysaccharides secreted by microphytobenthos (Sutherland et al. 1998). Several authors (Madsen et al. 1993, Underwood and Paterson 1993a, Tolhurst et al. 2002, Friend et al. 2003b) have demonstrated the increase of critical erosion shear stress with increasing EPS. Although EPS is expected to be the appropriate parameter to represent sediment stabilization, it cannot be used as a proxy parameter for large-scale mapping by optical remote sensing (Riethmüller et al. 2000).

Chlorophyll-a from microphytobenthos in the uppermost sediment surface can be detected and quantitatively estimated by means of optical remote sensing techniques (Hakvoort et al. 1998, Paterson et al. 1998). Hence, it may be an appropriate candidate for mapping critical erosion shear stress. Several authors have observed a significant positive relationship between critical erosion shear stress and Chlorophyll-a concentration on the intertidal (Riethmüller et al. 1998, Riethmüller et al. 2000, Austen et al. 1999, Paterson et al. 2000) and subtidal (Madsen et al. 1993, Sutherland et al. 1998, Lund-Hansen et al. 2002) flats. However, the detected relationships are often weak, suggesting that important interactions are being missed. For example, the variation in Chlorophyll-a contents could explain only 40 % of the variance in critical erosion shear stress in the Danish Wadden Sea (Andersen 2001a). Riethmüller et al. (2000) showed that the relationship between critical erosion

shear stress and Chlorophyll-a concentration can be highly significant at specific locations but the relationships vary from location to location and sometimes due to specific events, e.g. mass blooms of specific diatom species.

1.4.2. Benthic macrofauna

Depending on type of feeding, benthic macrofauna can be classified as "suspension feeders" and "deposit feeders". This classification is frequently used and works well for most species but some species may be both deposit feeders and suspension feeders depending on circumstances. Dauer et al. (1981) used the term "interface feeders" to refer to species that can switch between deposit and suspension feeding. An example is *Macoma balthica* which is often abundant on fine-grained tidal flats and may feed directly from the suspension at times but mostly is deposit feeding (Riisgård and Kamermans 2001). A further possible distinction is given by the fact that some organisms lead a sessile life, while others are motile (Heinzelmann and Wallisch 1991).

Suspension feeders including mussels and cockles extract their food from suspended particles in the water column. The filtered material will be deposited as faeces or pseudo faeces with settling velocities one order of magnitude higher then their constituent grains (Haven and Morales-Alamo 1966, Andersen and Pejrup 2002). Suspension-feeding organisms tend to enhance the flux of suspended material from the water column to the bed via suspension feeding and biodeposition (Widdows et al. 1998c).

Deposit feeders include a large number of worms, snails and mussels. They all take their food from the sediment surface (surface deposit feeders) or from below the surface (subsurface deposit feeders) (Riisgård and Kamermans 2001). The Polychaetes *Lanice conchilega* and *Heteromastus filiformis* are an example of surface and subsurface deposit feeders, respectively.

The influence of benthic macrofauna on erodibility of fine-grained sediments is ambiguous and both stabilization and destabilization can be expected. In some cases, both stabilization as well as destabilization of sediment by a single species was observed. For example, Gerdol and Hughes

(1994) found that the amphiphod *Corophium volutator* caused destabilization of the sediment due to grazing on microphytobenthos and reworking of the sediment by burrowing and tube formation. By contrast, Mouritsen et al. (1998) attributed the stabilization of sediment to the presence of *Corophium volutator*. They suggested that coating of the walls of burrowing holes by mucus was responsible for the observed stabilization.

Most benthic macrofauna species tend to increase the roughness of the bed either by actual presence of the animal itself, by tracking of the surface during the locomotion or by the excretion of fecal pellet or pseudo pellets (Nowell et al. 1981). This increase in roughness would increase the erodibility of sediments. The flume studies of Nowell et al. (1981) with the small bivalve *Transenella tantilla* showed that tracking activity of the bivalve doubled the boundary roughness and decreased the critical entrainment velocity by 20 % of the investigated marine sediments.

Many benthic macrofauna produce tubes (e.g. worm tubes) protruding few millimeters to centimeters above the bed and most obviously change the bottom roughness height (Graft and Rosenberg 1997). Animal tubes have been suggested in both the stabilization and destabilization of sediment (Eckman et al. 1981). Rhoads et al. (1978) postulated that the arbitrary effect of tubes will be related to the density of the tubes. Single or isolated tubes may cause local scour and hence destabilize sediments by deflecting fluid of relatively high momentum toward the bed (Eckman et al. 1981). By contrast, high density tube mats may produce a "skimming flow" that effectively protects the bed from erosion. In skimming flow, the region of maximum turbulent kinetic energy and shear stress production occurs away from the bed (Eckman et al. 1981). According to laboratory flume experiments of Nowell and Church (1979), skimming flow occurs when one-twelfth of the sediment surface is covered with tubes.

The erodibility of the bed may be also indirectly influenced by benthic macrofauna by modifying the bed characteristics, such as water content, organic content and particle size distribution. Bioturbation (digging and burrowing) activity of macrofauna loosens the bed material thus increasing the water content (Rhoads et al. 1978, Rowden et al. 1998, Cadée 2001, de Deckere et al. 2001). Both effects reduce the cohesion and hence decrease

the bed stability (Rhoads 1974, Rowden et al. 1998). According to Postma (1967), an increase in water content of fine-grained sediments from 50 % to 60 % can result in a decrease of the sediment stability of about 25 %. Bioturbation activity may also maintain porosity and prevents compaction (Meadows and Tait 1989). Underwood and Paterson (1993a) found that elimination of all biological activity with formaldehyde resulted in compaction of the sediment and an increase in the critical erosion shear stress.

Benthic macrofauna can also influence the sediment erodibility by production of fecal pellets (Widdows et al. 1998b, Andersen 2001b). Fecal pellets or pseudofaeces produced by cockles may indirectly increase surface sediment stability by stimulating the growth of microphytobenthos (Sündback 1984). In most cases, however, a decrease in sediment stability due to presence of pellets has been reported (Haven and Morales-Alamo 1966, Nowell et al. 1981, Taghon et al. 1984). Pelletization of the bed material by mobile deposit feeders results in high porosity at the surface and less compaction and cohesion, so enhancing erosion (Rhoads 1974). Andersen (2001b) has recently reported the effect of fecal pellet produced by mud snail *Hydrobia ulvae* on sediment erodibility at Kongsmark area, Danish Wadden Sea. He found that erosion rate increased with increasing fecal pellet content of the bed material. It was also found in this study that strong seasonal variation of the content of fecal pellets of the bed material causes a seasonal variation of the erosion rate with high erodibility in the summer period when the production of fecal pellet is high and low erodibility in the winter.

The erodibility of sediment can also be indirectly mediated by feeding activity of macrofauna. For example, *Corophium volutator* increase sediment erodibility indirectly by reducing benthic diatom biomass via grazing (Gerdol and Hughes 1994, de Deckere et al. 2000). Mud snails *Hydrobia ulvae* may indirectly enhance sediment erodibility by grazing on benthic diatoms (Austen et al. 1999, Andersen 2001b). By contrast, the presence of cockle beds may indirectly increase surface sediment stability by stimulating the growth of microphytobenthos through several mechanisms (Andersen et al. in review). These mechanisms include the effect of nutrient release, mainly ammonium, by the cockles (Swanberg 1991) and the increase of photosynthetically active

radiation (PAR) at the sediment by removing the seston and silt from the water column (Newel et al. 2002).

1.5. Instruments for determination of erodibility

1.5.1. Overview

Several techniques have been developed for making laboratory and in-situ measurement of the erodibility of cohesive sediment. They differ in size from about 10 cm to 3 m in diameter, and in test section areas from smaller than 0.01 m^2 to 1 m^2, and in weight from a few kilograms to more than 100 kg. Several of the larger instruments are the annular flume "Sea Carousel" described by Amos et al. (1992), the "VIMS Sea Carousel" (Maa et al. 1993), the In Situ Erosion Flume (ISEF; Houwing and Van Rijn 1998), and the straight flume "SEAFLUME" described by Young and Southard (1978).

Although the forcing of the water flow differs for each instrument, the applied technique is broadly the same, namely circulating or straight water flow are used to exert a shear force on the bed surface. The main disadvantage of straight flumes for use in the field is the size, which is necessary to produce a fully developed turbulent boundary layer at the point of observation in the test section. This makes deployment difficult and expensive. The infinite flow length of an annular flume results in a fully developed boundary layer, but sealing around the rotating annulus is difficult (Amos et al. 1992), causing aeration in subaerial deployments. The advantage of the annular and straight flume is that flow characteristics are reasonably close to the situation in open channel flow and they give good average values for thresholds and erosion rates due to large area at which they are measured (Black and Paterson 1997, Andersen 2001b).

Other techniques used for determination of erodibility of cohesive sediments are: (1) generating a water jet impacting on the sediment surface (e.g. the cohesive strength meter CSM; Tolhurst et al. 1999, 2000a); (2) generating a stream of water between an inverted bell-shaped funnel, placed at close range above the sediment surface (ISIS; Williamson and Ockenden 1996); (3) inducing fluid flow by a disc stirring combined with central suction (Microcosm; Gust and Müller 1997); (4) inducing turbulent motion by a

propeller at close range above the bed surface (EROMES and portable EROMES; Schünemann and Kühl 1991, Andersen 2001a; LABEREX chamber, Lund-Hansen et al. 2002).

Instruments of the latter type are smaller and therefore easier to handle. Due to their relatively small test section, the results are more sensitive to small-scale irregularities of the bed surface and the settings of the instrument on the bed surface. Disadvantages are therefore primarily found in the distribution of the bottom shear stresses which is often not quite regular in time and space (Houwing and van Rijn 1998).

The CSM is a small portable erosion device that uses a vertical jet of water to erode surface sediment (Paterson 1989). The occurrence and increase of eroded matter with generated bed shear stresses is monitored by light attenuation in the measuring cell. This instrument has been used to determine critical erosion shear stresses of intertidal mudflat and marsh sediments. It can be relatively easily transported and in-situ erosion tests undertaken rapidly, increasing the number of measurements. In addition, the device generates a wide range of equivalent bed shear stresses, enabling it to be used on a variety of sediment types, including salt marsh, biostabilized areas, desiccated sediments (Tolhurst et al. 1999). There are a number of disadvantages with the device: (i) unnatural flow structure – the flow is arguably dissimilar to that of a natural flow; (ii) the CSM can not be deployed underwater; (iii) critical erosion thresholds are defined by a certain level of light attenuation which can not be quantified in terms of erosion rates and hence the criterion for the onset of erosion depends strongly on the optical characteristics of the eroded material (Tolhurst et al. 2000b); (iv) erosion rates are not easily determined by use of the device.

ISIS (now called as SedErode) was developed by HR Wallingford, Oxford, United Kingdom (UK), to measure erosion shear stress directly on undisturbed intertidal muds (Williamson and Ockenden 1996, Black and Paterson 1997). ISIS consists of a circular, inverted, bell-shaped funnel that fits inside a cylindrical perspex column of 90 mm diameter with a 3 mm annular space around the edges. The bell head is positioned just above the sediment bed, at a typical distance of 4–8 mm from the lowest part of the bell head to the mud bed.

ISIS produces a steady, approximately uniform shear stress at the sediment water interface by recirculating water circumferencially through the gap then drawing the water through a hole at the center of the bell head. Shear stress at the bed is controlled by the recirculating rate. The point of surface erosion is recorded as an increase in turbidity (measured by a nephelometer) relating to a significant removal of material from the bed surface (Williamson and Ockenden 1996).

The Microcosm is a relatively small erosion device (30 cm in diameter), with a removable lid housing, a stirring disc and water input and output (Gust and Müller 1997, Black and Paterson 1997). The device generates a spatially uniform bed shear stress over the sediment surface by controlling the rotational speed of the lid and the rate of removal of fluid through the lid. The discharge rate from the pump and the revolution rate of the disc determine the stress over the bed in the chamber. The turbulence spectrum generated by this device matches those of channel flows. A circular hole in the lid allows water samples to be taken from the chamber to measure the suspended particulate matter (SPM) at every shear stress increment.

1.5.2. EROMES

The EROMES (Figure 1.2) has been used in several erosion studies (Schünemann and Kühl 1991, Austen et al. 1999, Riethmüller et al. 2000; Tolhurst et al. 2000b). Both critical erosion shear stress and erosion rate can be determined with the instrument. The original EROMES system was developed by the GKSS Research Centre (Germany) to investigate the erodibility of natural muddy sediments in the laboratory.

A portable field-version of the original EROMES has been designed, built, calibrated and tested by Andersen (2001a). The instrument resembles the laboratory (original) version but can be used *in situ* as well. The main advantages of the portable EROMES (Figure 1.2) are that it is able to produce data on both erosion thresholds, erosion rate and settling velocity of the eroded material and measurements can be done quite rapidly (Andersen 2001b).

The principle of EROMES is that the turbulence of the water is induced by a rotating propeller, causing erosion or resuspension of sediment. The

rotational flow in the chamber is significantly reduced by placing a series of vertical baffles around the chamber wall (Schünemann and Kühl 1991). The propeller revolutions have been converted to bed shear stress by use of a calibration on erosion of quartz sands with known critical erosion shear stress.

One of the disadvantages of EROMES system is that the fluctuations of turbulence generated by the propeller are large and the turbulent energy spectrum exceeds those found in natural channel flows by an order of magnitude (Gust and Müller 1997). On the other hand, it may resemble the conditions found on intertidal areas which is characterized by a combination of both waves and currents. In addition, bed shear stress generated by the device is not radially uniform over the sediment surface, i.e. bed shear stress increases with increasing distance toward the outer wall. Gust and Müller (1997) found that bed shear stresses are low at radii 0 mm (at the center) and 40 mm, and stresses are high at 20 mm and 30 mm from the center. The rough turbulence spectrum on the one side and the radial dependence of the imposed bed shear stress on the other side with an reduced area affected by the propeller do not allow a direct transfer of the data to field conditions or comparisons with other erosion devices. Still, they are used for relative comparisons of erodibility.

Two types of bed shear stress calibration have recently been applied for the EROMES: a direct measure of bed shear stress using a hot-film probe and an indirect calibration using the onset of erosion of quartz-sands with known critical bed shear stresses (Schünemann and Kühl 1991, Andersen 2001a). Highly fluctuating bed shear stresses were found during the calibration with the hot-film sensor due to the stirring motion of the propeller. The flow structure is assumed to be comparable to the quartz-sand calibration for bed shear stresses below 0.5 N m^{-2} due to the presence of a viscous sub-layer in both calibration experiments. Based on a comparison of the two methods, a good agreement was found between the quartz-sand experiments τ_s and the mean of the max one third of τ for the hot film measurements, $\tau_{1/3}$ (Figure 1.3). When calculating τ_s and $\tau_{1/3}$ for the complete range, a fairly good agreement is found for a radii of 10, 20 and 30 mm, although a maximum of 10 % difference is found at the highest bed shear stress (Andersen 2001a).

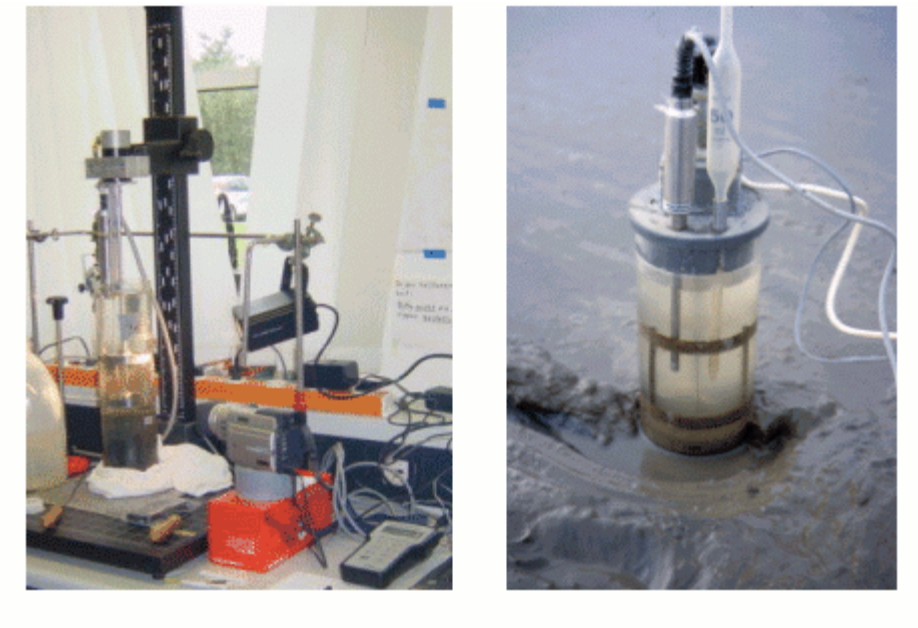

Figure 1.2. Photographs of Lab (left) and Portable EROMES (right).

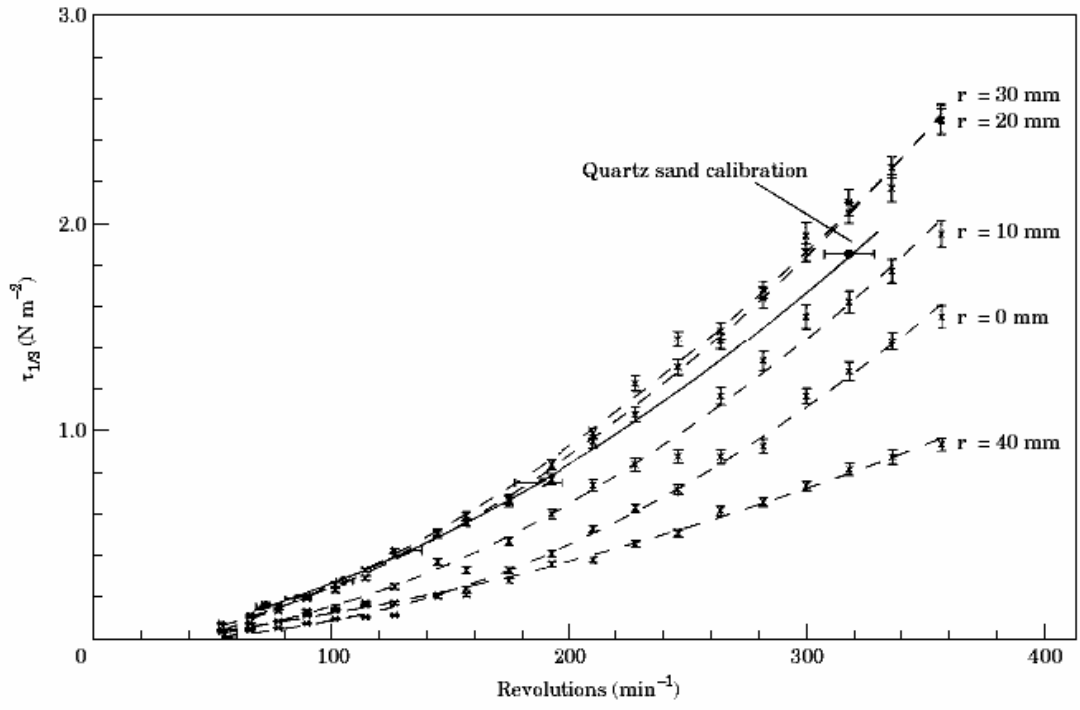

Figure 1.3. Comparison of the hot-film and quartz-sand calibrations for the portable EROMES (from Andersen 2001a).

In the present work, two lab and one in-situ systems of EROMES were used. The concentration of eroded material (SPM) in the EROMES system

was continuously determined by measuring the turbidity, using for one system a transmission sensor in a by-pass loop and for the second lab and the in-situ system an optical back scatter (OBS) sensor mounted 5 cm above the sediment water interface (Figure 1.4). The turbidity was calibrated against water samples taken for gravimetric analysis and calibration curves are produced for each erosion experiment. The SPM time series are used to calculate the erosion rate for each erosion step, giving a time averaged erosion rate. Due to problems with turbulence fluctuations and radially bed shear stress variations in the EROMES system, the resulting erosion rate is probably underestimated due to the fact that only selected parts in the test section are affected effectively by applied bed shear stress. Therefore, the resulted erosion rate is called "EROMES erosion rate". The critical erosion shear stress is determined by a significant increase of the erosion rate and is defined as the bed shear stress when the EROMES erosion rate exceeds a critical level of 0.01 g m^{-2} s^{-1}.

The results of critical erosion shear stresses EROMES (see chapter 2.3.1 for definitions and technical details) have been checked against other devices, namely the CSM, the ISIS and the Sea-Carousel (Tolhurst et al. 2000b). In case of the CSM, parallel close-by measurements were carried out, covering cases with widely differing diatom densities. For a consistent definition of critical erosion shear stress, the EROMES criterion, based on erosion rates, was transferred to an appropriate threshold of light attenuation measured in the by-pass loop. With this threshold criterion good agreement between both devices was achieved. To compare with ISIS and SEA Carousel, EROMES results were checked indirectly against published data (Williamson and Ockenden 1996, Amos et al. 1998) comparing the values of critical erosion shear stresses for comparable situations with negligible contribution of diatom stabilization and expected dominant impact of physical sediment properties. In the comparison, EROMES data were plotted against the sediment surface dry bulk density together with ISIS data from the Severn estuary, UK; and against sediment surface wet bulk density together with Sea carousel data from sites on the Canadian coast and the Humber estuary (Figures 1.5 (A) and (B)). Compared to ISIS, the ERMOES data agree in magnitude, trend and range of scattering. Compared to the Sea Carousel data, the trend and the range of

scattering also agree but the EROMES erosion shear stresses seem to be somewhat lower. This may be explained by the fact that for some Sea-Carousel data effects of biostabilization cannot be excluded. The agreement between EROMES and results from other devices suggests that EROMES works reasonably well with respect to measurements of critical erosion shear stresses. Comparisons made for measured erosion rates will be described in chapter 2.3.3.

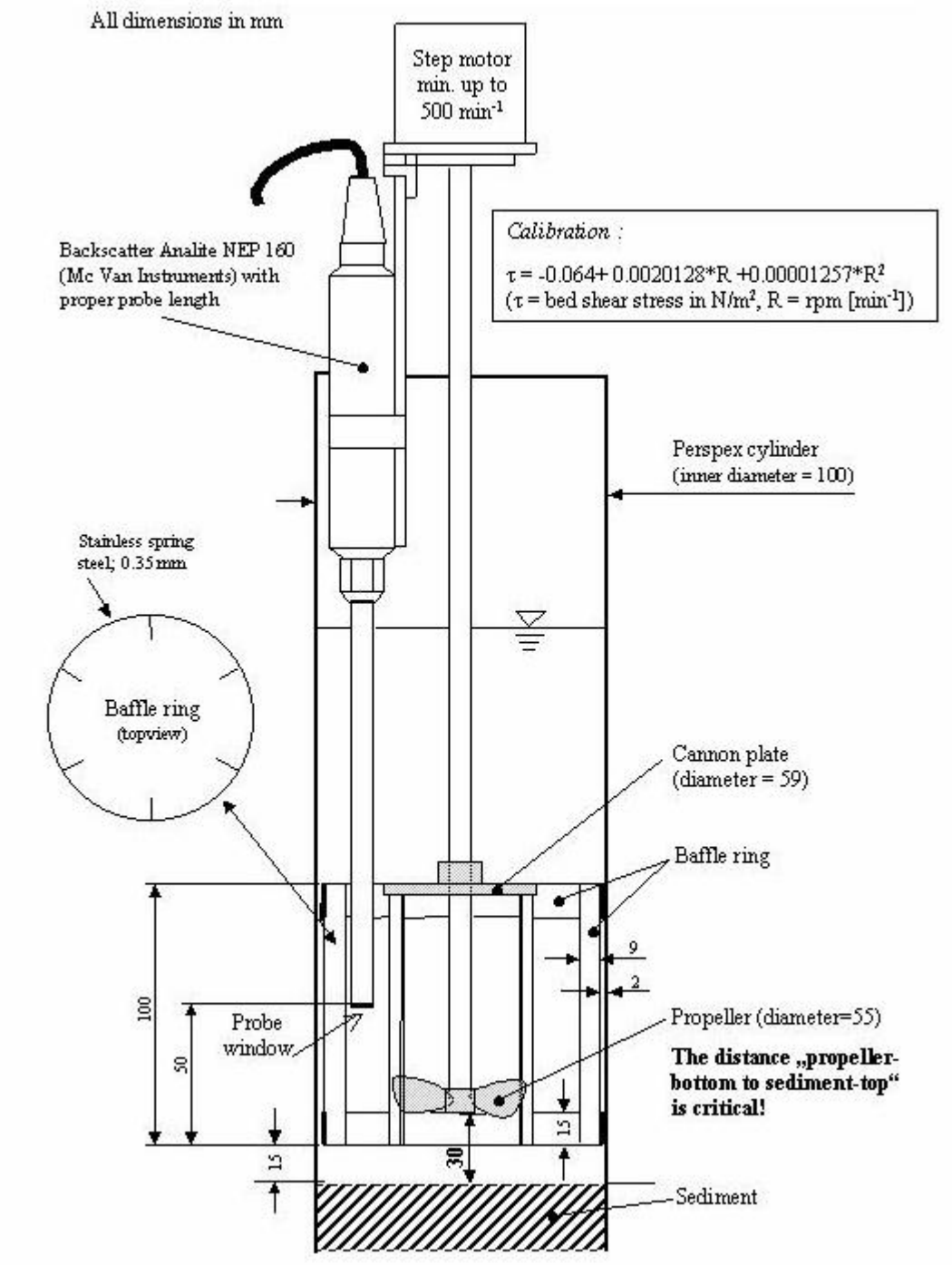

Figure 1.4. Schematic view of EROMES device with backscatter.

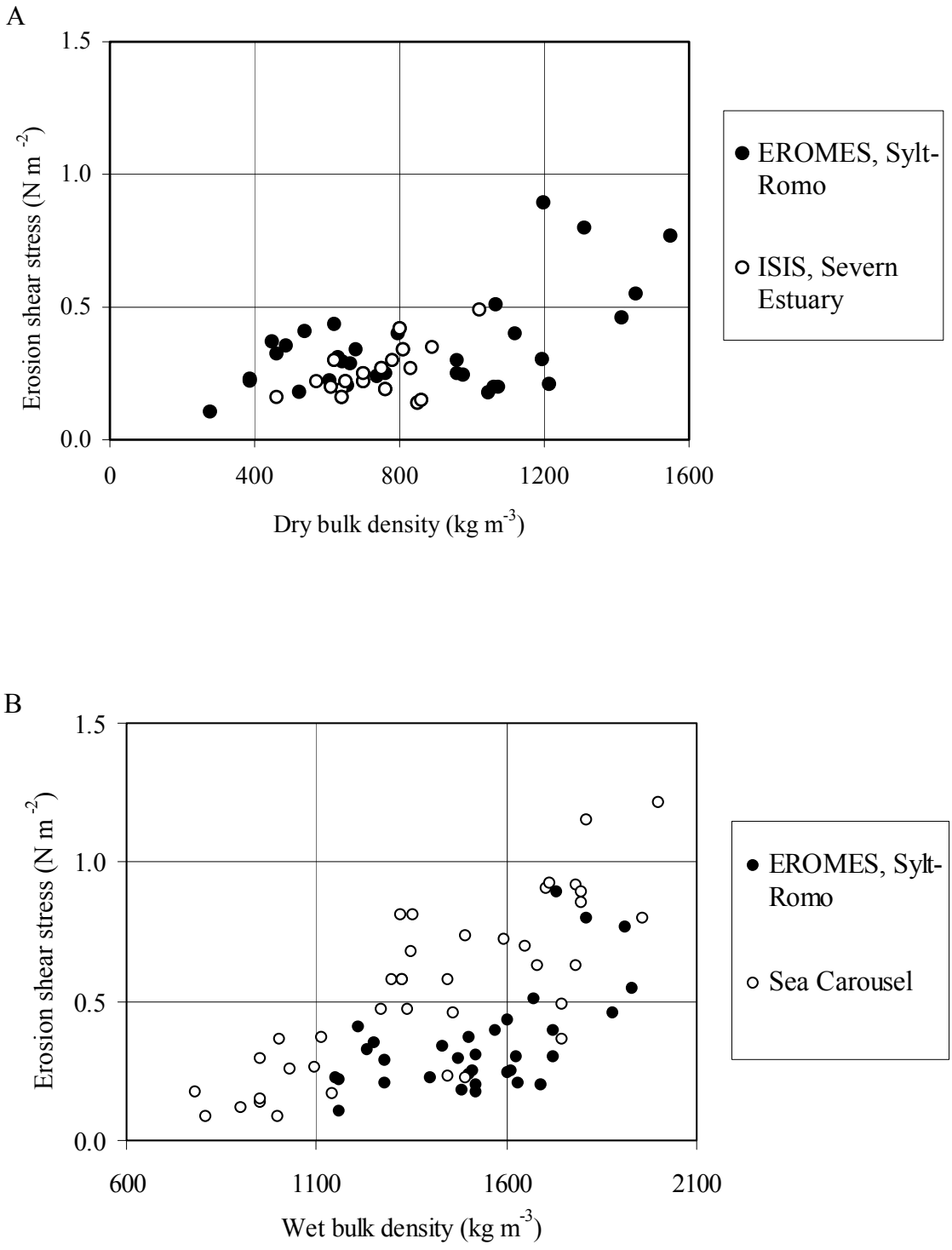

Figure 1.5. (A) Comparison of the relationship between erosion threshold and dry bulk density for EROMES and ISIS. (B) Comparison of the relationship between erosion threshold and dry bulk density for EROMES and Sea Carousel. For the EROMES, only data with a chlorophyll-*a* content less than 20 mg m^{-2} was used to reduce the influence of microbial stabilization on the thresholds (from Tolhurst et al. 2000b).

CHAPTER 2
FIELD WORKS AND METHODOLOGIES

2.1. Study site

The study was conducted on the "Dornumer Nacken", a back-barrier tidal flat located between the barrier island of Baltrum and the East-Frisian mainland coast in Lower Saxony, Germany (Figure 2.1). The site was selected because of its habitat variety and sound documentation of sediment distribution and biological properties over many years (van Bernem 1999). The mean tidal range is approximately 2.8 m and the tides are semi-diurnal. Depth-average tidal current velocities in the channels close to the inlet reach a maximum of up to 0.70 m s^{-1} and on the tidal flats of up to 0.25 m s^{-1} (Krögel and Flemming 1998).

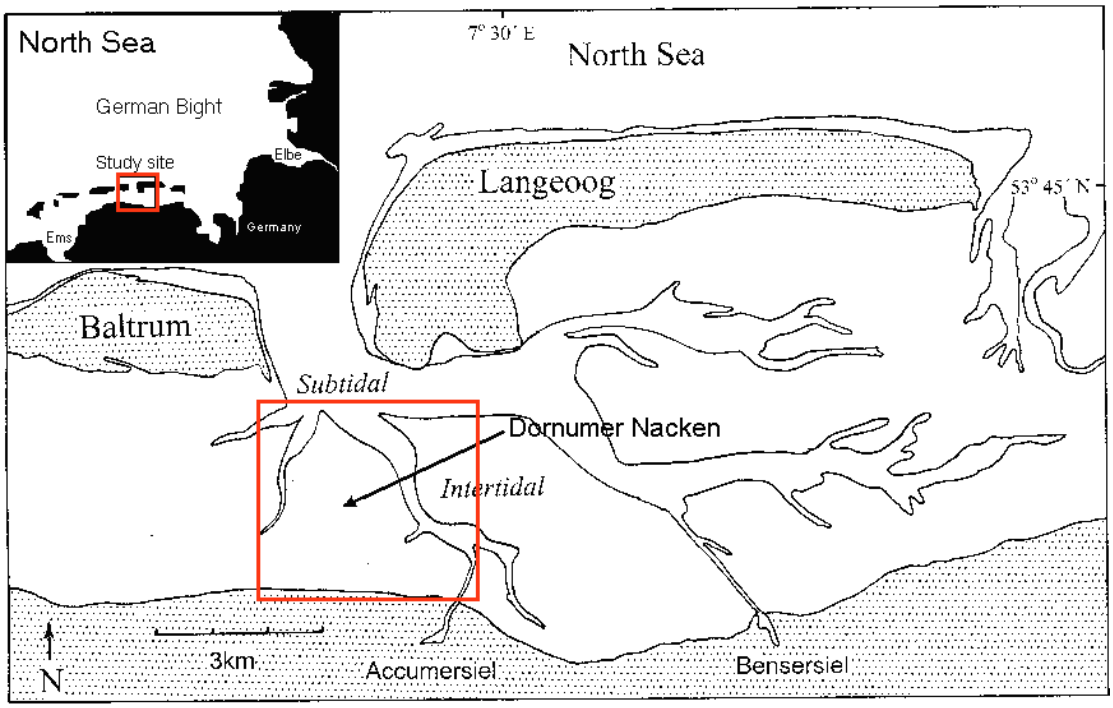

Figure 2.1. Map of the study site showing the Dornumer Nacken intertidal flats.

According to the diversity of habitats, the Dornumer Nacken can be divided into three main zones: exposed zone, middle zone, and inner zone, including a protected salt marsh area close to the mainland. The mud content increases towards the shoreline. The exposed zone is sandy, whereas the middle and inner zones are mixed tidal flats with a mud content of 20 to 40 % by weight. The mud content in the salt marsh is higher than 50 % by weight. The middle

zone is slightly less elevated (depression) and has shorter emersion time (i.e. four to five hours per tidal cycles) than the exposed and inner zones. The emersion time of the exposed zone is less than five hours per tidal cycles, while the inner zone is sub-aerially exposed for five to six hours per tidal cycles.

The habitat structure is homogenous in the outer (exposed) zone and dominated by sessile polychaetes, e.g. lug worm (*Arenicola marina*) and sand mason (*Lanice conchilega*). The middle zone shows a higher heterogeneity of habitat patterns including patches of changing density of the blue mussel (*Mytilus edulis*) and cockles (*Cerastoderma edule*). The inner zone shows again a predominantly homogeneous distribution of habitats characterized by small sessile polychaetes (e.g. *Heteromastus filiformis* and *Pygospio elegans*) and patches of the cockles *Cerastoderma edule* and *Macoma baltica.* In elevate areas the mud snail *Hydrobia ulvae* is the most abundant grazer on the sediment surface.

The sediment distribution at the study site was described in detail by Krögel and Flemming (1998). The pattern generally showed a distinct gradient in grain-sizes with coarser sediments and lower mud content close to the tidal inlet and increasing mud content towards the mainland dike (Figure 2.2). The distribution was attributed to the general decrease in hydrodynamic energy from the tidal inlet towards the mainland and to the different settling rates of sediment particles induced by seasonal changes in water temperature (Krögel and Flemming 1998). It is claimed by those authors that the distribution is adjusted to winter conditions with lowest settling velocities of sediment particles and highest the energy input.

2.2. Sampling strategy

2.2.1. Selection of sampling stations

On the tidal flat, six stations along a cross-shore transect of approximately 1.5 km length from immediately below the salt marsh to the middle of the tidal flat were chosen (designated A–F seawards in Figure 2.3). The principal motivation behind the selection of stations was to cover a range of parameters, which are expected to have a detectable effect on the critical erosion shear stress and the erosion rate. These parameters are energy

regime, exposure time, sediment type, and epibenthic and endobenthic macrofaunal assemblages

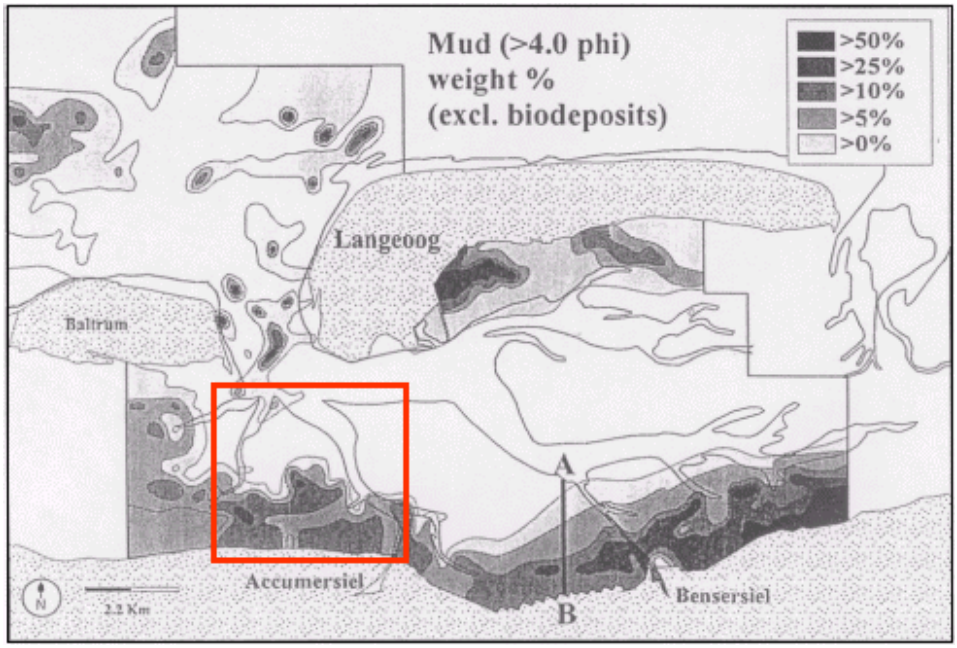

Figure 2.2. Mud distribution at the study site (Krögel and Flemming 1998).

Station A is located close to the salt marsh. This station is continuously exposed for up to seven days between successive spring and neap tidal cycles and inundated only around spring tides and during storm surges. Station B is located in the *Hydrobia* dominated strip, approximately 130 m from the shoreline and exposed for six hours per tidal cycle. Stations C and E are within areas dominated by sessile worms, whereas station D is in the cockle bed area. Stations C, D, and E are approximately 700, 700, and 1000 m away from the shoreline, respectively. While the distance between the outermost station F and the shoreline is approximately 1500 m. It was characterized by blue mussel patches of about 5 m in diameter and 10–15 m apart. The sampling location was in between these patches. Stations C – F had similar emersion time of about four to five hours per tidal cycle.

The sediments at station A varied from muddy sand to sandy mud with mud content ranging from 46 % to 68 %. The sediments at stations B, C and E consisted of slightly muddy sand to muddy sand, with mud content generally less than 37 %. Station D was classified as muddy sand with mean mud

content of 41 %. The sediment at station F varied from slightly muddy sand to sandy mud with mud content ranging from 18 to 70 % (classification after Flemming 2000). Figure 2.4 shows the morphological features of the sediment surface at each of the six sampling stations.

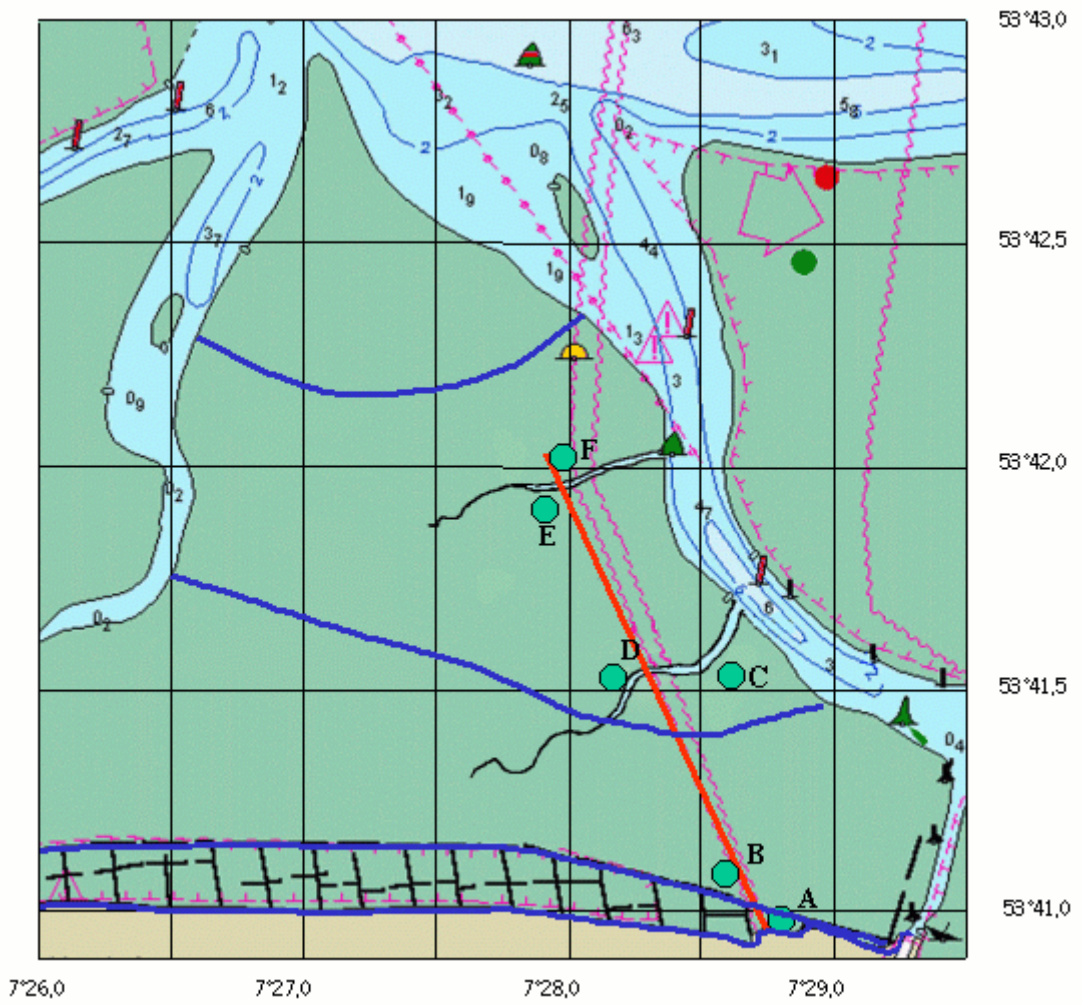

Figure 2.3. The cross shore transect and the six sampling stations. The blue lines indicate the approximate boundaries between the described zones as suggested by habitat field mappings (C. van Bernem, personal communication).

Geomorphological structures (bedforms) were present at all stations during the sampling periods. The bedforms were characterized by irregular crest and troughs system. The bedforms were aligned more or less normal to the shoreline, with wavelengths of 0.5–1 m and heights 0.1–0.15 m. The crests were lower at station D with height of 0.02 to 0.05 m. The elevated crests emerged at low tide and tended to dry out during emersion (Figure 2.5). The

depressions or troughs acted as drainage channels which often contained trapped or slowly running water during most of the emersion period.

Figure 2.4. Photographs of the morphological features of the sediment surface at sampling stations A–F.

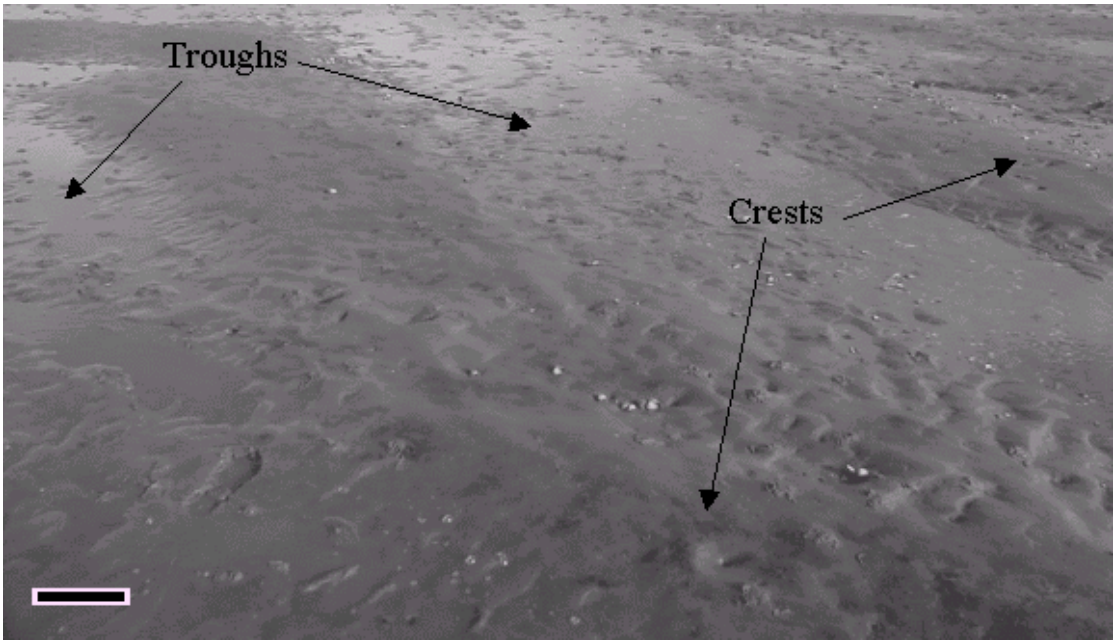

Figure 2.5. Photograph of morphological feature with a pronounced crest and trough system at station E. Crests are the emergent elevated parts, and troughs are depression parts (scale bar = 0.15 m).

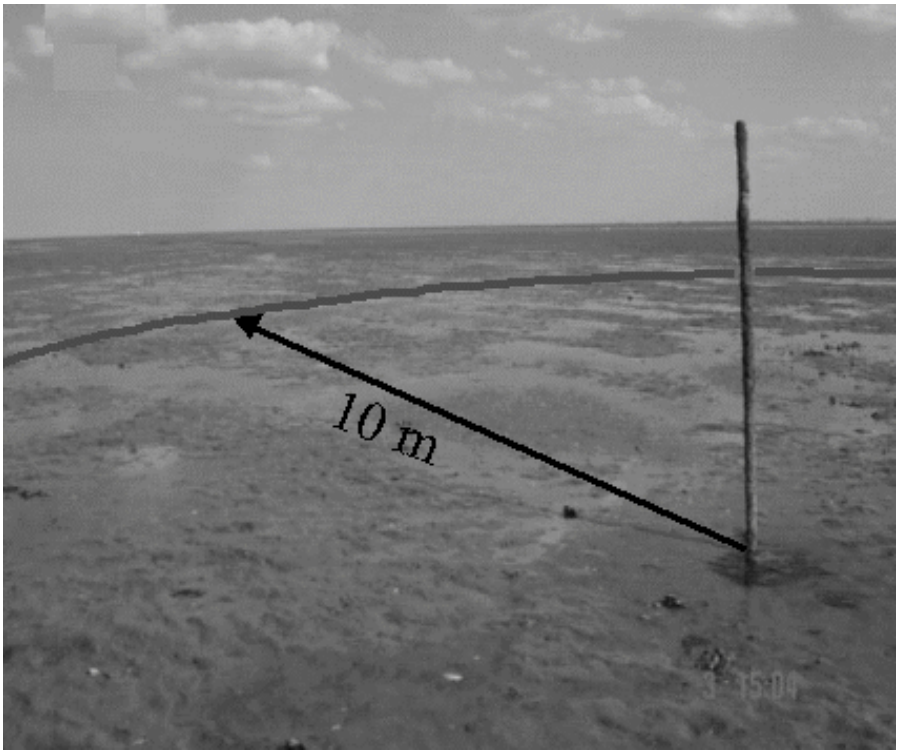

Figure 2.6. The sampling positions within each station are located in a circle with radius 10 m.

2.2.2. Selection of samples at each station

The samples were collected within a 10-m radius of a permanent marker at each station (Figure 2.6) except for station D. At D, the samples were collected along a transect with a spacing of approximately 10 m between each sample. The transect was 50 m long and oriented perpendicular to a small gully. The sampling was conducted at approximately 1 hour after the sampling stations were exposed (low tide). The actual choice of the sampling positions was guided by the objective to cover a representative set of surface types within each station. To minimize sample surface disturbance during transport this choice was biased to surfaces which were visually undisturbed and free of surface water and benthic macrofauna structure. The samples were taken at crests and troughs of the bedforms in 2002 to compare the erodibility of crests and troughs. In 2001, the samples were mostly taken on the crests only.

2.2.3. Temporal (seasonal) sampling pattern

Sampling was conducted from spring to autumn because biological influences on sediment properties and hence erodibility were expected to be higher than in winter. In 2001, samples were taken in April, May, June, and October to examine the potential seasonal variability of erodibility on the tidal flat as a whole. April and May are representing the spring situation, June represents early summer, and October the conditions in autumn. The tidal flat was also visited during September 2001, but no sampling was made due to stormy weather and water set up. In 2002, the sampling was conducted in June and September. The number of samples per station and sampling date was considerably increased for the examination of cross-shore variations. Additionally, the 2002 sampling was aimed to investigate temporal variations of sediment erodibility at each station by comparing June and September data. Additional *in situ* erosion measurements using portable EROMES were conducted at station D in June and September 2002. The temporal pattern of sampling is presented in Table 2.1.

2.2.4. Measured parameters

The physical and biological sediment parameters (properties) that were measured included:

– Surface parameters (1 mm layer)

  - physical: wet bulk density, grain-size distribution, and water content
  - biological: microphytobenthos assemblages, chlorophyll-a, colloidal carbohydrate, extracellular polymeric substance (EPS), organic content and fecal pellet content;
- Depth integrated parameters
  - physical (0–5 cm layer): wet bulk density, grain-size distribution, and water content
  - biological (0–5 cm layer): chlorophyll-a and organic content
  - benthic macrofauna (0–10 cm layer).

Table. 2.1. Number of samples collected at each station in 2001 and 2002.

	2001				2002	
Station	April	May	June	October	June	Sep.
A	–	–	–	–	7	6
B	1	2	2	2	4	6
C	1	2	3	2	5	4
D	–	–	–	–	14	14
E	1	2	2	3	9	4
F	1	1	3	2	13	6

2.3. Methods

2.3.1. Erosion measurements with Lab EROMES

A 10-cm diameter perspex tube was used to collect the sediment core for erosion measurements. The cores were immediately transported to a nearby mobile laboratory. Particular care was taken to avoid any disturbance during transport and storage of the cores. The selected core sites had to be completely free of surface water; hence, no water could exert stress on the sample surface when the cores were moved during the subsequent transport. Before excavation, the cores were sealed to prevent any vertical movement of the sample inside the cylinder. Next, the cores were transported by sledge across the tidal flat and then carefully carried from the shoreline to the nearby

mobile laboratory. At the laboratory, they were carefully filled with local seawater to a level of 30 cm by pouring it slowly over a plate positioned 1 cm above the sample surface. Despite great care being taken, this process nevertheless stresses the surface to a certain degree; therefore, the cores were allowed to stand for at least one hour and at most 18 hours before the start of the erosion experiment.

Two lab EROMES systems were used to determine the critical erosion shear stresses and erosion rates. During each erosion experiment, the applied bed shear stress was initially started from 0.05 N m^{-2} and increased in steps of 0.1 N m^{-2} every 5 minutes. The experiments were ended when the turbidity in the system reached saturation. The concentration of eroded material (SPM) in the system was continuously determined by measuring the turbidity using for one system a transmission sensor in a by-pass loop and for the second system an OBS-sensor mounted 50 mm above the sediment water interface. The turbidity was calibrated against water samples taken for gravimetric analysis, and calibration curves were produced for each erosion experiment (Figure 2.7a and b). The SPM time series can then be used to calculate the EROMES erosion rate for each erosion step, giving a time averaged erosion rate over five minutes.

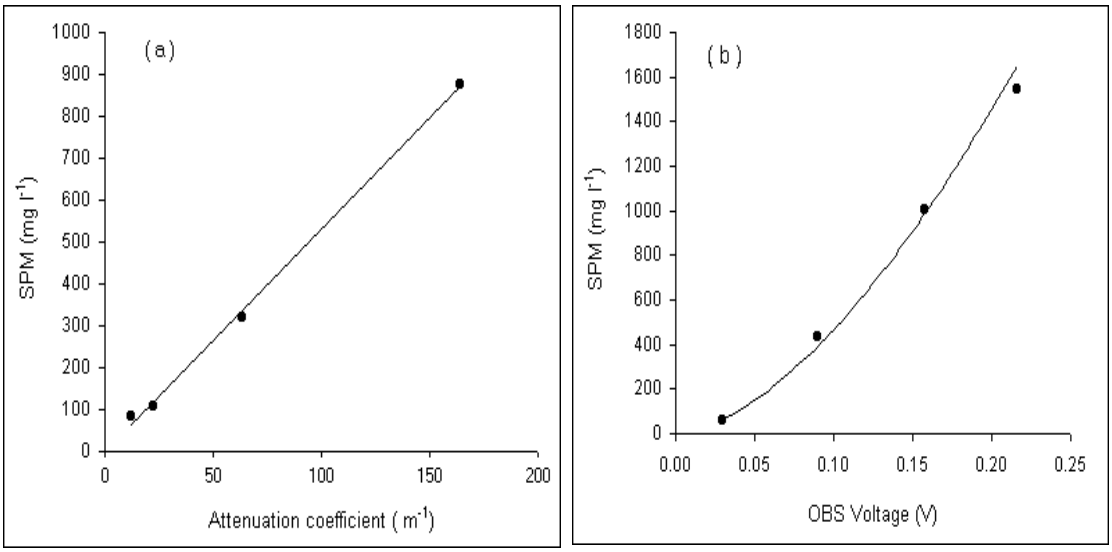

Figure 2.7. Calibration curves for suspended particulate matter (SPM) versus (a) transmission sensor and (b) OBS output.

Critical erosion shear stress is defined as the bed shear stress when the EROMES erosion rate exceeds a critical level of 0.01 g m^{-2} s^{-1}. Below the critical shear stress, loose and fluffy materials that settled during the resting period of the cores are eroded and resuspended. In the presence of filter feeders (e.g. *Cerastoderma edule*, *Macoma baltica*), negative erosion rates due to filter feeding activity of the fauna were often observed. The exact value of critical erosion shear stress was determined by applying a linear regression to the observed rate around the critical erosion rate of 0.01 g m^{-2} s^{-1}. The evaluation procedure to compute critical erosion shear stress is illustrated in Figure 2.8b for a sample taken in 2001 at the station B.

2.3.2. *In situ* erosion measurements with portable EROMES

The equipment was originally described by Schünemann and Kühl (1991) and the portable version described in detail by Andersen (2001a). Basically, the erosion instrument consists of a 10-cm diameter perspex tube that is pushed into the undisturbed bed sediment. The tube is gently filled with local seawater and the eroding unit is placed on top of the tube. This eroding unit consists of a propeller that generates bed shear stresses and an OBS-sensor, which monitors the changing suspended sediment concentration (SSC).

During each erosion experiment, the bed shear stress was increased in steps of 0.1 N m^{-2} every two minutes from 0.1 N m^{-2} to 1.0 or 1.5 N m^{-2} (depending on the critical erosion shear stress of the bed). Samples for the calibration of the OBS-sensor were withdrawn from the instrument during each experiment and filtered through pre-weighed Millipore 0.45 µm CEM filters. The method to determine critical erosion shear stress is similar to that used for Lab EROMES.

2.3.3. EROMES erosion rate

Erosion rate for each applied bed shear stress was calculated from suspended particulate matter (SPM) time series which measured at every five minutes. The erosion rates, which are reported here, are the average erosion rates during the application of the bed shear stress from 1.0 to 2.0 N m^{-2}. In order to facilitate direct comparison with earlier publications using the portable EROMES (e.g. Andersen 2001a), erosion rate data derived from portable

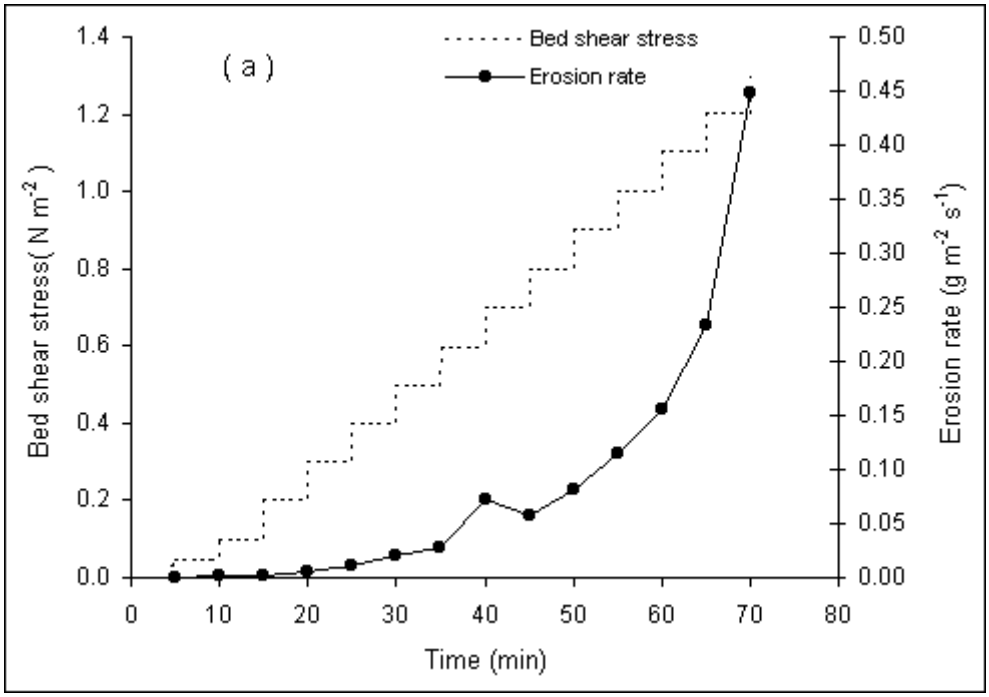

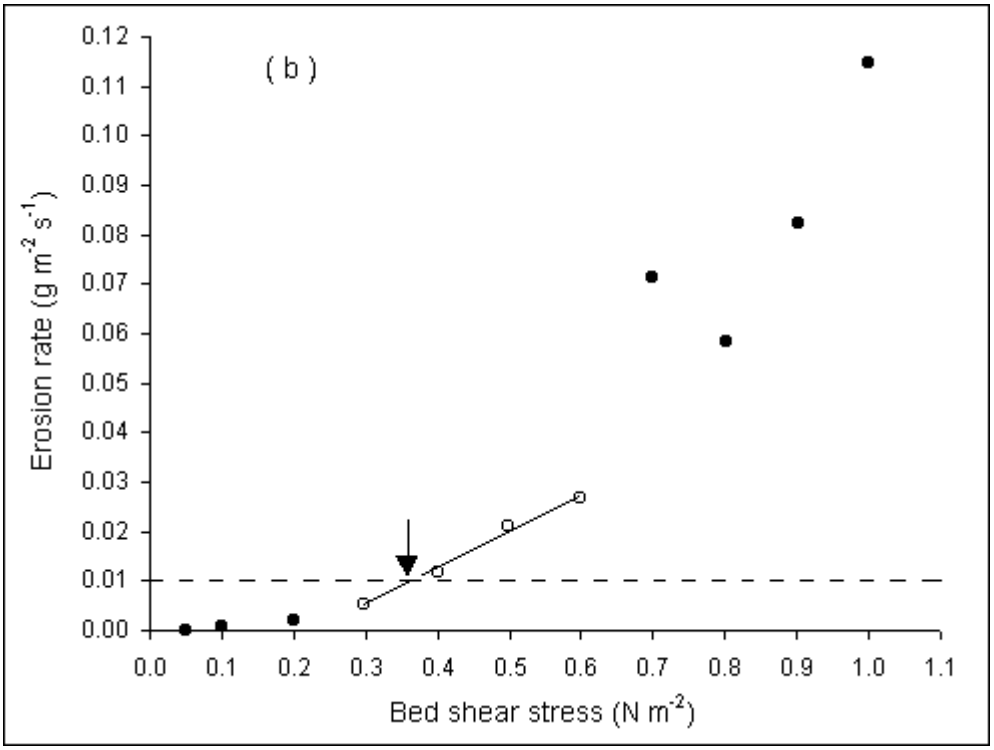

Figure 2.8. An example of the output of erosion experiment using the EROMES. (a) The stepwise increase in applied bed shear stress and the variation in erosion rate during the erosion experiment. (b) Erosion rate versus bed shear stress for the same experiment. To determine the critical erosion shear stress, a linear function is fitted to the data in the region around the critical erosion rate of 0.01 g m^{-2} s^{-1} (open circles). A critical shear stress of 0.35 N m^{-2} is found for this experiment.

EROMES are calculated from 2 minutes increments and as the average erosion rate for the bed shear stress increments from 0.5–1.0 N m^{-2}.

The best fit of the power relationship between log erosion rate and log excess bed shear stress ($\tau_b - \tau_{cr}$) was made at each erosion experiment to smooth out the fluctuations of erosion rate (Figure 2.9). The fit was done according to the following formula: $\log E = \log A + B \log(\tau_b - \tau_{cr})$ where E is the erosion rate, τ_b is the applied bed shear stress, τ_{cr} is the critical erosion shear stress, A and B are intercept and slope, respectively. From this fit, smoothed and consistent erosion rates as well as SPM concentrations can be calculated as a function of bed shear stress. The power law approach was used to generated the best fit because the increase erosion rate with increasing applied bed shear stress exhibit a power law relationship rather than linear or exponential form.

The best fit described above was also used to extrapolate the erosion rates for the cases where the erosion experiments were ended due to the saturation of the turbidity (optical devices) in the EROMES system. This allows us to make a comparison between sample erosion rates at high bed shear stress, i.e. bed shear stress above the turbidity saturation. The smoothed and extrapolated erosion profiles presented in chapter 4 (Figure 4.4) were generated by plotting the mean of SPM concentration of 4 to 10 samples against bed shear stress at every shear stress increment.

To examine whether erosion rate derived from EROMES are comparable with those from other erosion devices, the EROMES erosion rate data were indirectly checked with published results from the *in situ* annular flume device (Widdows et al. 1998a). In the comparison, EROMES erosion rates were plotted against the applied bed shear stress together with *in situ* annular flume data from the Skeffling mudflat, Humber estuary (UK). Noted that erosion rate data of *in situ* annular flume presented here were deduced directly from graph shown by Widdows et al. (1998a). Compared to *in situ* annular flume, EROMES data agrees in magnitude and trend of the increase erosion rate with increasing bed shear stress (Figure 2.10). This suggests that a comparable and reasonable erosion rate still can be derived from EROMES although the device generates large turbulence fluctuations and not radially uniform bed shear stress over the sediment surface.

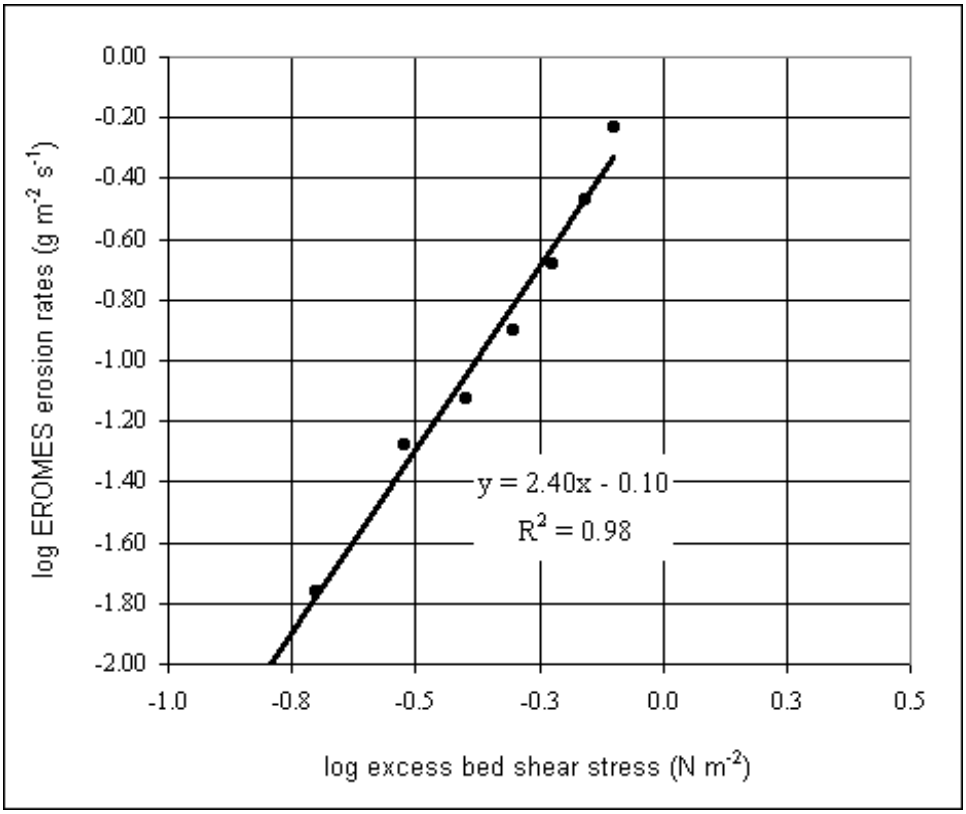

Figure 2.9. Log EROMES erosion rate as a function of log excess bed shear stress.

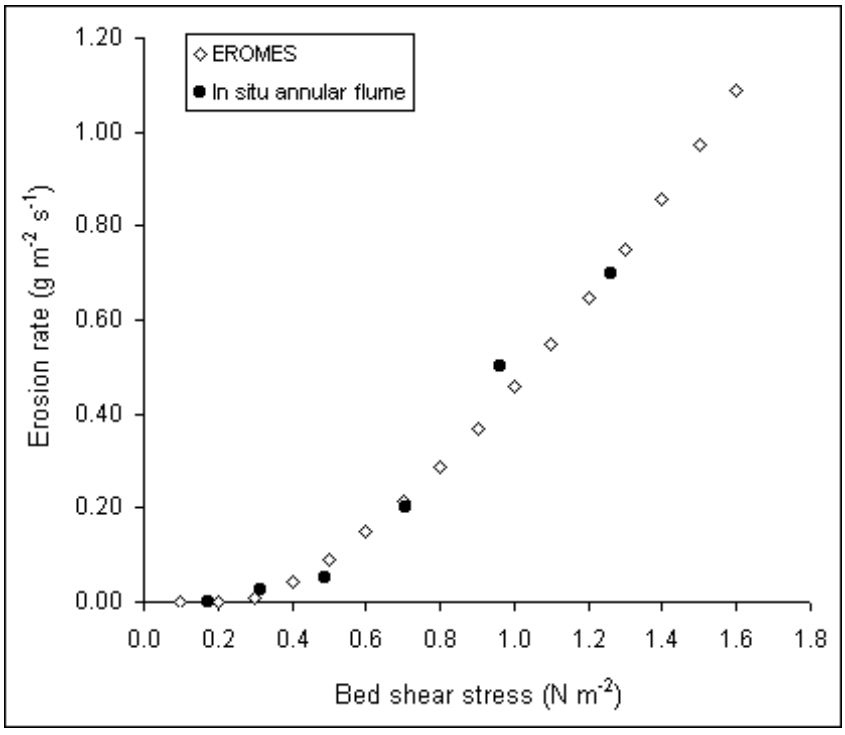

Figure 2.10. Comparison of the relationship between erosion rate and bed shear stress for EROMES and *in situ* annular flume.

2.3.4. Physical and biological sediment properties measurements

The upper 1 mm of surface sediments was carefully scraped in the direct neighbourhood of each erosion core to collect sufficient material for the sub-samples and to integrate over small scale patchiness. If the diatom distribution inside the core was visibly very patchy, the scrapped area was chosen to approximate the fraction of diatom coverage visible in the core. The samples were well mixed and sub-samples were taken to measure wet bulk density, grain-size distribution, water content, organic content, microphytobenthos assemblages, chlorophyll-a, colloidal carbohydrate and EPS concentration of the bed material.

Additional samples integrating the upper 0–5 cm of the sediment were taken to compare with the data from geological works (e.g. Flemming and Delafontaine 2000) and to distinguish more actual conditions (upper mm) from more persistent ones. The samples were taken with a small perspex tube core of 5 cm diameter. Cores were taken in triplicate and the three samples were pooled into one sample for analysis of wet bulk density, grain-size distribution, water content, organic content and chlorophyll-a.

A different sampling strategy was chosen for the samples probed with the portable EROMES. These measurements were carried out in close cooperation with a scientist from the University of Copenhagen which used the following method: a surface scrape of the topmost 1 mm of the bed was analyzed for grain-size distribution, fecal pellet content, organic content, chlorophyll-a, colloidal carbohydrate and EPS concentration. Additional samples of the topmost 5 mm of the bed were taken with a syringe (diameter 21 mm, five samples pooled into one sample) and analyzed for wet bulk density. To examine the vertical distribution of mud content at station D, a sediment core was collected by means of a 7-cm diameter aluminum pipe (100-cm long). The core was sliced into 2 cm sections and examined for their mud content

Sediment chlorophyll-a concentration

Sediment samples were freeze-dried prior to the determination of chlorophyll-a. Chlorophyll-a concentrations were measured using the acetone extraction and reverse-phase column HPLC technique of Wright et al. (1991).

In this procedure, pigments were extracted by adding 2–3 ml of 100 % acetone to the 1–2 g freeze-dried sediment sample and extraction for 24 hours in the dark at -40 ^{o}C. The extract was filtered using a spartan 0.2 µm filter. 20–50 µL of the extract was injected to the separation column of HPLC.

The HPLC system consisted of multiwavelength detector (Jasco MD-915), autosampler (851-AS), Line degaser (DG-980-503), ternary gradient unit (LG-980-02), intelligent HPLC pump (PU-980), and intelligent column thermostat (CO-1560). The reversed phase column used was nucleosil 5 µm C18. The flow rate was 1 ml/minute and the three solvents used were eluant A: 80 % methanol: 20 % 0.5 M ammonium acetate (ph 7.2), eluant B: 90 % acetonitrile: 10 % water, eluant C: 100 % ethyl acetate. Chlorophyll-a eluted at 27 minutes, and analysis of peak area and retention time was used to quantify the pigment. The following equation was used for the identification of chlorophyll-a (Friend 2001):

$$\text{Pigment content (µg/g)} = \frac{A\ x\ V\ x\ 10}{0.5\ x\ RF\ x\ 1000\ x\ W}$$

Where A = peak area from HPLC chromatogram

V = volume of acetone extract (ml)

RF = response factor (3514 for Chlorophyll-a)

W = weight of sample (g DW)

Chlorophyll-a content (µg/g) was then converted to concentration by area (mg m^{-2}) by using the following equation:

$$\text{Chlorophyll-a concentration (mg m}^{-2}\text{)} = A \times B \times \left[1 - \frac{C}{100}\right]$$

where A = chlorophyll-a in µg/g, B = sediment wet bulk density (g cm^{-3}), and C = sediment water content (%).

Sediment carbohydrate concentration

Sediment samples were freeze-dried prior to the determination of carbohydrate. Two different fractions of carbohydrate were determined: the colloidal fraction and EPS in the colloidal fraction (Underwood et al. 1995). In this procedure, 5 ml of saline water (25 ^{o}/oo) were added to 100–150 mg of

dry sediment. The samples were then left for 15 minutes at 20 °C, followed by centrifugation for 15 minutes at 2500 rpm. 1 ml of the supernatant (from 5 ml extract) was used for the determination of the colloidal fraction. To obtain the EPS in the colloidal fraction, 7 ml of cold ethanol (2–4 °C) was added to 3 ml of the supernatant (from 5 ml extract) to a final concentration of 70 %. The sample was incubated overnight at 5 °C, followed by centrifugation for 15 minutes at 2500 rpm. The supernatant was subsequently discarded and the pellets that contained EPS resuspended in 1ml of distilled water. Finally, the colloidal carbohydrate and EPS in the colloidal fraction was determined using the phenol-sulfuric acid assay with glucose as a reference (Dubois et al. 1956).

Water content

The water content of the sediment was determined by drying 1–2 g of fresh sediment samples in an oven to constant weight for 24 hours at a temperature of 105 °C. The sediment water content (%) was calculated from the difference between wet and dry weight. The following formula was used to calculate the sediment water content:

$$\text{Water content (\%)} = \frac{Sample\ wet\ weight - Sample\ dry\ weight}{Sample\ wet\ weight} \times 100$$

Wet bulk density

To determine the sediment wet bulk density, fresh sediment was put in a plastic container under continued stirring until it was completely filled. The sample was weighed and the weight of the container was subtracted. The wet bulk density of the sample is the ratio of wet weight to wet total volume (here 48 cm^3).

Organic content

Organic content was determined by loss on ignition of 1–2 g dry sediment after combustion for one hour at 550 °C. The following formula was used to calculate the sediment organic content:

$$\text{Organic content (\%)} = \frac{DW_{105} - DW_{550}}{DW_{105}} \times 100$$

where DW_{105} = dry weight of sample after oven drying at 105 °C

DW_{550} = dry weight of sample after combustion at 550 °C

Grain-size analysis

Sediment samples were freeze-dried prior to the determination of grain-size distribution. The sediment was prepared for grain-size analysis by adding 300 ml of tap water to 2.5 g of sediment and then adding 30 ml of 30 % v/v hydrogen peroxide (H_2O_2) to the sediment slurry. This removes organic material and thereby cleans the sediment particles. The sediment slurry was stored overnight in an oven (100 °C) to evaporate the H_2O_2. Once cooled, the sediment slurry was sieved using a sieve with mesh size of 300 µm. On the fraction < 300 µm the determination was done by means of a Galai Cis-1 laser particle size analyzer, with a specific analytical size intervals of 1 µm. This analyzer is equipped with a module for measurements in the range between 2 and 300 µm. For samples probed with the portable EROMES, grain size analyses were carried out by use of a Malvern Mastersizer/E laser-sizer after careful dispersion in 0.01 M $Na_2P_4O_7$ and ultrasonic treatment for three minutes prior to analysis.

Normalized water content

It has been shown by Flemming and Delafontaine (2000) that water content increases with mud content: muddy sediments have a higher porosity than sandy sediments in contrast to expectation taking into account only the grain-size. The relationship was observed to be site-specific reflecting different degrees of compaction. The same phenomenon has been observed for sediments taken from the upper mm (Riethmüller et al. 2000). Effects of sediment compaction (e.g. due to drying) can not directly be derived from the water contents when the mud content is changing accordingly. To compensate for this effect a site-specific reference for the relation between water and mud content has to be established.

In the samples taken at the Dornmer Nacken, the described behaviour is also to be seen (see Figure. 3.1a). The saltmarsh site, Station A, has consistently lower water contents than most data from the other stations

reflecting the drying and consolidation due to longer emersion periods and energetically calmer conditions. Data from Station F showed a wide scatter which may be attributed to the small-scale variability in the hydrodynamic conditions caused by the blue mussel patches. A reference line (Water content $_{predicted}$) between water and mud content for this study area was computed by a linear regression pooling the data from stations B, C, D and E:

Water content $_{predicted}$ = (0.4693 x mud content) + 23.44

To examine the effect of drying on sediment erodibility, a normalized water content was defined in the following way:

$$\text{Normalized water content (\%)} = \frac{Water\ content_{\ measured}}{Water\ content_{\ predicted}} \times 100$$

Values above 100 % denote relatively loosened sediment with higher water content, whereas values below 100 % indicate compaction, e.g. due to drying. The normalized water content is dependent on the site-specific relationship between water content and mud content. Hence, it is not a universal variable but it can show the relative degree of compaction for given mud content.

2.3.5. Microphytobenthos assemblages

Another sub-sample of some 2 g weight was transferred immediately into 10 ml glass receptacles with lid and in case of fixation covered with 4 % phormol approximately 1 cm above the sediment surface. For the light microscopy, the samples were filled up to 10 ml with demineralised water. After shaking carefully, a sample of 50 µl was taken out of the suspension, transferred onto a glass slide and covered with a cover slip. Five uniformly distributed traverses were counted out across the glass cover. Under these conditions, the benthic diatoms found can be approximately divided into apparently alive or dying individuals and empty valves, according to the condition of the protoplast. Taxonomical determination was performed using the keys of Hustedt (1930, 1959), Pankow (1990), Hartley (1996) and Tomas (1997).

2.3.6. Fecal pellet content

Fecal pellets originating from *Heteromastus filiformis* at station D were determined by gentle wet-sieving of a sub-sample at 63 µm and examination of the retained material under microscope in order to estimate the fecal pellet content in this material. The retained material was subsequently given an ultrasonic treatment for 2 minutes and wet-sieved at 63 µm again in order to separate fecal pellet material, sand and shell-fragments.

2.3.7. Benthic macrofauna

After performing the erosion experiment, the upper 10 cm of the sediment was sieved using a sieve with mesh size of 0.5 mm and subsequently preserved in formaldehyde (4 % after dilution). The macrofauna species were identified and counted. It should be noted that the true density of the cockle derived from erosion core data was probably underestimated. This is due to the fact that when cockles were present at or close to the edge of the cores, the sediment surface would often crack and the cores would be discarded for erosion experiment (Andersen et al. in review).

2.3.8. Statistical analysis

Pearson product moment correlation was used to investigate the correlation between the various parameters. One-way ANOVA ($\alpha = 0.05$) was used to test differences in critical erosion shear stress and erosion rate between stations for each sampling period in 2002 (spatial differences) and between sampling dates (i.e. between June and September 2002) for each station (temporal differences). Prior to analysis, log (n+1)-transformations were made to satisfy the assumptions of normality and homoscedasticity (Fowler and Cohen 1997). A LSD (least significance difference) multiple comparison test was used to locate any spatial differences identified by ANOVA ($\alpha = 0.05$). The significance of the difference in mean values between crests and troughs of the bedforms were statistically examined using the *t*-test.

Stepwise multiple linear regression (SMR) models were constructed to examine sediment physical and biological parameters apparently correlating with critical erosion shear stress, and possibly regulating it. The models had

critical erosion shear stress as dependent variable, and mud content, normalized water content, chlorophyll-a, EPS, and the density of dominant macrofauna species as possible independent variables which might correlate with the dependent variable (Kocum et al. 2002).

The statistical analysis focused on determining the relative effects of major physical and biological variables on critical erosion shear stress data. In order to achieve this, the stepwise multiple regression function of the Statistical Package for Social Sciences (SPSS) computer program (SPSS Inc., USA) was used. This enabled construction of models to determine which combination of variables could best explain the most variation in critical erosion shear stress. The minimum probability of *F* (p_{in}) for a variable to enter the equation was set at 0.05 and probability of *F* to remove a variable (p_{out}) from the equation was set at 0.1. Prior to analysis, log (n +1)-transformations were made to satisfy the assumptions of normality distribution of the variable. Based on these criteria, stepwise multiple regression was used to develop the models, using the given set of initial variables, and to determine which variables were significantly correlated with the critical erosion shear stress.

2.3.9. Sources of error

- Tolhurst et al. (2000b) noted that critical erosion shear stresses may changes during transport from the field to the laboratory and resting of the excavated cores. However, Comparison of the *in situ* with the laboratory measurement shows that the critical erosion shear stress derived from lab EROMES fall about the values derived from *in situ* portable EROMES of comparable chlorophyll-a concentration (Figure 2.11). This suggests that the physical and biological properties and hence the strength of the sediment were negligible changed during transport, handling and storing (resting) under laboratory condition.
- Wet bulk density, water content, organic content, grain size distribution, chlorophyll-a, colloidal carbohydrate, and EPS values were determined from the samples obtained outside (direct neighborhood) of the each erosion core. It was impossible to measure the properties of the same sediment used for the erosion measurement without disturbing the sample, and the resulting spatial heterogeneity could decrease

correlation between critical erosion shear stress and measured physical and biological sediment surface parameters. The errors due to the difference in properties of sediment taken inside and outside of the erosion core have not been quantified.

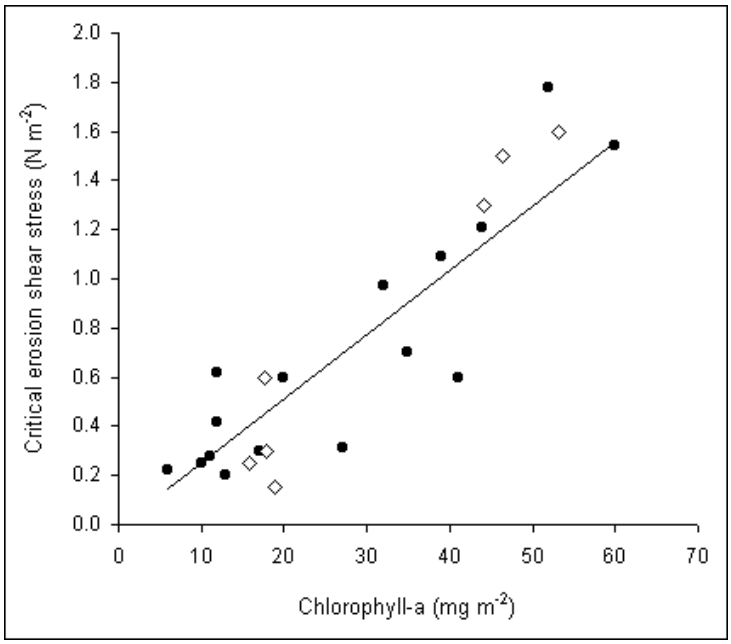

Figure 2.11. A plot of the chlorophyll-a concentration versus the critical erosion shear stress. Filled circles: EROMES *in situ*; diamonds: EROMES in the laboratory.

- Small-scale patchiness of biofilm, cracks and holes inside the erosion core might change the stability of surface sediment as erosions usually start from the cracks and holes. The magnitude of the errors due to the patchiness of biofilm, cracks, and holes are difficult to quantify.
- Errors in the determination of water content due to evaporation of the samples occurred during the weighing procedure (K. Wirth, personal communication). The decrease water content due to evaporation was estimated to be 0.002 %. This decrease is very small and hence negligible.
- The determination of wet bulk density is very sensitive to the homogenization during the filling procedure and it is important to ensure that the plastic container is completely filled.
- Scraping: 1 mm thickness is only by estimation. Increase or decrease of the vertical resolution of the scrapping method might change the

strength of the relationship between critical erosion shear stress and chlorophyll-a and carbohydrate concentration. Errors in the thickness could have been as much as ± 1 mm (i.e. the thickness of the spatula used to take the scrape samples).

- Grain-size analysis comparison for selected samples revealed that values derived from laser particle size analyzer (Galai CIS) agree reasonably well with those derived from sieving method: the difference for fraction <63 μm was found to be less than 6 %.
- Homogenization of the sub-samples. The errors due to homogenization process are examined by plotting wet bulk density against water content. As shown in Figure 2.12, the correlation between wet bulk density and water content is very good (r = 0.97) and it agrees reasonably well with the theoretical curve of the relationship between wet bulk density and water content for quarzt sand with density of 2.65 g cm^{-3}. This suggests that the errors due to homogenization were very small.

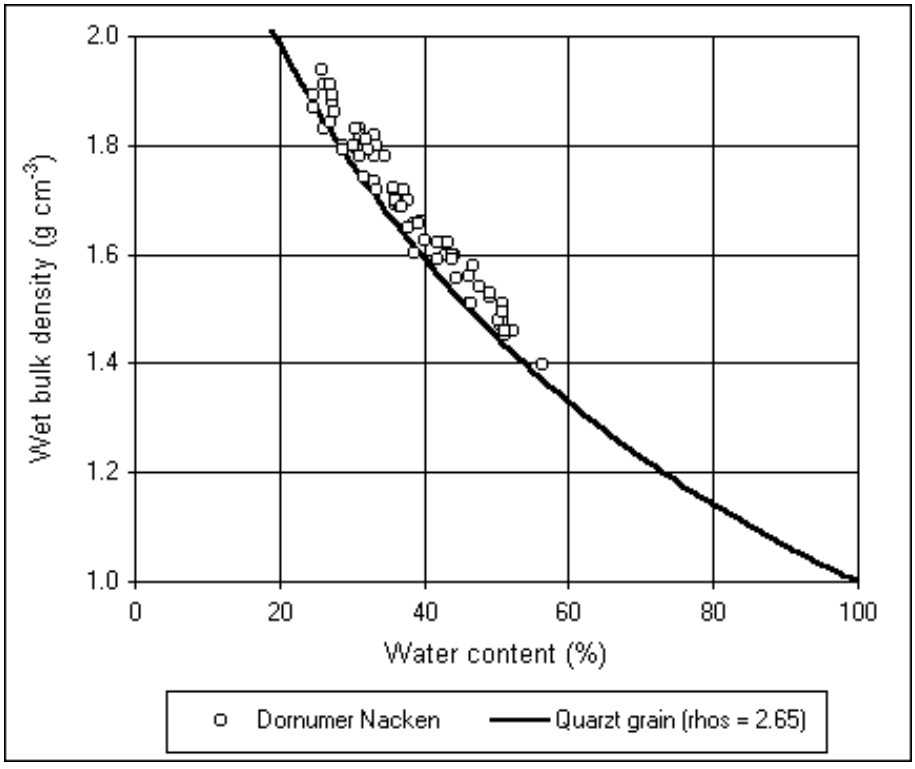

Figure 2.12. A plot of the wet bulk density versus water content present in the upper 1 mm sediment surface.

- The errors in determination of chlorophyll-a using HPLC may arise during extraction, injection to HPLC, analysis and interpretation of the peak area from HPLC chromatogram. The magnitude of the errors is estimated to be ± 5 % (K. Heymann, personal communication).

CHAPTER 3

GENERAL FEATURES OF THE DATA

The purposes of this chapter are:

- to present an overview of the data
- to show the general relationships between the different parameters, e.g. which ones are so close related that only the one which is considered as functionally more important will be considered further (e.g. EPS and colloidal carbohydrate, Water content and wet bulk density, mud content and water content and organic content).
- to describe evident structures (e.g. site specific dependencies) which will be discussed in more detail in the following chapters.
- to get an idea of the main processes
- to formulate hypotheses which will be considered further in the following chapters.

3.1. Sediment surface parameters

The mean values with standard errors of wet bulk density, water content, normalized water content, mud content, median grain-size, organic content, chlorophyll-a, colloidal carbohydrate, EPS concentration, critical erosion shear stresses and EROMES erosion rates are listed in Table 3.1. This table gives a general overview of data collected in June and September 2002 where all stations were sampled in a comparable way. The corresponding data for Stations B, C, E, and F in 2001 are listed in Appendix 1. The data presented in table 3.1 will be discussed in detail in chapter 5.

To show the relationships between the different parameters, data from 2001 and 2002 were considered together since no temporal differences in the relationships could be detected. The relationship between mud content and water content, chlorophyll-a and EPS concentration are shown in Figure 3.1. In general, the water content increased with increasing the mud content (Figure 3.1a) as discussed already in chapter 2 (section 2.3.4). However, no clear relationship between the mud content and the chlorophyll-a and EPS concentration was observed.

Table 3.1. Critical erosion shear stress, erosion rate and determined physical and biological properties of surface sediment at stations A – F in June (J) and September (S) 2002 (mean ± S.E, n = 4–14).

	Date	StationA	Station B	Station C	Station D	Station E	Station F
Critical shear stress (N m^{-2})	J	1.10 ± 0.46	0.58 ± 0.05	0.52 ± 0.12	0.36 ± 0.09	0.54 ± 0.09	1.16 ± 0.19
	S	1.53 ± 0.39	0.60 ± 0.04	1.54 ± 0.27	1.04 ± 0.12	1.34 ± 0.37	2.39 ± 0.28
Erosion rate (g m^{-2} s^{-1})	J	0.24 ± 0.12	1.73 ± 0.29	0.69 ± 0.09	0.50 ± 0.11	1.58 ± 0.63	0.15 ± 0.04
	S	0.07 ± 0.04	1.42 ± 0.80	0.04 ± 0.03	0.59 ± 0.31	0.88 ± 0.62	0.01 ± 0.01
Wet bulk density (g cm^{-3})	J	1.63 ± 0.01	1.76 ± 0.04	1.85 ± 0.02	1.69 ± 0.01	1.83 ± 0.01	1.65 ± 0.04
	S	1.65 ± 0.04	1.71 ± 0.01	1.63 ± 0.01	1.55 ± 0.04	1.61 ± 0.06	1.50 ± 0.04
Water content (%)	J	42 ± 1.1	34 ± 1.5	27 ± 0.9	37 ± 0.5	28 ± 0.7	40 ± 2.0
	S	40 ± 2.7	36 ± 0.2	39 ± 0.0	46 ± 2.6	42 ± 5.1	50 ± 2.7
Normalized Water content (%)	J	81 ± 2	98 ± 3	83 ± 2	86 ± 3	93 ± 2	98 ± 4
	S	80 ± 2	102 ± 2	104 ± 1	108 ± 4	120 ± 3	122 ± 5
Mud content (%)	J	60 ± 1	23 ± 1	19 ± 1	42 ± 3	15 ± 1	38 ± 6
	S	55 ± 4	26 ± 2	29 ± 1	40 ± 3	25 ± 7	37 ± 3
Median grain-size (μm)	J	50 ± 1	101 ± 1	118 ± 2	80 ± 5	128 ± 2	104 ± 12
	S	58 ± 7	97 ± 2	97 ± 1	81 ± 3	113 ± 10	98 ± 6
Organic content (%)	J	3.4 ± 0.2	2.4 ± 0.1	2.2 ± 0.1	3.0 ± 0.1	2.0 ± 0.1	4.3 ± 0.6
	S	5.5 ± 0.6	3.6 ± 0.1	4.6 ± 0.1	5.1 ± 0.5	4.6 ± 0.9	6.2 ± 0.4
Chlorophyll-a (mg m^{-2})	J	39 ± 6	48 ± 7	83 ± 8	14 ± 1	50 ± 6	93 ± 4
	S	57 ± 2	48 ± 2	160 ± 18	41 ± 4	72 ± 6	91 ± 2
Colloidal carbohydrate (mg m^{-2})	J	878 ± 188	836 ± 0	1600 ± 25	173 ± 42	928 ± 161	1557 ± 164
	S	1424 ± 320	1835 ± 115	3505 ± 525	1016 ± 182	2475 ± 105	3102 ± 556
EPS (mg m^{-2})	J	163 ± 45	144 ± 0	217 ± 15	27 ± 7	113 ± 23	318 ± 41
	S	363 ± 77	352 ± 32	982 ± 205	204 ± 30	784 ± 111	877 ± 164

Figure 3.2 shows the relationship between EPS concentration and chlorophyll-a concentration and normalized water content. EPS generally increased with increasing chlorophyll-a but the relationships between these two parameters were not strong except at stations C and D. No correlation at all between EPS and chlorophyll-a was observed at station B. These results suggest that the variation of EPS was not solely controlled by the abundance of microphytobenthos (measured as chlorophyll-a concentration). EPS increased with decreasing normalized water content at station A. An opposite trend was observed at station E. No clear relationship between EPS and water content was observed at other stations.

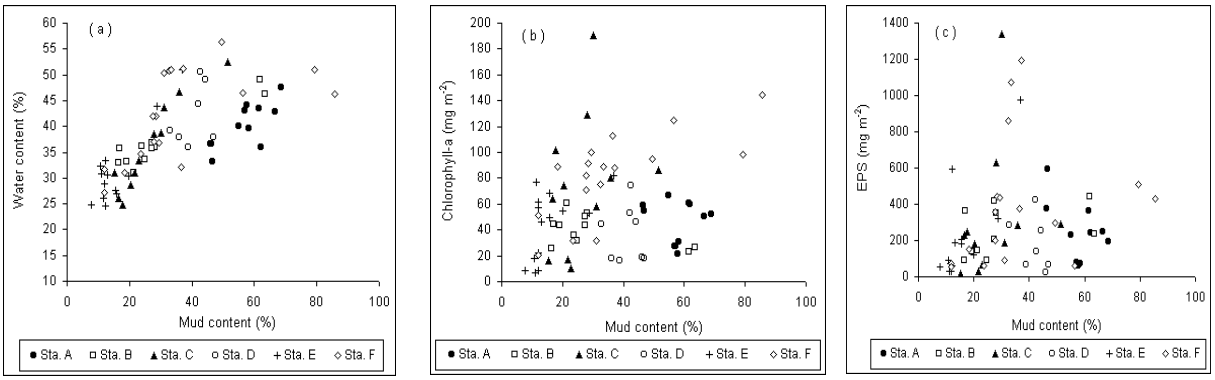

Figure 3.1. Scatter plots of mud content versus (a) water content, (b) chlorophyll-a, and (c) EPS present in the upper 1 mm sediment surface.

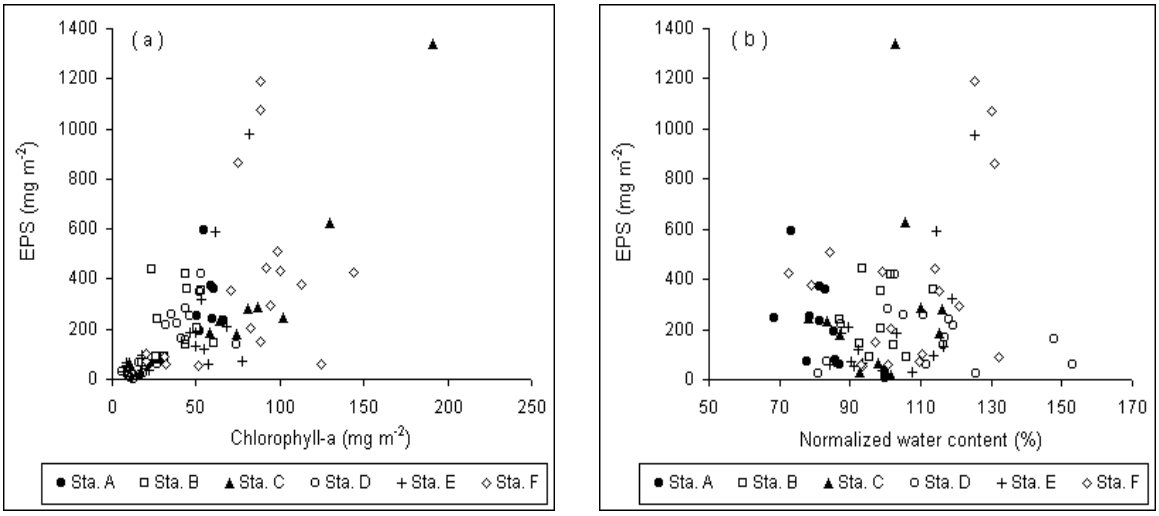

Figure 3.2. Scatter plots of EPS versus (a) chlorophyll-a and (b) normalized water content present in the upper 1 mm sediment surface.

As parameters such as wet bulk density, water content, median grain size, and mud content was highly correlated (see Appendix 3), only one of them which considered as functionally more important will be considered further. In this case only mud content will be considered further. Similarly, colloidal carbohydrate and EPS was highly correlated and only EPS will be considered further due to EPS has been regarded as a functionally closer proxy to biofilm stability (Paterson 1994).

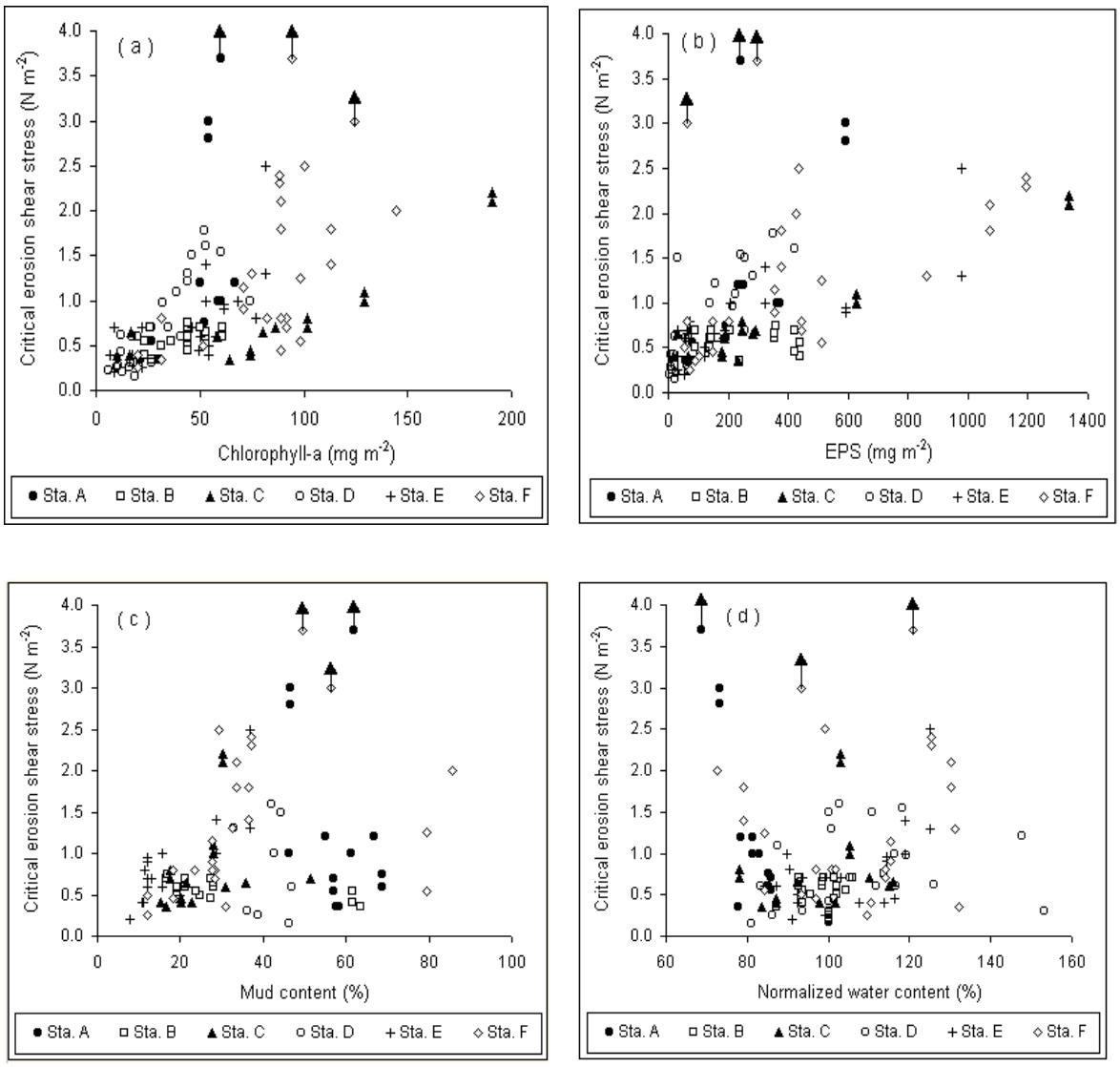

Figure 3.3. Scatter plots of critical erosion shear stress versus (a) chlorophyll-a, (b) EPS, (c) mud content, and (d) normalized water content present in the upper 1 mm sediment surface. The data with arrows were omitted in the linear regression analysis because the upper limit of the erosion device was reached.

The relationships between critical erosion shear stress and chlorophyll-a, EPS concentration, mud content and normalized water content are shown in Figure 3.3. The critical erosion shear stress generally increased with increasing chlorophyll-a and EPS concentration but the slopes of the increase differed from station to station. Critical erosion shear stress seems to be uncorrelated with the mud content. Critical erosion shear stress increased with decreasing normalized water content at station A. This relationship was unique to station A. The relationships between critical erosion shear stress and normalized water content were not clear at other stations (Figure 3.3d).

The relationships between the station mean erosion rate and critical erosion shear stress are shown in Figure 3.4. Erosion rate decreased with increasing critical erosion shear stress both in June and September 2002. The observed negative correlation between erosion rate and critical erosion shear stress is obviously due to the fact that as the surface of the sediment becomes more resistant to erosion, the erosion also is influenced.

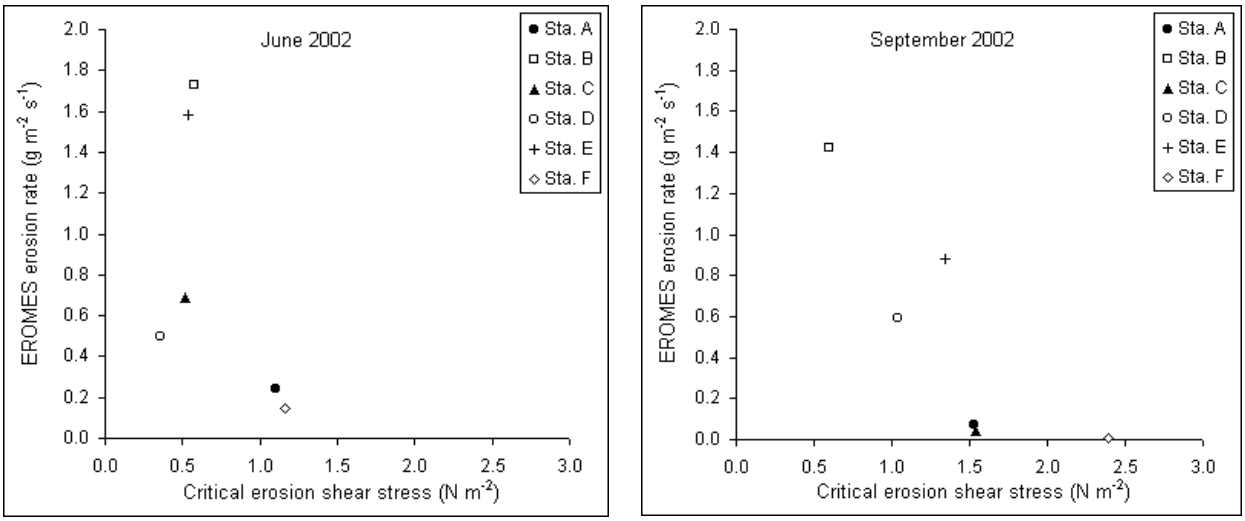

Figure 3.4. Scatter plots of the station mean erosion rate versus critical erosion shear stress in June and September 2002.

Figure 3.5 shows the relationships between erosion rate and chlorophyll-a, EPS concentration, mud content and normalized water content. In general, the erosion rates seem to be uncorrelated with chlorophyll-a, EPS concentration, mud content and normalized water content. The observed low values at high chlorophyll-a, EPS concentration, and mud content are simply due to the station specific behavior.

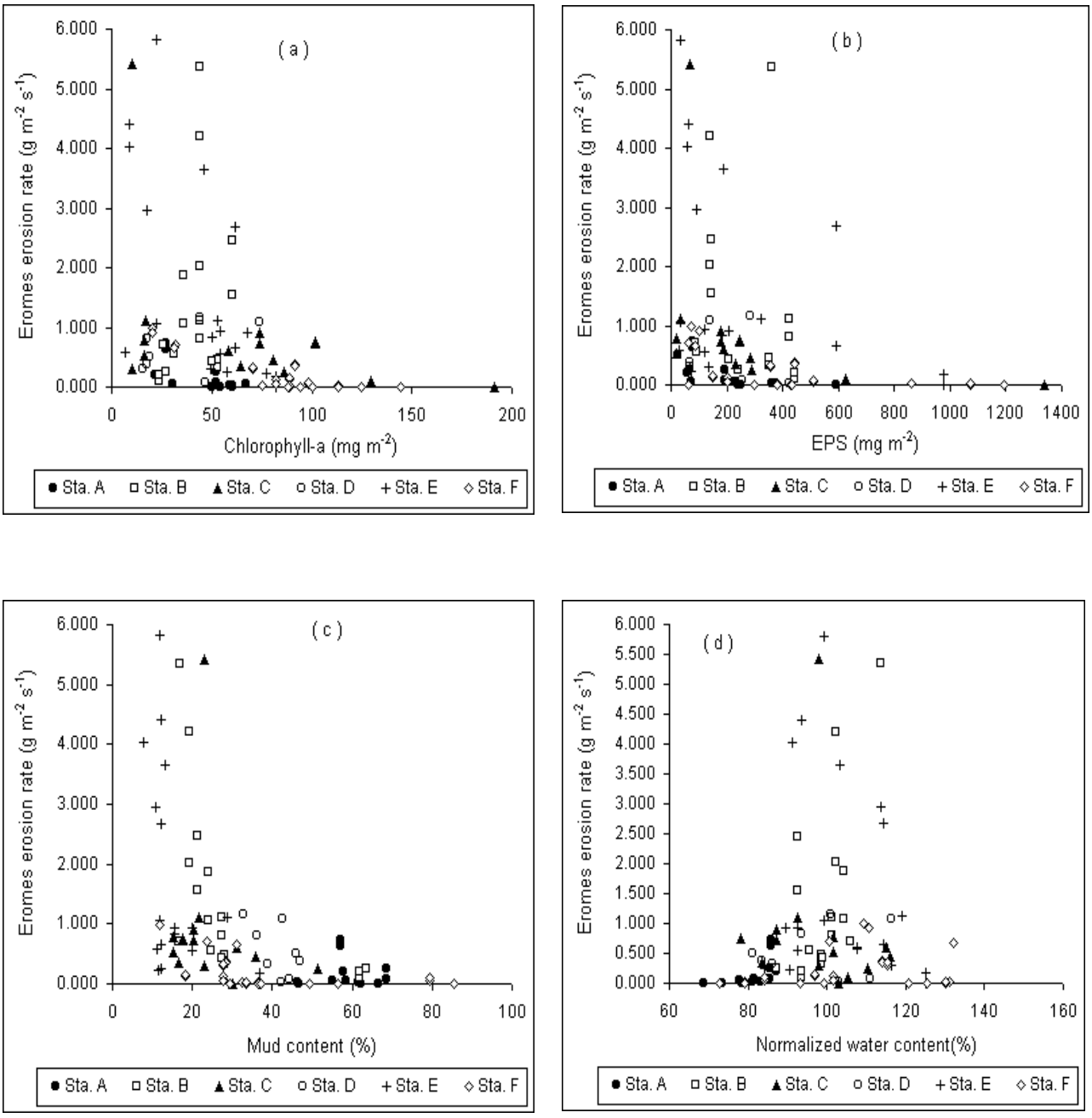

Figure 3.5. Scatter plots of erosion rate versus (a) chlorophyll-a, (b) EPS, (c) mud content, and (d) normalized water content present in the upper 1 mm sediment surface.

3.2. Comparison between surface (1 mm) and depth integrated (0–5 cm) sample

The relationship between mud content and water content for sediment taken at the upper most layer (1 mm) and subsurface layer (0–5 cm) are shown in Figure 3.6. With comparable amount of mud content, the water

contents of subsurface sediment were lower than those at upper 1 mm layer suggesting that subsurface sediments were more consolidated. It should be noted that the scatter of the surface (upper 1 mm) data was due to the specific of the different stations. The scatter was comparably low for the subsurface data (upper 0–5 cm). The upper 0–5 cm points with very high mud content stem from the station A. These points did not show increase of water content with mud content due to the effect of drying at station A.

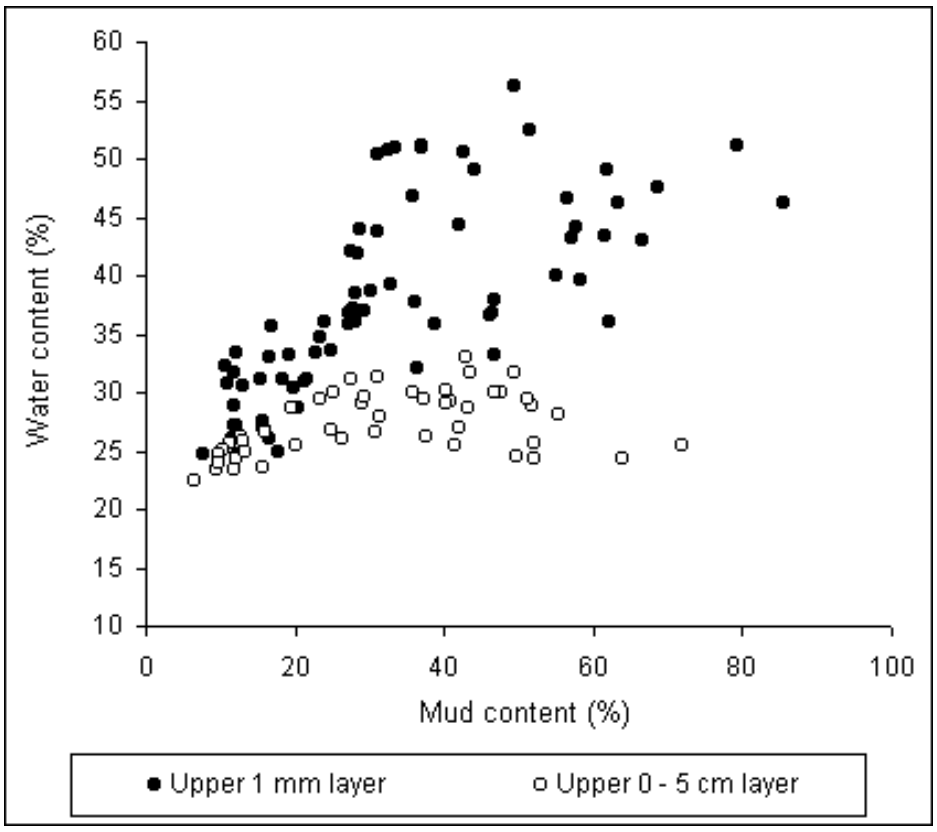

Figure 3.6. Comparison of the relationship mud content/water content between upper 1 mm and 0–5 cm sediment surface.

3.3. Microphytobenthos assemblages

About 42 species of microphytobenthos were identified but eight epipelic benthic diatom species dominated all samples: *Cylindrotheca gracilis*, *Navicula A*, *Navicula B*, *Nitzschia A*, *Nitzschia closterium*, *Melosira westii*, *Cymatosira belgica*, and *Gyrosigma fasciola*. The dominant microphyto-benthos species at each station during the study is given in Table 3.2.

Table 3.2. The dominant microphytobenthos species at stations A–F in 2001 and 2002.

Station A	Station B	Station C
– *Cylindrotheca gracilis* – *Navicula B* – *Nitzschia closterium*	– *Navicula B* – *Nitzschia closterium* – *Melosira westii*	– *Nitzschia A* – *Merismopedia A* – *Merismopedia B*
Station D	**Station E**	**Station F**
– *Nitzschia closterium* – *Navicula B*	– *Cymatosira belgica* – *Amphora A* – *Navicula A*	– *Gyrosigma fasciola* – *Navicula A* – *Merismopedia A*

3.4. Benthic macrofauna

The density of dominant macrofauna species in the erosion cores at each station during 2002 is given in Table 3.3. The result of benthic macrofauna analysis in 2001 is given in Appendix 2. The dominant species can be divided into four functional groups, i.e. subsurface bivalves (*Macoma baltica*, *Cerastoderma edule*), epibenthic gastropods (*Hydrobia ulvae*), tube building worms (*Capitella capitata, Heteromastus filiformis, Lanice conchilega, Pygospio elegans*, and *Tubificoides benedeni*), and subsurface vagile sediment dwellers (*Eteone longa*, *Hediste diversicolor,* and *Tharyx killariensis*).

Hydrobia ulvae has been shown to destabilize surface sediments through their grazing and tracking activities and fecal pellet production (Blanchard et al. 1997, Andersen 2001b). The impact of *Macoma baltica* on sediment erodibility was primarily due to bioturbation and feeding on the surface sediment, which loosened the surface and increase surface roughness (Widdows et al. 1998c). Tube building worms may stabilize sediment by binding particles with secretions used to construct their tube (Yingst and Rhoads 1978).

Table 3.3. The average density (individual m^{-2}) of dominant macrofauna species in June (J) and September (S) 2002 at the study site. (□) highest density of species on stations A– F].

Species	Date	Station A	Station B	Station C	Station D	Station E	Station F
Capitella capitata	J	3094	0	306	45	57	343
	S	5393	0	191	9	0	85
Cerastoderma edule	J	0	510	0	45	0	157
	S	0	340	0	146	0	0
Eteone longa	J	91	0	0	55	0	0
	S	403	191	0	45	0	0
Hediste diversicolor	J	637	0	0	1447	0	1107
	S	1274	0	0	1037	0	0
Heteromastus filiformis	J	146	0	866	2511	85	813
	S	2293	255	1433	4140	96	1040
Hydrobia ulvae	J	1674	13,854	0	0	0	0
	S	828	24, 862	0	0	0	0
Lanice conchilega	J	0	0	0	355	0	3224
	S	0	0	0	200	0	0
Macoma baltica	J	3840	828	917	1729	934	1489
	S	6285	1104	64	182	64	212
Pygospio elegans	J	5514	64	0	373	170	255
	S	2887	786	96	136	0	255
Tharyx killariensis	J	0	318	382	519	1401	1813
	S	0	701	350	646	159	106
Tubificoides benedeni	J	3258	414	764	1647	170	2793
	S	8981	1486	478	864	64	658

In 2002, the tube building worms *Heteromastus filiformis, Pygospio elegans,* and *Tubificoides benedeni*, and bivalve *Macoma baltica* occurred commonly over the entire sampling stations and represented a major part of

the total number of macrofauna. Other species such as *Hydrobia ulvae* was present only at station A and B and absent at other stations. *Hydrobia ulvae* and *Macoma baltica* observed at station A were probably imported from the outer nearby areas (e.g. station B) during the spring tide floods. *Lanice conchilega* was only present at stations D and F and absent at other stations. *Cerastoderma edule* was abundant at station B and D both in June and September.

The mean density of *Cerastoderma edule* was higher in June than in September 2002 at station B. An opposite trend was observed at station D. The mean densities of *Heteromastus filiformis* were higher in September than in June 2002 at all stations. In contrast, the densities of *Macoma baltica* were lower in September than in June 2002 at all stations except stations A and B. *Hydrobia ulvae* was more abundant in September than in June 2002 at station B but opposite trend was observed at station A (Table 3.3).

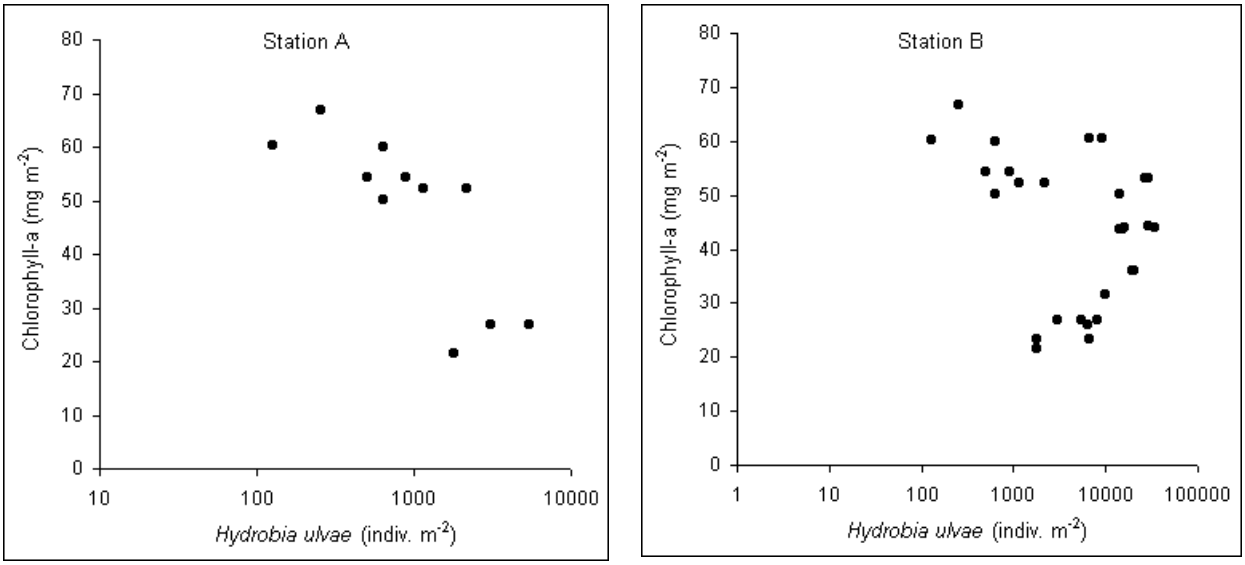

Figure 3.7. Scatter plots of *Hydrobia ullvae* density versus chlorophyll-a concentration at stations A and B.

The relationships between *Hydrobia ulvae* density and chlorophyll-a concentration at stations A and B are shown in Figure 3.7. The chlorophyll-a concentration decreased with increasing *Hydrobia ulvae* density at station A. This trend was not observed at station B. At this station, high values of chlorophyll-a were only found at low *Hydrobia ulvae* densities. By contrast, a broad range of chlorophyll-a values was observed at high *Hydrobia ulvae*

densities. There was no correlation between *Macoma baltica* density and chlorophyll-a concentration (Figure 3.8).

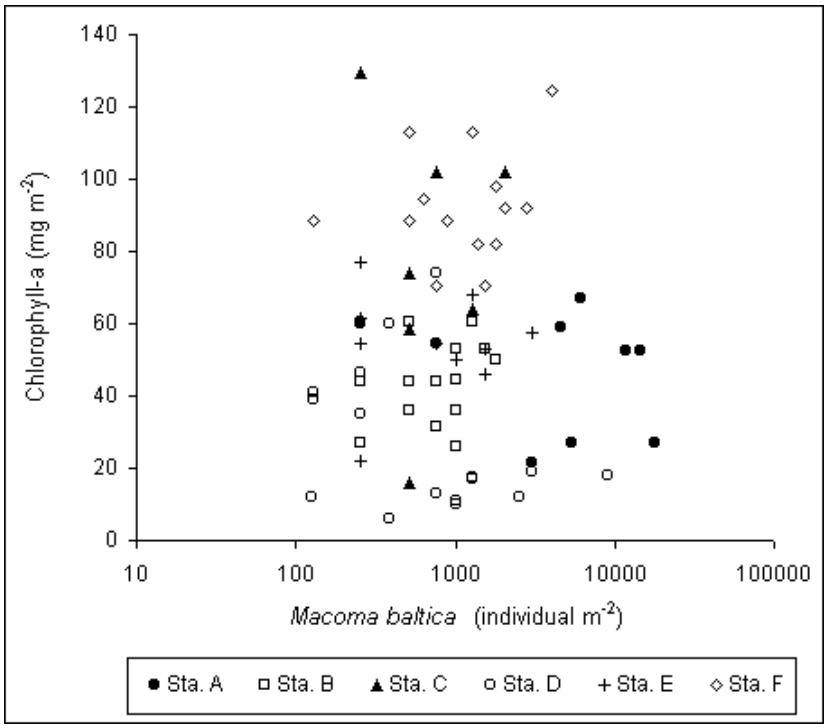

Figure 3.8. Scatter plots of *Macoma baltica* density versus chlorophyll-a concentration at the study site.

3.5. Comparison with abiotic sediment erosion

The measured critical erosion shear stresses can be compared to the critical erosion shear stress of abiotic non-cohesive sediment, which can be determined from knowledge of grain density and size and the fluid properties by using one of the version of the Shields parameters. Here, the threshold Shields parameter for cohesionless grains θ_{cr} was calculated using a formula proposed by Soulsby and Whitehouse (1997):

$$\theta_{cr} = \frac{0.30}{1+1.2D_*} + 0.055\left[1 - \exp\left(-0.020D_*\right)\right]$$

with dimensionless grain-size, $D_* = \left[\frac{g\,(s-1)}{\nu^2}\right]^{1/3} d$

With the Shields parameter the abiotic non-cohesive sediment critical erosion shear stress ($\tau_{cr\text{-}Shields}$) can be calculated as follows:

$$\tau_{cr-Shields} = \theta_{cr} \left[(\rho_s - \rho)\, g\, d \right]$$

where ρ and ρ_s are fluid and sediment density, respectively, $s = \rho_s / \rho$, g is acceleration due to gravity, d is grain diameter, and ν is kinematic viscosity of water. For this purpose, ρ_s was taken as 2650 kg m^{-3}, ρ as 1027 kg m^{-3}, g as 9.81 m s^{-2} and ν as 1.36 x 10^{-6} $m^2 s^{-1}$.

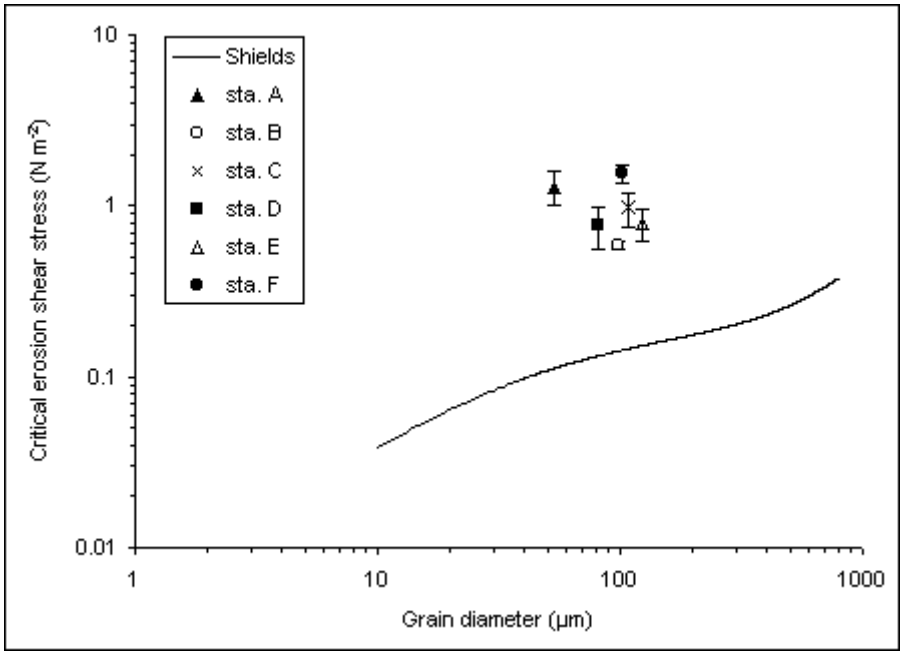

Figure 3.9. Measured critical erosion shear stress in 2002 (mean ± SE) and compared to $\tau_{cr-Shields}$ of quartz grain in seawater of 10 °C and salinity 35 °/oo (Soulsby and Whitehouse 1997).

As shown in Figure 3.9, critical erosion shear stresses at all stations fall above Shields predicted values and the divergence can not solely be attributed to difference in erosion threshold criteria. The discrepancy between the measured critical erosion shear stress and abiotic non-cohesive sediment values is most likely caused by the existence of benthic diatoms. Even in the sand flat with lack of visible diatom biofilm, Lelieveld et al. (2003) still found an increase of sediment critical shear stress relative to abiotic sediment by up to factor of 14, highlighting that visible diatom biofilms are not a prerequisite for measurable sediment stabilization. In this case the stabilization is most likely due to gluing by sessile diatoms which do not form a bioflim.

The differences in critical erosion shear stress between natural sediment and abiotic sediment may be also caused by the effect of cohesiveness associated with natural sediments, which will increase the critical shear stress. As suggested by Mitchener and Torfs (1996), the mode of erosion changes from cohesionless to cohesive behaviour at low mud contents (< 62.5 μm) added to sand, with a transition occurring in the region 3 % to 15 % mud by weight. The mud content of sediment at all stations were above the transition region of 3–15 % suggested by Mitchener and Torfs (1996) to impart cohesive properties on sediment.

Differences in critical erosion shear stress between natural and abiotic sediments have been often expressed in terms of a biostabilization index, $S_B = [\tau_{cr}(measured) / \tau_{cr}(Shields)]$ (e.g. Manzenrieder 1983). This index (S_B) represents the discrepancy in critical erosion shear stress relative to abiotic value and provides a platform for analyzing the biological effects. The denominator in the formula to calculate S_B need not necessarily be the Shields critical shear stress, and some workers use wintertime (i.e. minimum biological influence) values (Grant et al. 1982) or laboratory determined values on sterilized sediment (Grant and Gust 1987). Here, the biostabilization index S_B, was calculated from the ratio of mean critical erosion shear stress at each station ($\tau_{cr\ measured}$) during 2002 to critical shear stress for cohesionless grain ($\tau_{cr\ Shields}$) or Shields predicted values presented in Figure 3.9. The way to calculate the biostabilization index S_B, is similar to that of Friend et al. (2003b). Noted that Shields curve presented in Figure 3.9 was used to calibrate the EROMES.

The highest S_B was 11.6 at station A, whereas the lowest index of 4.2 occurred at station B. A comparison of these biostabilisation indices with indices from other studies is somewhat difficult due to the different methods to calculate the biostabilisation indices. For example, Yallop et al. (1994) reported a biostabilization index of 2.9 for intertidal mudflat sediment at Portishead in the Severn Estuary, UK. These authors calculated the biostabilization index from the ratio of sediment with visible biofilm to sediment with non-biofilm. The value derived from such method is likely to be an underestimate because although biofilm formation was not apparent this does not suggest a lack of biotic activity (Yallop et al. 1994).

3.6. Conclusions

- The mud content was strongly correlated with the water content, which water content increased with increasing mud content. However, the mud content seems to be uncorrelated with either the chlorophyll-a or EPS concentration.
- The EPS concentration was strongly correlated with the chlorophyll-a concentration at stations C and D but in most cases the relationships between these parameters were weak.
- The critical erosion shear stress generally increased with increasing chlorophyll-a and EPS concentration but the slopes of the increase differed from station to station.
- The increase in critical erosion shear stress with decreasing normalized water content was unique to station A. In most cases no correlation between these parameters was observed.
- The erosion rate generally decreased with increasing critical erosion shear stress. The erosion rate seems to be uncorrelated with the chlorophyll-a, EPS, mud content, and normalized water content.
- Sediments taken at subsurface layer (0–5 cm) were more consolidated compared to those taken at upper 1 mm layer. This was reflected by the lower increase of water content with mud content for sediment taken at 0–5cm layer.
- The microphytobenthos at the study site was dominated by epipelic diatom.
- The dominant benthic macrofauna at the study site can be divided into four functional groups, i.e. subsurface bivalves, epibenthic gastropods, tube building worms, and subsurface vagile sediment dwellers.
- The measured critical erosion shear stresses fall above the abiotic sediment values, giving a biostabilization index of 4.2 to 11.6. Differences in critical erosion shear stress between natural and abiotic sediments are likely caused by the effect of biostabilization and by cohesive behaviour of natural sediments.

The formulated hypotheses below will be considered in the next chapters:

- Small-scale variations of critical erosion shear stress and erosion rate are influenced mainly by microphytobenthos (chapter 4).
- Small-scale variations of critical erosion shear stress and erosion rate are influenced directly or indirectly by benthic macrofauna (chapter 4).
- Physical processes of drying influences small-scale variations of critical erosion shear stress (chapter 4).
- Erosion characteristics and physical and biological properties of surface sediment are affected by the presence of geomorphological structures (bedforms) (chapter 4).
- There is a synergistic effect of physical processes (i.e. drying) and biological processes (i.e. biostabilization) on sediment surface stability (chapter 4).
- Spatial and temporal variation of critical erosion shear stress and erosion rate of surface sediment are controlled mainly by micro-phytobenthos (chapter 5).
- Spatial and temporal variation of critical erosion shear stress and erosion rate of surface sediment are influenced directly or indirectly by benthic macrofauna (chapter 5).
- Emersion period affects sediment surface erodibility (chapter 5).
- Mud content affects critical erosion shear stress and erosion rate of surface sediment (chapter 5).
- Critical erosion shear stress can be predicted satisfactory from chlorophyll-a concentration alone (chapter 6).
- Critical erosion shear stress can be predicted better by a combination of two or more potential proxies (chapter 6).

CHAPTER 4

SMALL-SCALE (WITHIN STATION) VARIATION OF SEDIMENT ERODIBILITY

4.1. Introduction

The physical and biological parameters that affect sediment erodibility (e.g. EPS production, drying, and macrofaunal grazing) can change significantly on spatial-scales of a few meters to a few kilometers. Therefore, small and large-scale variations in erodibility can be expected due to these changes. This chapter is set out to determine the small-scale variations of sediment erodibility within a 10-m radius of a permanent marker at each station. A better understanding of those and the processes that cause the variations is expected also to elucidate the large-scale variations of sediment erodibility at the study site.

We start with the microphytobenthos since this is the most obvious effect on sediment erodibility variations as shown in Chapter 3, then followed by the effects of benthic macrofauna, drying, and geomorphological structures. The effect of cockle *Cerastoderma edule* and polychaetes worm *Heteromastus filiformis* was studied in more detail because these two species are abundant benthic species at many tidal flats and no studies have specifically aimed at a determination of these species effect on sediment erodibility. This specific study was carried out at station D where *Cerastoderma edule* and *Heteromastus filiformis* were observed to be abundant during the period of this study.

In this study, data set from 2001 and 2002 are included since no temporal difference in the relationships of between parameters could be detected. Major questions addressed are: (1) Does small-scale variation of sediment erodibility mainly influenced by microphytobenthos? (2) Is sediment erodibility related to other sediment parameters such as mud content or normalized water content in the sediment? (3) Does benthic macrofauna have influential role on the small-scale variation of sediment erodibility? (4) Is there any synergistic effect of physical processes and biological processes on sediment stability? (5) Does the presence of geomorphlogical structures (bedforms) affect the sediment erodibility?

4.2. Results

The widest range of critical erosion shear stress for erosion was observed at station F with a range of 0.25–3.70 N m^{-2}, while the narrowest range of the values were measured at station B with a range of 0.35 – 0.75 N m^{-2}. The critical erosion shear stresses varied from 0.35 to 3.70, 0.35 to 2.20, 0.15 to 1.78, 0.20 to 2.50 N m^{-2} at station A, C, D, and E, respectively. The widest range of erosion rate was observed at station E with a range of 0 – 5.812 g m^{-2} s^{-1}. The narrowest rate was observed at station A with a range of 0 – 0 .736 g m^{-2} s^{-1}. A wide range of erosion rate was also observed at stations B (0.093–5.355 g m^{-2} s^{-1}) and C (0 – 5 .416 g m^{-2} s^{-1}). Similar to station A, the erosion rates did not vary much at stations D (0.033–1.161 g m^{-2} s^{-1}) and F (0 – 0 .993 g m^{-2} s^{-1}).

4.2.1. Effect of microphytobenthos

Critical erosion shear stress increased with increasing chlorophyll-a concentration at all stations (Figure 3.3a) and the relationships between these variables were significant at all stations except stations A and B (Appendix 4, 5 and 6). However, the strength of the relationships between critical erosion shear stress and chlorophyll-a differed from station to station. The correlations were high at stations C (r = 0.88), D (r = 0.83), and E (r = 0.65) but relatively low at stations A (r = 0.49), B (r = 0.51) and station F (r = 0.59). The slopes of the increase in critical erosion shear stress with increasing chlorophyll-a also differed from station to station. For example, the increase of critical erosion shear stress with chlorophyll-a was much steeper at station D compared to that at station C (see Figure 3.3a).

Critical erosion shear stress were also significantly correlated with colloidal carbohydrate and EPS concentrations at all stations except station B (Appendix 4, 5 and 6 and Figure 3.3b). Similar to chlorophyll-a, the correlation between critical erosion shear and colloidal carbohydrate and EPS was highly site specific. For example, the slope of the increase critical erosion shear stress with EPS was much higher at station D (0.0035) than at station C (0.0013).

A significant negative correlation was found between the erosion rate and chlorophyll-a at station E ($r = 0.54$, $P < 0.01$). At station F, the erosion rate was negatively correlated with chlorophyll-a ($r = 0.87$, $P < 0.01$), colloidal carbohydrate ($r = 0.64$, $P < 0.01$) and EPS ($r = 0.58$, $P < 0.01$, Appendix 6). No significant correlation between the erosion rate and either chlorophyll-a, colloidal carbohydrate or EPS was found at other stations.

4.2.2. Effect of benthic macrofauna

Hydrobia ulvae

The density of mud snails, *Hydrobia ulvae,* was positively correlated with erosion rate at station A ($r = 0.93$, $P < 0.01$; Figure 4.1). This means that a high erosion rate is related to a high density of *Hydrobia ulvae* and vice versa. It was expected that *Hydrobia ulvae* and *Cerastoderma edule* present with high densities at station B would have a direct significant effect on the variations of erodibility of surface sediment. However, no direct effects of these macrofauna on variations of either erosion shear stress or erosion rate were observed there. There was a negative correlation between chlorophyll-a and the density of *Hydrobia ulvae* at station A (Figure 3.7)

Macoma baltica

Specifically, there was no significant direct effect of bioturbator *Macoma baltica* on either critical erosion shear stress or erosion rate at any station. While a decrease in the chlorophyll-a concentration was observed with the density of *Hydrobia ulvae* at station A, there was no correlation between chlorophyll-a concentration and *Macoma baltica* density at any station (Figure 3.8). This was also true for all other macrofauna species listed in Table 3.3.

Patches of Mytilus edulis

Sediment parameter such as normalized water content and mud content varied considerably at station F. These large variations were attributed to the small-scale variability in the hydrodynamic conditions caused by the presence of blue mussel patches.

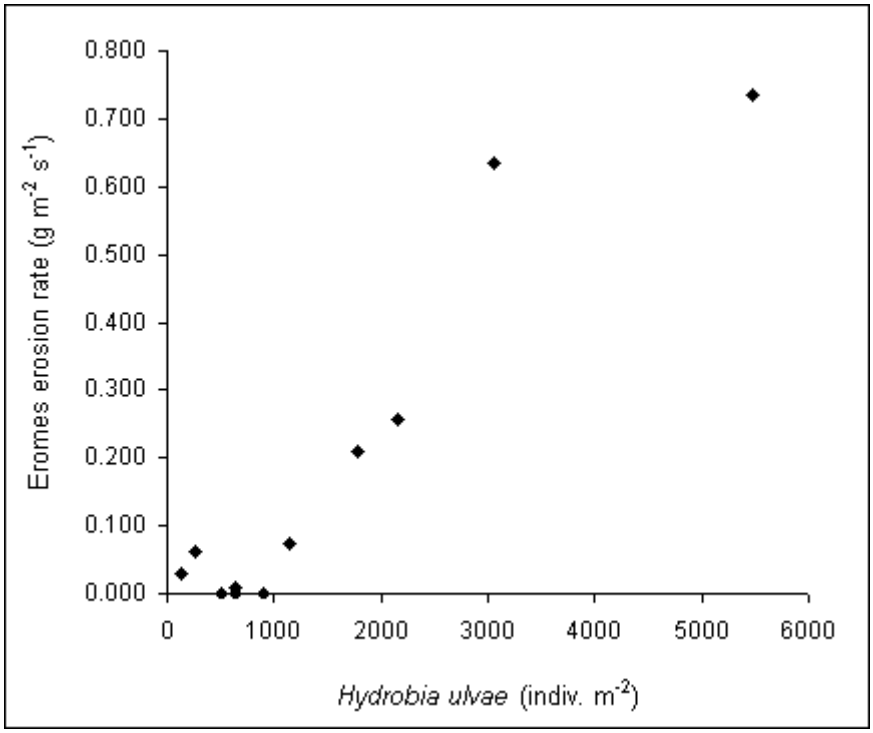

Figure 4.1. Scatter plot showing the relationship between erosion rate and density of *Hydrobia ulvae* at station A.

Cerastoderma edule and *Heteromastus filiformis*

The results show that there was no correlation between the critical erosion shear stress and the density of *Cerastoderma edule* and *Heteromastus filiformis* This was also true for the erosion rate. Fecal pellets from *Heteromastus filiformis* were observed in all samples with a content between 8 and 24 % by weight. Grain-size analyses carried out on disaggregated pellets from *Heteromastus filiformis* revealed that the texture of the pellets with a mud content of about 77 % was significantly finer than that of surface sediments (41 %). This fine-grained material is obviously picked up by the worm at depths of about 10 to 30 cm and the result is a pronounced decline in the mud content at this depth (Figure 4.2).

4.2.3. Effect of drying

The degree of drying was estimated by the computed normalised water contents. At all stations outside the saltmarsh, no correlation between normalized water content and erosion parameters was detected. Only at

station A, the erosion shear stress was negatively correlated with normalized water content of sediment ($r = 0.83$, $P < 0.01$, Figure 3.3d).

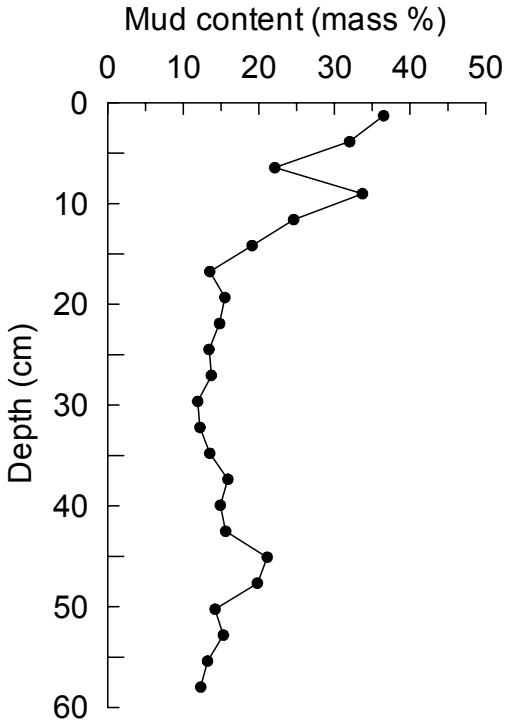

Figure 4.2. The vertical variation of the mud-content at station D. The decrease with depth is assigned to the conveyor-belt feeder *H. filiformis*.

4.2.4. Effect of geomorphological structures

To examine the effect of geomorphological structures (bedforms) on small-scale variation of sediment erodibility, the data was sorted into samples collected from the crests and troughs of the bedforms at each station. Here only data from 2002 was used. The critical erosion shear stresses and erosion rates at station D were determined by means of the portable EROMES, while at the other stations critical erosion shear stresses and erosion rates were determined by means of the Lab EROMES. It should be noted again that the erosion rates reported here are calculated as the average erosion rate for the bed shear stress increments from 0.5 to 1.0 N m^{-2} for station D and from 1.0 to 2 N m^{-2} for other stations. Results clearly indicate an effect of these geomorphological structures on the sediment erodibility.

Critical erosion shear stress and erosion rate

Sediments on the crests had generally higher critical erosion shear stresses and lower erosion rates than those in the troughs. The mean erosion shear stresses and erosion rates on the crests and in the troughs at each station are shown in Figure 4.3. The results of the statistical significance tests between crests and troughs for critical erosion shear stress, erosion rate and physical and biological sediment parameters are listed in Table 4.1.

Table 4.1. Level of significance of the difference between crests and troughs for critical erosion shear stress, erosion rate and physical and biological sediment parameters [ns: not significant (P > 0.05), based on t-test].

	Station A	Station B	Station C	Station D	Station E	Station F
Critical erosion stress	P < 0.05	ns	ns	ns	P < 0.05	ns
Erosion rate	P < 0.05	ns	ns	P < 0.05	P < 0.05	P < 0.05
Median grain-size	ns	ns	ns	ns	ns	P < 0.05
Mud content	ns	ns	ns	ns	ns	ns
Chlorophyll-a	P < 0.05	P < 0.05	ns	ns	P < 0.01	P < 0.01
Colloidal carbohydrate	P < 0.01	ns	ns	ns	P < 0.05	ns
EPS	P < 0.01	ns	ns	ns	P < 0.05	ns
Wet bulk density	P < 0.01	ns	ns	ns	ns	ns
Norm. Water content	P < 0.05	ns	ns	ns	ns	ns
Organic content	ns	ns	ns	ns	ns	ns

Crests had significantly higher critical erosion shear stresses than troughs at station A (P < 0.05) and station E (P < 0.05), but not at stations B, C, D and F. Differences were also observed in the erosion profiles of the crests and troughs, with crests tending to have shallower erosion profiles at all stations. Note that only selected stations where crests and troughs showed quite

pronounced difference in erosion profile are shown (Figure 4.4). Erosion rates were significantly lower on the crests than in the troughs at station A ($P < 0.05$), D ($P < 0.05$), E ($P < 0.05$), and F ($P < 0.01$), but no significant difference was observed at station B and C, although erosion rates were lower on the crests than in the corresponding troughs.

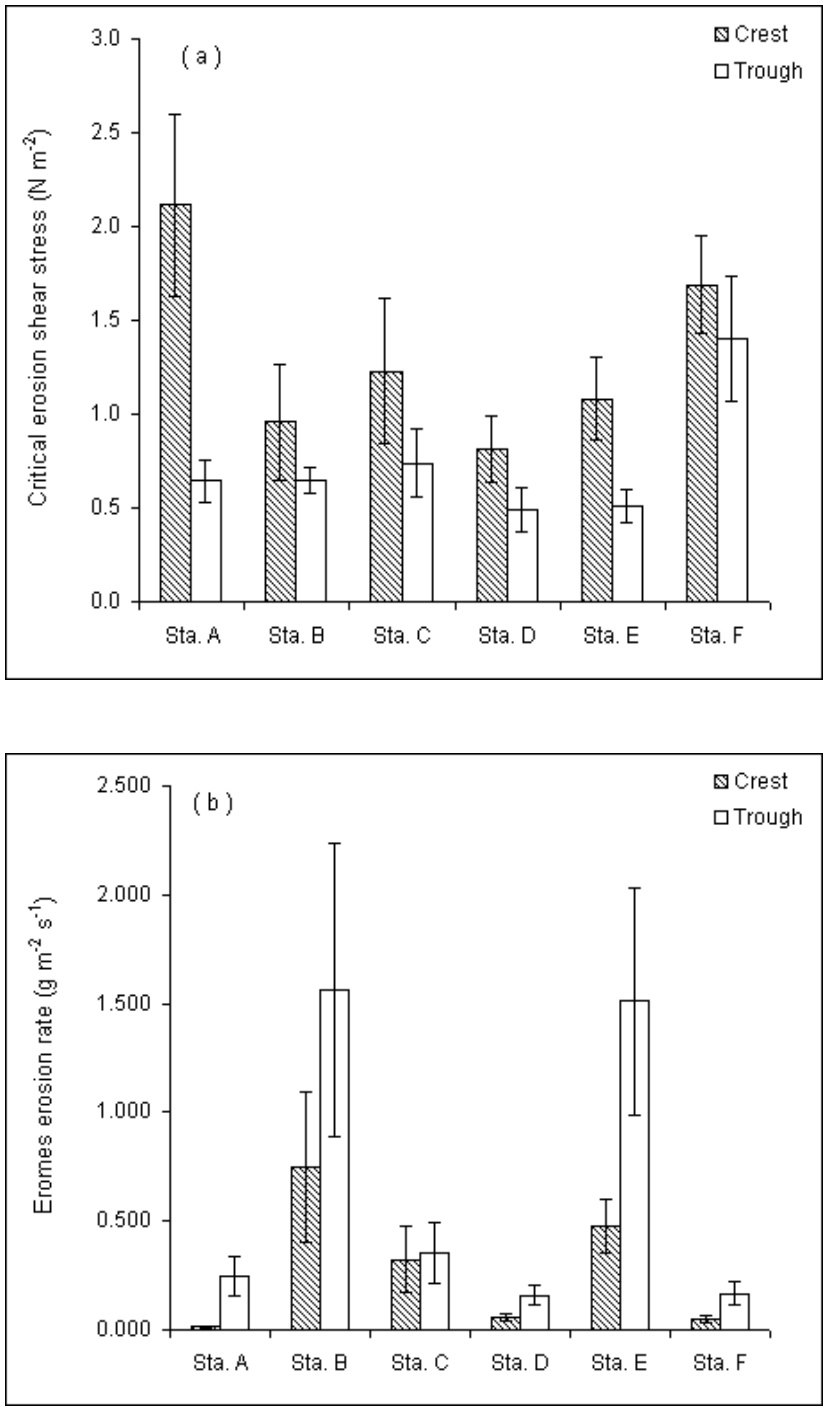

Figure 4.3. (a) Critical erosion shear stress and (b) erosion rate on the crests and in troughs at each station (mean ± S.E, n = 4–11).

Chlorophyll-a, colloidal carbohydrate, and EPS

Figure 4.5 shows the mean chlorophyll-a and EPS concentrations on the crests and in the troughs at the stations. Crests contained significantly higher chlorophyll-a than troughs at station A ($P < 0.05$), B ($P < 0.05$), E ($P < 0.01$) and station F ($P < 0.01$). There was no significant difference in chlorophyll-a concentration between crests and troughs at station C and D, although the concentrations were higher on the crests than in the troughs.

Crests had significantly higher colloidal carbohydrate contents than troughs at station A ($P < 0.01$) and E ($P < 0.05$) but the content was not significantly different at station C, D and F. Colloidal carbohydrate was slightly higher on the troughs than crests at station B but the difference was not significant. Similarly, EPS concentrations were significantly higher on the crests than in the troughs at station A ($P < 0.01$) and E ($P < 0.05$) but not significantly different at station B, C and F.

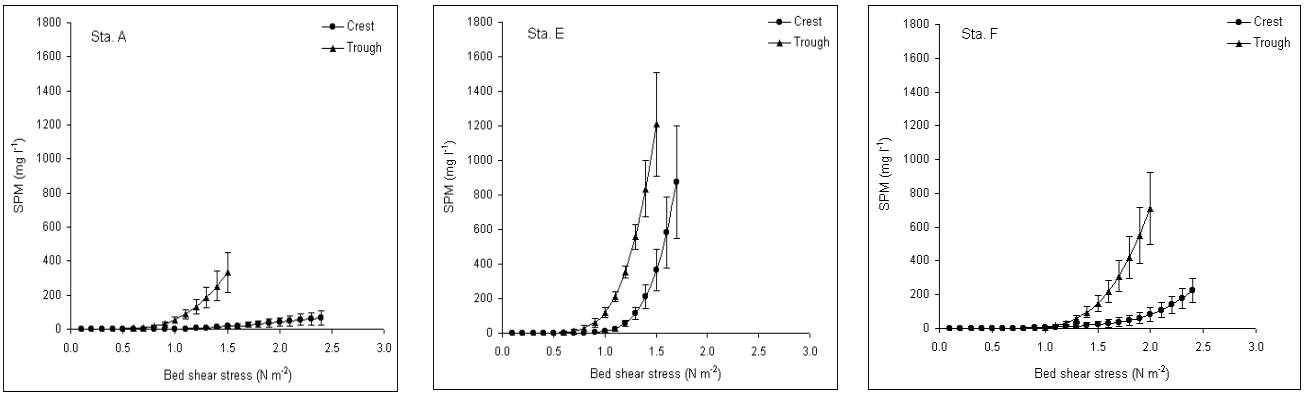

Figure 4.4. The average erosion profiles derived by EROMES erosion analysis of sediment on the crests and troughs at station A, E, and F (mean ± S.E, n = 4–10).

Grain-size, normalized water content, wet bulk density, and organic content

The mean mud content (fine-grain fraction < 63 μm) and normalized water content are shown in Figure 4.6. No significant difference in mud content and median grain-size between crests and troughs was observed at any of the stations except station F ($P < 0.05$, Table 4.1).

There was a significant difference between crests and troughs with respect to normalized water content and wet bulk density at station A ($P < 0.05$,

P < 0.01, respectively), with the crests being drier and denser than the troughs. No significant difference was observed between crests and troughs at the other five stations with respect to these parameters. No significant difference in organic content between crests and troughs was observed at any of the stations.

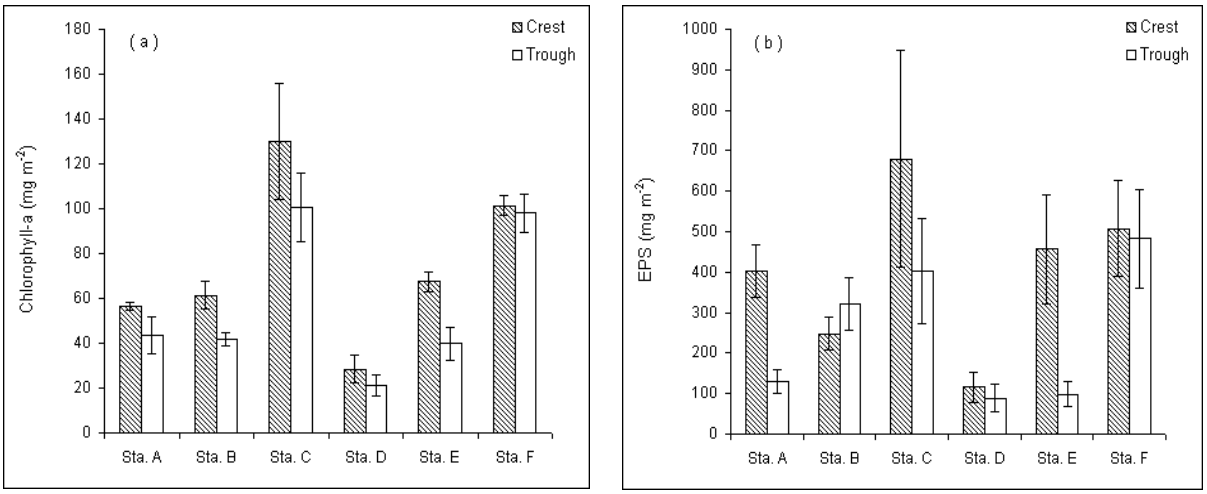

Figure 4.5. (a) Chlorophyll-a and (b) EPS concentration of surface sediment on the crests and troughs at each station (mean ± S.E, n = 4–11).

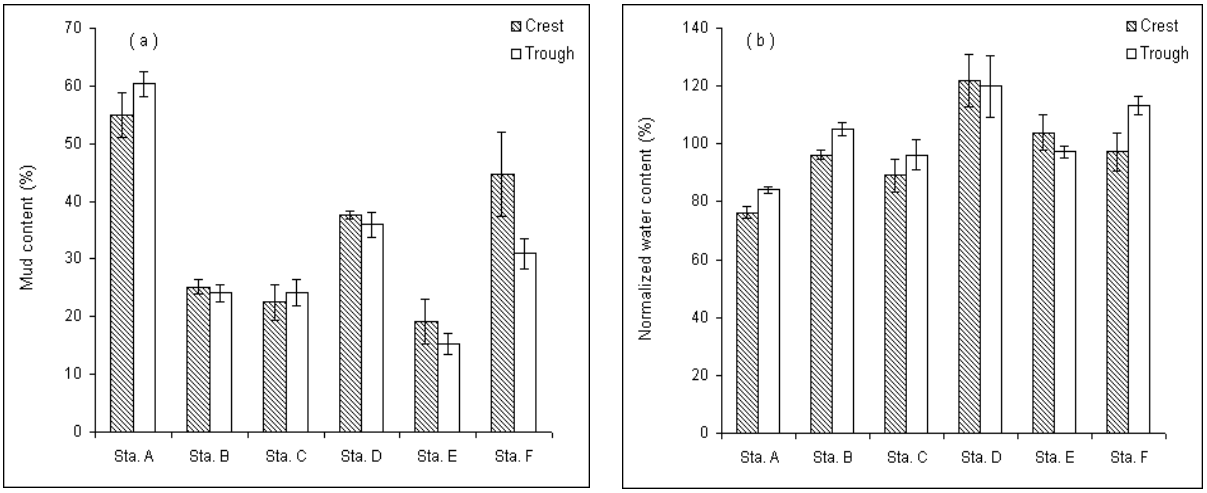

Figure 4.6. (a) Mud content and (b) normalized water content of surface sediment on the crests and troughs at each station (mean ± S.E, n = 4–11).

4.3. Discussion

4.3.1. Effect of microphytobenthos

Critical erosion shear stress generally showed stronger correlation with chlorophyll-a, colloidal carbohydrate, and EPS than other sediment

parameters. These results indicated that the variations in erodibility at each station were controlled to a large degree by microphytobenthos present (in this environment mainly consisting of benthic diatoms). A similar influence of microphytobenthos has been found in many studies, which are listed in the introduction (see chapter 1).

On the other hand, the correlation between chlorophyll-a concentration and sediment erodibility is highly site specific. This was also observed in previous studies and ascribed to the differences in e.g., sediment texture, shelter and biotic community structure as supposed by Riethmüller et al. (2000) and demonstrated by Defew et al. (2002). The weak correlations between critical erosion shear and chlorophyll-a and EPS observed at some selected stations (e.g. stations B and F) can be attributed to the influence of other physical and biological factors that contribute some of the variations in the data. The influences of these factors may be indirect and non-linear. The differences in slopes of increase in critical erosion shear with chlorophyll-a or EPS can also be attributed to the influences of these factors.

4.3.2. Effect of benthic macrofauna

The direct effect of benthic macrofauna on the sediment erodibility was only locally detectable and less dominant compared to the effect of microphytobenthos.

Hydrobia ulvae

The mud snail *Hydrobia ulvae* was the only analyzed benthic macrofauna significantly correlated to sediment erodibility at station A: the erosion rate increased at this station with increasing density of *Hydrobia ulvae* (Figure 4.1). From the literature, *Hydrobia ulvae* can enhance erodibility directly by moving through the surface sediment and by loosening the sediment through pelletization of the surface material (Blanchard et al. 1997, Andersen 2001a).

It is also likely that *Hydrobia ulvae* indirectly affect the sediment erodibility at station A by reducing the stabilizing effect of microphytobenthos (Austen et al. 1999). This was supported by the fact that microphytobenthos biomass (measured as chlorophyll-a) decreased with increasing *Hydrobia ulvae* densities at station A (Figure 3.7).

The correlation between chlorophyll-a and critical erosion shear stress was low at station B. This was probably due to the small range of the chlorophyll-a concentration at this station. High density of *Hydrobia ulvae* was probably responsible for the low microphytobenthos biomass (measured as chlorophyll-a) as these snails feed mainly on benthic diatoms (Lopez and Kofoed 1986).

Macoma baltica

The influences of *Macoma baltica* on sediment erodibility have been reported in several previous studies (Widdows et al. 1998c, Widdows et al. 2000a). In the Skeffling, Humber estuary (UK), Widdows et al. (2000a) found a significant decreased in critical erosion velocity with increasing *Macoma baltica* density. A significant positive correlation between mass of sediment eroded m^{-2} and *Macoma baltica* density, has also been recorded in the Westershelde (The Netherlands, Widdows et al. 2000b). However, in the present study the direct influence of *Macoma baltica* on small-scale (within station) variability of critical erosion shear stress and erosion rate was not detected. Moreover, the abundance of microphytobenthos did not seem to be affected by the grazing activity of *Macoma baltica*. This was indicated by the lack of correlation between *Macoma baltica* density and chlorophyll-a concentration.

Patches of Mytilus edulis

The variations of critical erosion shear stress, normalized water content, and mud content were large at Station F. This may be attributed to the within station hydrodymical variability due to the presence of patches of *Mytilus edule* and an overall sheltering of this area. The weak correlation between critical erosion shear stress and chlorophyll-a and EPS concentration at station F was unclear, but may also be related to the small-scale hydro-dynamic variability at this station.

Cerastoderma edule and erodibility

No direct effect of the presence of *Cerastoderma edule* with respect to sediment erodibility was observed. This may be due to two opposing effects: although *Cerastoderma edule* is not a deposit-feeder, it locally removes microphytobenthos from the surface by movement of his siphons, as

recognisable by the characteristic 1 cm diameter holes in the biofilm coverage directly above this bivalve. On the other hand, there are indications for an indirect stabilisation by *Cerastoderma edule*. A laboratory study by Swanberg (1991) suggested that the presence of *Cerastoderma edule* may actually increase the stock of benthic diatoms. Her study showed a stimulating effect of *Cerastoderma edule* on microphytobenthos, mainly by increasing the level of ammonium in the water. However, in this study the potential effect of *Cerastoderma edule* in enhancing stock of benthic diatoms was not pronounced. This is reflected by the fact that density of *Cerastoderma edule* was high at stations D but the chlorophyll-a concentration was relatively low (see also chapter 5).

The presence of other deposit feeders may also hamper the stabilization potential of *Cerastoderma edule.* As an example, *Cerastoderma edule* and *Hydrobia ulvae* have been found to be able to co-exist at high densities on a mudflat in the Danish Wadden Sea (T.T..J. Andersen et al., in preparation). This implies that the possible stimulating effect of the presence of *Cerastoderma edule* on microphytobenthos may be completely overridden when a deposit feeder like *Hydrobia ulvae* is present as it will feed on the microphytobenthos and greatly increase the erodibility if present in high numbers (Austen et al. 1999, Andersen 2001a). Additionally, some observations indicate that the cockle may tend to destabilize the sediment surface if is present in very high numbers (R. Riethmüller, unpublished data).

Cerastoderma edule and biodeposition

The faeces and pseudo-faeces produced by *Cerastoderma edule* are very fragile and it was not possible to discern any of these after gentle wet-sieving at a 63 µm sieve. This is consistent with the study of Austen (1997) who also found that pellets produced by *C. edule* were rare in sediments from mixed mudflats of the Lister Dyb tidal basin. Due to the fragile nature of the pellets, it was not possible to determine the contribution of these to the total fine-grained content of the surface material. However, a comparison of the rate of biodeposition and the sediment accumulation rate at the site provides an idea of the contribution. The biodeposition rate of *C. edule* is dependent on both the density of the animal, the suspended sediment concentration and perhaps

to some extent also season. For a density of 135 individuals m^{-2} in the Oosterschelde (the Netherlands), Smaal et al. (1986) calculated a deposition of 81 g m^{-2} per day. The density at the sampling station is of the same order (146 individuals m^{-2}) and assuming biodeposition for 300 days each year (allowing for reduced/absent biodeposition during the winter period), a gross-deposition of 24 kg m^{-2} per year is found. For comparison, with the estimated accretion rate of 0.7 cm per year (T.J. Andersen, unpublished data), the average dry bulk density of 0.98 g cm^{-3} and the average mud content of 41 %, the net-deposition of mud at the site is 2.4 kg m^{-2} per year – an order of magnitude lower. This indicates that a substantial part of the fine-grained material deposited at the site may be biodeposits from *C. edule* and is in accordance with the early observations of Verwey (1952) who found that the biodeposits originating from *M. edulis* and *C. edule* made up a significant portion of the total accumulation of fine-grained material in the Dutch Wadden Sea area. The gross-deposition being much larger than the estimated net-deposition shows that a large part of the biodeposits are resuspended quickly after deposition.

Heteromastus filiformis and erodibility

The finer texture of the fecal pellets compared to the texture of the surface material is caused by the preferential ingestion of the finer particles of the sediment by *Heteromastus filiformis*. This will decrease the fine-grained content of the subsurface sediment and increase the content at the surface as observed in the vertical profile of the mud content (Figure 4.2).

The fecal pellets on average contributed to 11 % of the surface material, and correction for the fine-grained content of the fecal pellets reduces the mud content of the surface sediments from 41 to 36 % – a reduction of about 12 %. Therefore, *H. filiformis* obviously increases the mud content of the surface material. Even without fecal pellets from *Heteromastus filiformis*, the mud content is still 36 % which shows that most of the fine-grained surface material is in the form of other aggregates and some of this material is fecal pellets and pseudo-faeces produced by *Cerastoderma edule*. It should be stressed that the vertical variation of the mud content at the site does not result from increasing sedimentation of fine-grained material but merely reflects the

strong sediment reworking by *Heteromastus filiformis*. A study on sediment reworking by *Heteromastus filiformis* in the Dutch Wadden Sea was reported by Cadée (1979) who showed that at a measured average density of 500 individuals m^{-2}, this species alone could account for sediment reworking of about 4 cm per year. This is due to the feeding at depth (10–20 cm; up to 30 cm in the winter) and deposition of pellets at the sediment surface. An even stronger reworking must be expected at the present study site due to the higher density of the species.

4.3.3. Effect of drying

From literature it is expected that dewatering through drying and drainage would have a significant effect on sediment stability (Anderson and Howell 1984). A significant positive effect of drying (in terms of normalised water content) on sediment stability was only found at the most landward station (A) where emersion periods or subaerial exposures are long. No such effects were found at the seaward stations, probably due to the short emersion periods for significant drying to occur. At station A, critical erosion shear stress increased significantly with EPS concentration and decreased with normalised water content (Figures 3.3b and 3.3d). A reduced water content should result in a sediment with increased strength and hence resistance to erosion (Whitehouse et al. 2000b). An increase in sediment stability due to drying during long air exposure has been previously demonstrated by Amos et al. (1988) and subsequently confirmed by Paterson et al. (1990). There is evidence that the capacity of EPS in binding sediment particles together is increase when the surface matrix of EPS becomes dehydrated (Paterson 1988). Therefore, the combination of drying and microphytobenthos (EPS) stabilization may have a synergistic effect on sediment stability at station A. On the other hand, the increase of critical erosion shear stress with EPS was not higher compared to station D and part of station F, pointing to a potential other source that influence the dependence of critical erosion shear stress on EPS.

4.3.4. Effect of geomorphological structures

The results of this study suggest that the presence of bedforms may introduce different modes of erosion. The sediments deposited on the crests

were more stable than those in the troughs. This result supports the study of Paterson et al. (2000) who also found higher sediment stability on the crests (ridge) than in the troughs (runnel) at the Skeffling mudflat, Humber Estuary, UK.

Two parameters were used to characterize the erodibility of the bed at the study site: critical erosion shear stress and erosion rate. Significantly higher critical erosion shear stresses on the crests were observed only at two stations (A and E), the difference at the other three stations being statistically not significant, although critical erosion shear stresses were in general higher on the crests than in the corresponding troughs in all cases.

A more pronounced effect of bedforms on sediment erodibility was found when considering the erosion rate. These were significantly lower on the crests than in the troughs at all stations except stations B and C. Differences in erodibility between crests and troughs are thus better represented by means of erosion rate rather than critical erosion shear stress in this study. The difference in erodibility between crests and troughs is also illuminated by their erosion profiles. As shown in Figure 4.4, mean erosion profiles for the crests are lower than for the troughs, the patterns being particularly clear for the sediments of station A, E and F. This suggests that much more sediment was eroded in the troughs once the bed shear stresses exceeded the critical values.

In this study, the difference in erodibility between crests and troughs can not be explained by mud content, median grain-size and organic content as crests and troughs are generally not significantly different with respect to these parameters. Instead, the differences in erodibility can be explained by the following physical and biological processes.

The differences between crests and troughs may firstly come from their physical characteristics (Blanchard et al. 2000). Crests are completely emerged during low tide and progressively dry out, whereas troughs are often covered with a thin layer of trapped or slowly running water. Consequently, sediment would be drier on the crests. A reduced water content results in a sediment with increased strength and hence greater resistance to erosion (Anderson and Howell 1984, Amos et al. 1988, Paterson et al. 1990). However, in the present study the effect of drying on normalized sediment

water content was apparent only at station A. This was probably due to the relatively long emersion time here. In addition, the ability of surface diatom biofilms to retain water in order to avoid desiccation and to maintain diatom viability may substantially reduce drying of the surface sediment on the crests (Christie et al. 2000) at the other stations.

Secondly, the physical characteristics prevailing in the troughs may also prevent carbohydrate-mediated stabilisation of the sediment (Blanchard et al. 2000). As observed in this study, the troughs generally contained less chlorophyll-a, colloidal carbohydrate and EPS than crests (Figure 4.5.). There are two explanations for the lower concentrations of both carbohydrate and chlorophyll-a in the troughs than those on the crests. Firstly, the carbohydrates freshly excreted by microphytobenthos in the troughs are probably rapidly dissolved in the thin layer of trapped water (Paterson et al. 2000) and may be washed out with the slowly running water (Blanchard et al. 2000). Secondly, a decrease in light due to overlying turbid water probably results in a lower activity of microphytobenthos in the troughs. All of these mechanisms may lead to a decrease in the potential biostabilization by microphytobenthos in the troughs of the bedforms (Blanchard et al. 2000).

Since water contents on the crests were not significantly higher at stations B–F, the higher sediment stability on the crests was evidently not associated with drying effects. Instead, biostabilisation by benthic diatoms through secretion of mucopolysaccharides seems to play a more important role in stabilizing the sediment surface on these crests. This was particularly true for station E where chlorophyll-a, colloidal carbohydrate and EPS concentrations were significantly higher on the crests than in the troughs.

By contrast, the most landward station (A), where benthic diatom biomasses were relatively low and the emersion periods longer, the physical processes (drying and compaction) seem to be the most important mechanism for the enhanced sediment stability on the crests. This is supported by the fact that the sediments on the crests were significantly drier at this station.

At the same time, concentrations of colloidal carbohydrate and EPS were also found to be significantly higher on the crests. One has to note that the

mechanisms of motile diatoms in stabilizing sediments are related to the physical characteristics of the mucilage produced for locomotion. If the mucopolysaccharide matrix at the surface becomes dehydrated it is possible that the sediment will become more tightly bound in the thickening matrix. Therefore, drying of sediment and dehydration of the mucopolysaccharide matrix may act together to raise the sediment stability (Paterson 1988) on the crests compared to the troughs. It is evident that this synergistic effect most likely occurs at station A where the emersion period is long enough to allow for significant drying.

4.4. Conclusions

The small-scale variation of sediment erodibility at each station was mainly controlled by microphytobenthos. However, the dependence of critical erosion shear stress on chlorophyll-a or EPS differed from station to station suggesting that the relationship between these parameters was highly site specific. The direct effect of benthic macrofauna on sediment erodibility was only detected at station A where the erosion rate decreased with increasing *Hydrobia ulvae* density. It is also possible that *Hydrobia ulvae* indirectly affect the sediment erodibility at station A by reducing the stabilizing effect of microphytobenthos. No direct or indirect effect of other macrofauna species on the sediment erodibility was observed. Both the presence of *Cerastoderma edule* and *Heteromastus filiformis* will increase the content of fine-grained sediments at the surface compared to abiotic situation.

The significant effect of drying (in terms of normalized water content) on sediment stability was only observed at station A where the emersion periods or subaerial exposure are long. Drying of sediment due to prolonged subaerial exposure will increase the capacity of EPS in binding sediment particles together. Therefore, drying and microphytobenthos (EPS) may have synergistic effect on sediment stability at station A.

The sediments deposited on the crests of bedforms were found to be more stable than those in the troughs. Two different processes were identified for the difference in erodibility between crest and troughs: (1) at stations B–F, the higher benthic diatom biomass on the crests is likely to stabilize the sediment surface of these features. (2) At station A (most landward station), where the

tidal emersion period is longer and benthic diatom biomass is relatively low, physical processes (drying, compaction) are more important for sediment stability on the crest.

CHAPTER 5

LARGE-SCALE (BETWEEN STATION) VARIATION OF SEDIMENT ERODIBILITY

5.1. Introduction

In this chapter, the large-scale (hundred of meters) spatial and temporal variation of erodibility is examined. Only data from 2002 are used to describe the spatial (between station) differences in erodibility. To investigate seasonal changes, data of 2001 are included when examining the erodibility of the studied transect as a whole.

Major questions addressed in this study are: (1) Is there a spatial (between station) and temporal variation of erodibility and sediment parameters? (2) if yes, how large is the variation? (3) What are the main processes that cause the spatial and temporal variation of sediment erodibility?

5.2. Results

Grain-size, normalized water content, and organic content

Mud contents were considerably higher both in June and September at station A compared to other seawards stations (Table 3.1 and Figure 5.1a) suggesting that station A is associated with a low energy environment. The mean mud contents at station A were 60 % and 55 % in June and September, respectively. The mean mud contents at stations B, C and E were generally less than 30 % both in June and September. The mean mud contents were slightly higher at stations D and F compared to those at stations B, C, and E both in June and September. Mean mud contents were higher in September than in June at stations, B, C, and E but the opposite pattern was observed at stations A, D and F (Table 3.1 and Figure 5.1a).

Mean normalized water content generally decreased from station F towards the shoreline both in June and September 2002 (Figure 5.1b). In June, the normalized water content decreased from about 90 % at station F to 80 % at station A. This decrease was gradual compared with September when the normalized water contents decreased from about 120 % at station F to 80 % at station A. The normalized water content was lower in June than in September at all stations except stations A and B where the contents

remained constant. No consistent spatial variation in organic content was evident in both June and September 2002. However, a general increase from June to September was observed (Table 3.1).

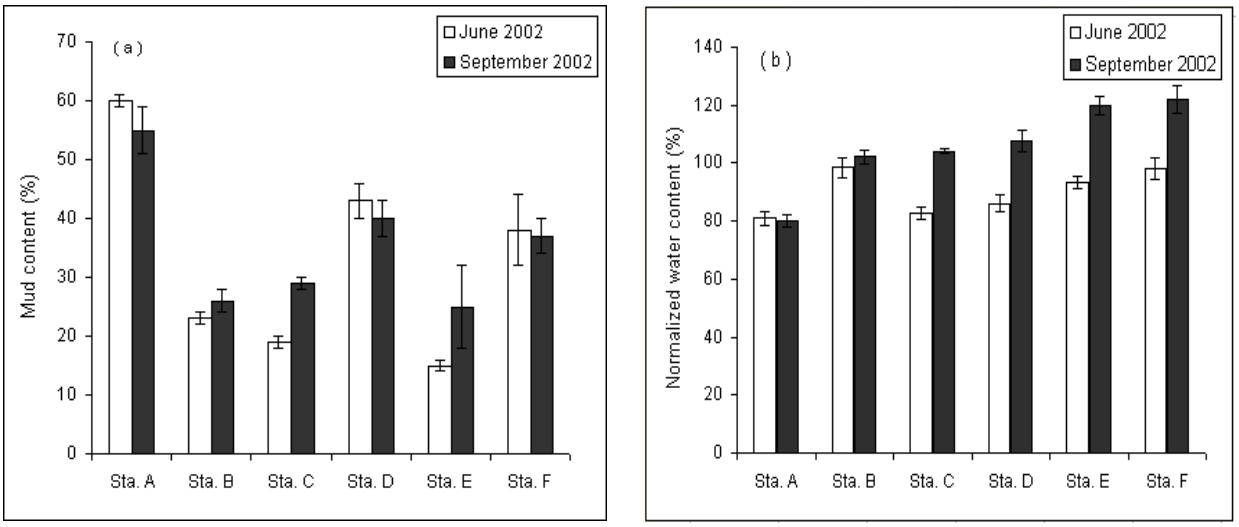

Figure 5.1. Spatial variation of the (a) mud content and (b) normalized water content at stations A–F for June and September 2002 (mean ± SE, n = 4–14).

Chlorophyll-a, colloidal carbohydrate and EPS

The spatial variations of chlorophyll-a, colloidal carbohydrate, and EPS concentrations for June and September 2002 are shown in Figure 5.2. All three parameters showed nearly the same patterns as a consequence of the same source in most cases (i.e. microphytobenthos). Two maxima were observed: one at station C and another one at station F. The lowest concentrations were measured at station D both in June and September (Table 3.1 and Figure 5.2). In general, an increase of these parameters from June to September was observed at all stations. The only two exceptions found were constant level of Chlorophyll-a concentrations at the stations B and F.

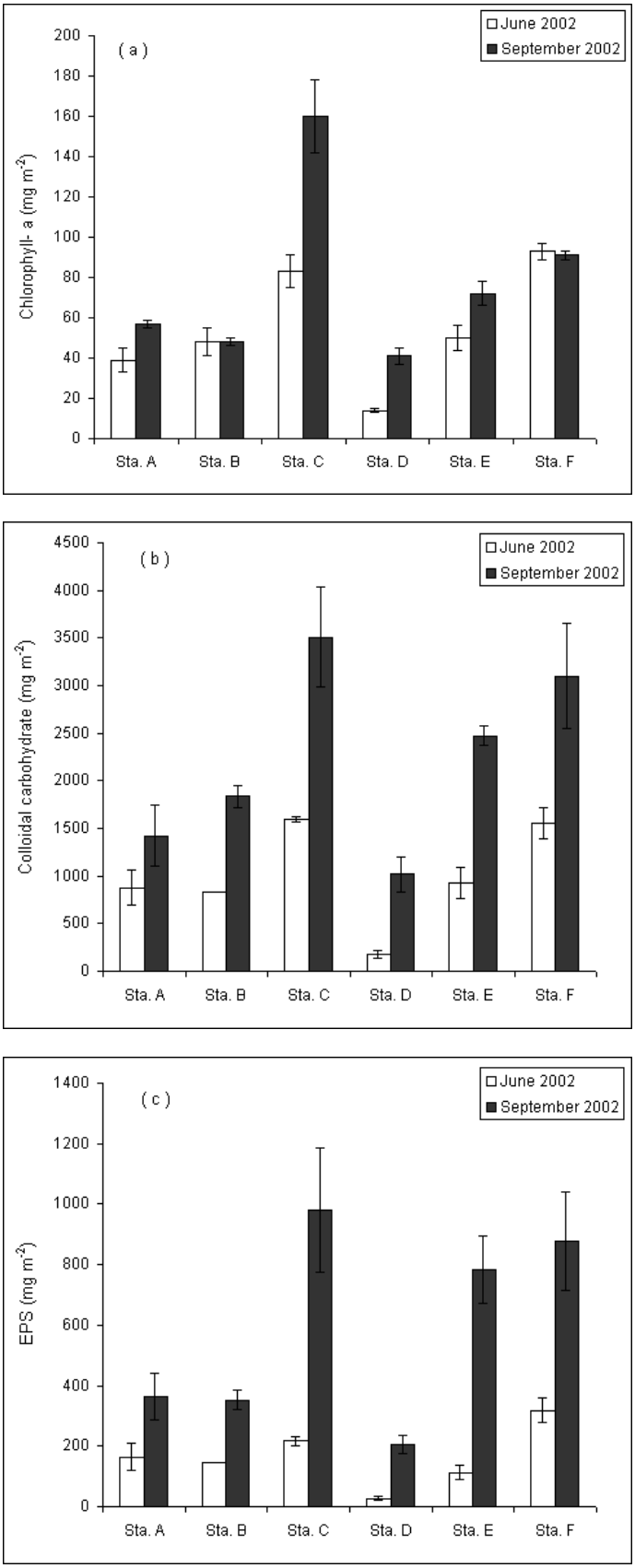

Figure 5.2. Spatial variation of the (a) chlorophyll-a, (b) colloidal carbohydrate, and (c) EPS at stations A– F for June and September 2002 (mean ± SE, n = 4–14).

Benthic macrofauna

As described in chapter 3, *Hydrobia ulvae* was present only at stations A and B, while other species such as *Heteromastus filiformis*, *Pygospio elegans*, *Tubificoides benedeni*, and *Macoma baltica* occurred commonly over the entire sampling stations (Table 3.3*). Hydrobia ulvae* were more abundant in September than in June 2002 at station B but the opposite was observed at station A (Figure 5.3). *Cerastoderma edule* were abundant at stations B and D both in June and September 2002. The mean density of this cockle was higher in June than in September at station B but the opposite was observed at station D (Table 3.4). The mean densities of *Heteromastus filiformis* were higher in September than in June 2002 at all stations (Table 3.4). By contrast, the densities of *Macoma baltica* were lower in September than in June 2002 at all station except stations A and B (Table 3.4 and Figure 5.4). No consistent spatial and temporal pattern was observed for other species listed in Table 3.4. The spatial and temporal variation of the mean density of sum of tube building worms is shown in Figure 5.5. The densities of these worms were higher in September than in June 2002 at all stations except stations E and F (Figure 5.5).

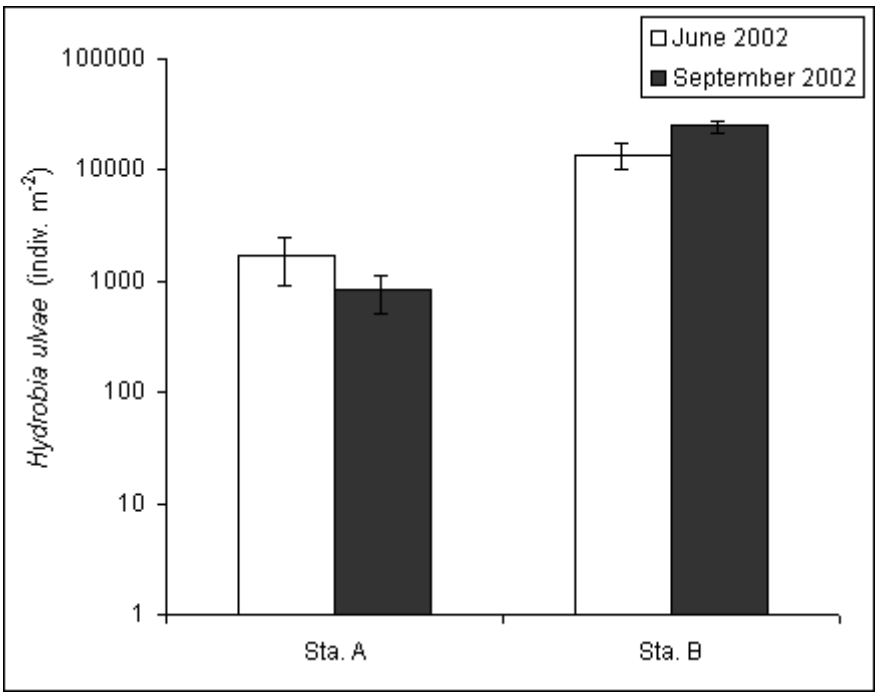

Figure 5.3. Spatial and temporal variation of the *Hydrobia ulvae* density at stations A and B (mean ± SE, n = 4–7).

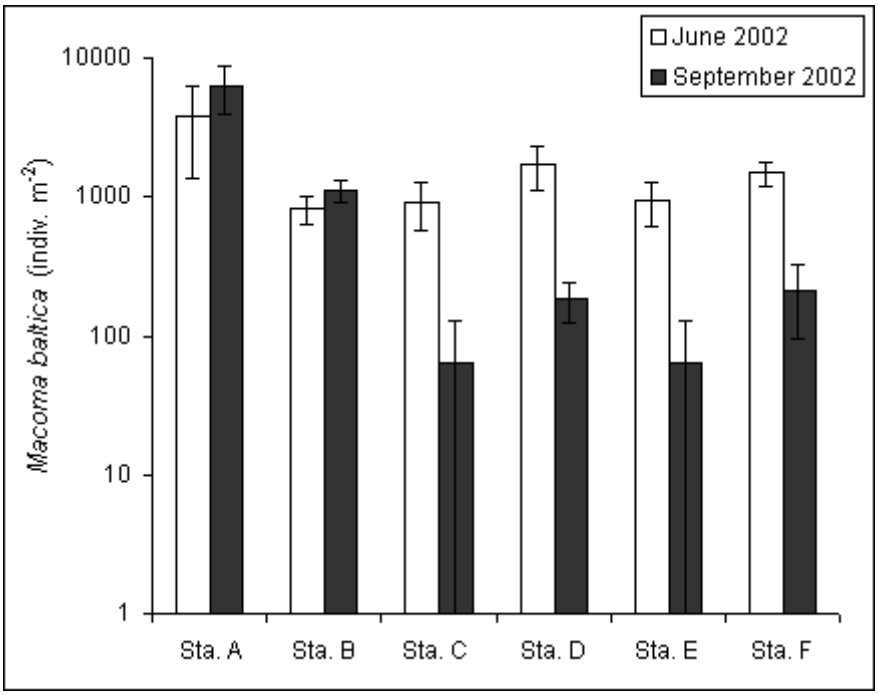

Figure 5.4. Spatial and temporal variation of the *Macoma baltica* density at stations A – F (mean ± SE, n = 4– 14).

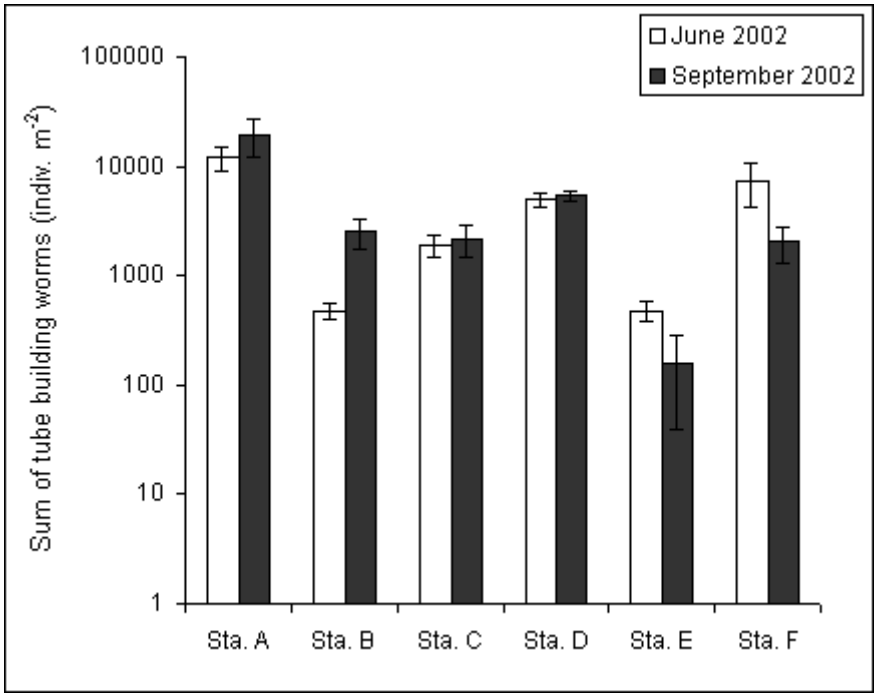

Figure 5.5. Spatial and temporal variation of the mean density of sum of tube building worms at stations A– F (mean ± SE, n = 4– 14).

Critical erosion shear stress and erosion rate

Mean critical erosion shear stresses varied from 0.36 N m^{-2} at station D in June to 2.39 N m^{-2} at station F in September (Table 3.1 and Figure 5.6). Spatial differences were more significant in September than in June (Table 5.1a). In June, station F had significantly higher mean critical erosion shear stress than other stations except stations A and B (Table 5.1a). Critical erosion shear stress was significantly lower at station D compared with those at stations A and F. In June, the average critical erosion shear stresses were comparable in magnitude at stations A, B, C, and E with a value of some 0.5 N m^{-2}. In September, station F had also significantly higher mean critical erosion shear stress than other stations except station C (Table 5.1a). The mean critical erosion shear stress was significantly lower at station B compared to those at all other stations except station D.

As in the case of colloidal carbohydrate and EPS concentrations, critical erosion shear stresses at stations C– F showed significant increase from June to September, contrasted by minor differences at stations A and B (Figure 5.6). Indeed, ANOVA showed that critical erosion shear stresses were significantly higher in September than in June at stations C– F but not at stations A and B (Table 5.1b). Changes in the coefficient of variation (cv; temporal standard deviation / temporal mean) for critical erosion shear stress support trends of increased temporal variability at stations C (cv = 0.70), D (cv = 0.68), E (cv = 0.55), and F (cv = 0.53) compared with stations A (cv = 0.23) and B (cv = 0.04).

Erosion rates reported here are calculated as the average erosion rate for the bed shear stress increments from 1.0 to 2.0 N m^{-2}. Erosion rate data derived from portable EROMES at station D were not included in the analysis because erosion rates derived from this device are calculated from 2 minute time increments and as the average erosion rate for the bed shear stress increments from 0.5–1.0 N m^{-2}. The mean erosion rate showed differences in space and time over two orders of magnitudes: the lowest rate of 0.01 g m^{-2} s^{-1} was observed at station F in September, while the highest value was 1.73 g m^{-2} s^{-1} at station B in June (Table 3.1 and Figure 5.6b). In general mean erosion rates were higher in June than in September which is expected

since critical erosion shear stresses increased. The only exception is station D where the mean erosion rate was not significantly higher in September than June. The differences between June and September were significant only at stations C and F. The highest rates on the average were measured at station B, while the lowest rates were observed at stations A and F. The results of statistical significance test between stations for erosion rate are listed in Table 5.2.

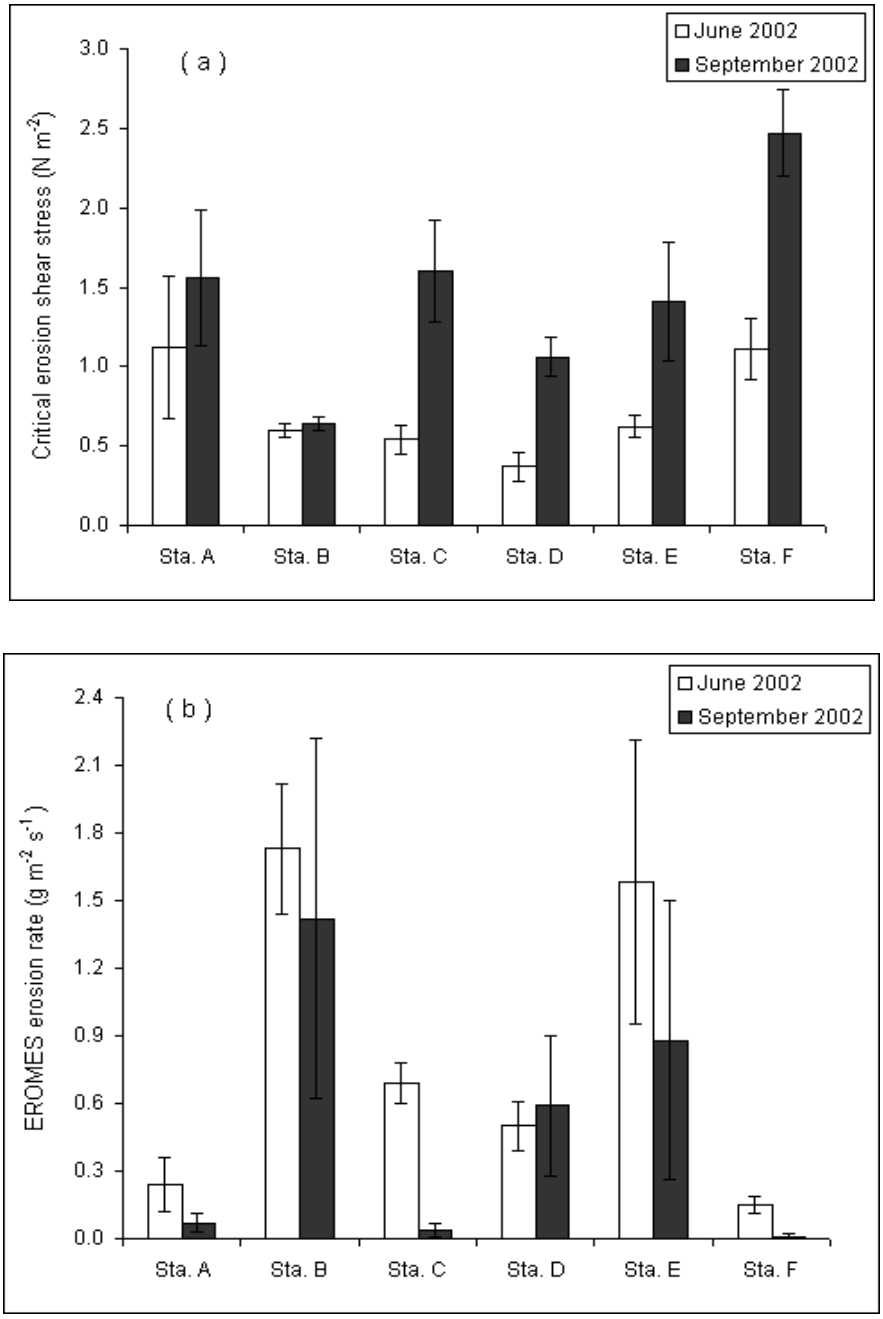

Figure 5.6. Spatial and temporal variation of the (a) critical erosion shear stress and (b) erosion rate at stations A– F (mean ± SE, n = 4– 14).

Table 5.1. Results of one-way ANOVA carried out to detect differences in critical erosion shear stress with station (a) or time (b) as the factor.

Month	*F*-value	*p*-value		Level of significance of differences between stations (LSD multiple comparison test)				
(a) Spatial analysis								
June	4.68	**0.002**		Sta. A	Sta. B	Sta. C	Sta. D	Sta. E
			Sta. B	ns	_			
			Sta. C	ns	ns	_		
			Sta. D	p = **0.005**	ns	ns	_	
			Sta. E	ns	ns	ns	ns	_
			Sta. F	ns	ns	p = **0.024**	p = **0.000**	p = **0.008**
September	6.75	**0.000**	Sta. B	p = **0.006**	_			
			Sta. C	ns	p = **0.006**	_		
			Sta. D	ns	ns	ns	_	
			Sta. E	ns	p = **0.031**	ns	ns	_
			Sta. F	p = **0.021**	p = **0.000**	ns	p = **0.000**	p = **0.015**
(b) Temporal analysis								
Sta. A	1.07	0.323						
Sta. B	0.18	0.677						
Sta. C	15.41	**0.006**						
Sta. D	25.90	**0.000**						
Sta. E	8.64	**0.013**						
Sta. F	13.75	**0.002**						

Significant *p*-values are in bold

ns: not significant (p > 0.05)

Table 5.2. Results of one-way ANOVA carried out to detect differences in erosion rate with station (a) or time (b) as the factor.

Month	*F*-value	*p*-value		Level of significance of differences between stations (LSD multiple comparison test)				
(a) Spatial analysis								
June	7.914	**0.000**		Sta. A	Sta. B	Sta. C	Sta. D	Sta. E
			Sta. B	p = **0.000**	-			
			Sta. C	ns	p = **0.024**	-		
			Sta. D	ns	p = **0.006**	ns	-	
			Sta. E	p = **0.000**	ns	ns	p = **0.024**	-
			Sta. F	ns	p = **0.000**	p = **0.044**	ns	p = **0.000**
September	3.610	**0.014**	Sta. B	p = **0.006**	-			
			Sta. C	ns	p = **0.011**	-		
			Sta. D	p = **0.036**	ns	p = **0.047**	-	
			Sta. E	ns	ns	ns	ns	-
			Sta. F	ns	p = **0.003**	ns	p = **0.021**	ns
(b) Temporal analysis								
Sta. A	1.216	0.294						
Sta. B	0.615	0.455						
Sta. C	29.185	**0.001**						
Sta. D	0.841	0.395						
Sta. E	1.999	0.185						
Sta. F	6.248	**0.023**						

Significant *p*-values are in bold

ns: not significant (p > 0.05)

Seasonal pattern of the study transect erodibility as a whole

To examine the seasonal pattern of the erodibility of the intertidal flat as a whole, data from stations B, C, E, and F were pooled and grouped according to the sampling period. Data from stations A and D were excluded because these two stations were not sampled during 2001. The highest mean mud content of 65 % was observed in April 2001, while the lowest content of was observed in June 2001 (15 %). The mean mud contents were comparable for other sampling periods with contents somewhat less than 30 % (Figure 5.7a). The mean normalized water content varied between 90 % in April 2001 and 110 % in May 2001 and September 2002 (Figure 5.7b). The seasonal variation of mean organic content was fairly similar to mud content with highest value in April 2001 and lowest in June 2001 (Figure 5.7c).

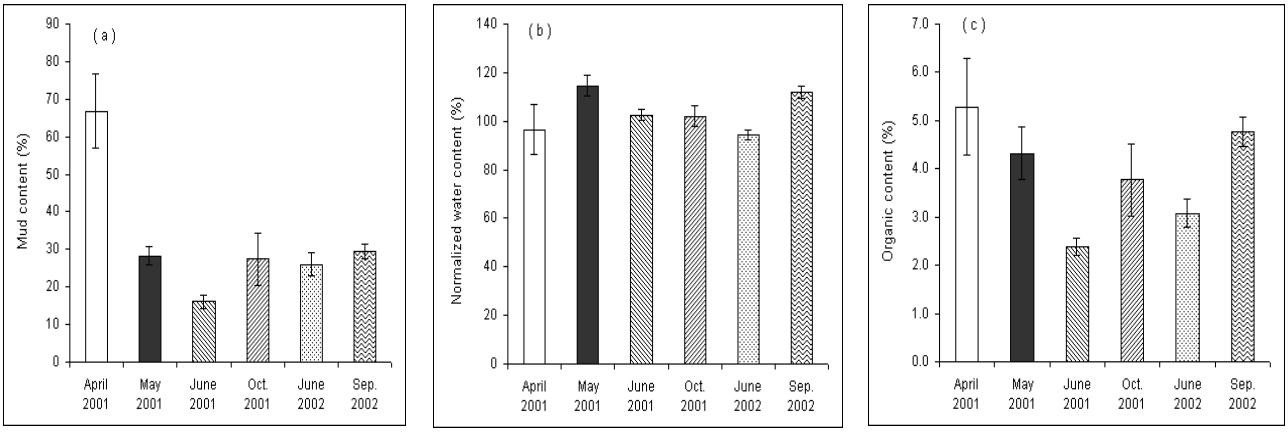

Figure 5.7. Seasonal variation of the (a) mud content, (b) normalized water content, and (c) organic content at the study site (mean ± SE, n = 4– 31).

Chlorophyll-a, colloidal carbohydrate, and EPS showed nearly the same pattern with low concentrations in June and October 2001 and high concentrations in September 2002 (Figure 5.8). The seasonal variation of mean *Cerastoderma edule*, *Hydrobia ulvae*, *Macoma baltica*, and sum of tube building worms density are shown in Figure 5.9. The highest density of *Cerastoderma edule* was in October 2001 (1020 indiv. m^{-2}), with low numbers in September 2002, and they were absent in April 2001. *Hydrobia ulvae* were more abundant in September 2002 than other sampling periods. The highest density of *Macoma baltica* was in June 2002, with low numbers in April 2001, and they were absent in October 2001. The highest and lowest densities of

sum of tube building worms were in May 2001 and September 2002, respectively.

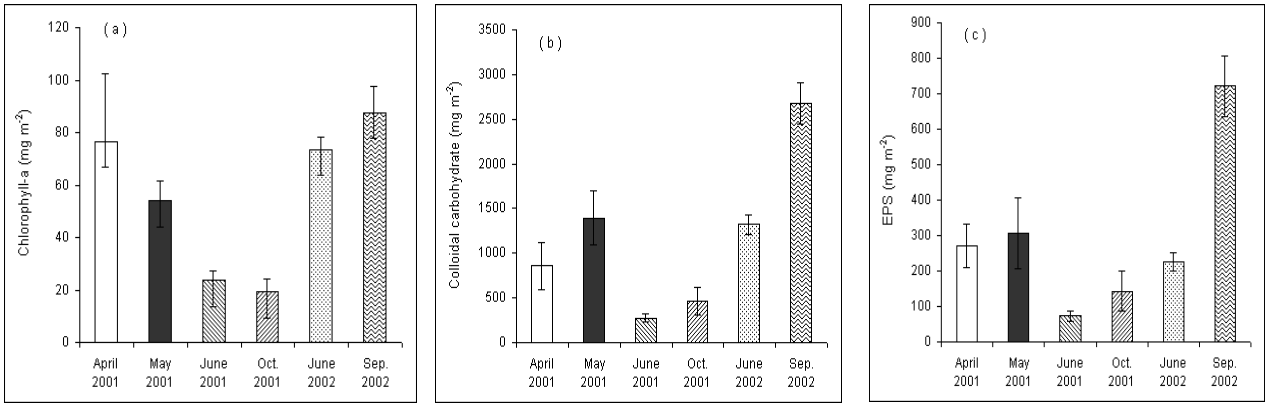

Figure 5.8. Seasonal variation of the (a) chlorophyll-a, (b) colloidal carbohydrate, and (c) EPS concentration at the study site (mean ± SE, n = 4– 31).

The seasonal variations of mean critical erosion shear stress and erosion rate are shown in Figure 5.10. The mean critical erosion shear stresses were lower in June and October 2001 than those at all other sampling periods. The highest mean critical erosion shear stress was observed in September 2002 with value of 1.47 N m^{-2}. An opposite trend was found accordingly in erosion rate, which was higher during June and October 2001. Erosion rate was considerably lower in April 2001 compared to other sampling periods.

5.3. Discussion

Variation in physical and biological sediment parameters

Generally, on tidal flats mud content increases with increasing elevation due to lower current velocities (van Straaten and Kuenen 1957, Postma 1961). This has been observed on a tidal flat in the Ems-Dollard estuary (Colijn and Dijkema 1981) and on the same area in the East Frisian Wadden Sea (Krögel and Flemming 1998). Similar with these findings, finer sediment with high mud content was observed at the most landward station (A) and the mud content decreased seaward (Figure 5.1a). Stations D and F did not follow this general pattern probably due to the presence of high amount of biodeposits. As discussed in chapter 4, *Cerastoderma edule* and *Heteromastus filiformis* contribute a considerably high amount of fine-grained material at station D. A similar phenomenon may also occur at station F where

mussels *Mytilus edulis* enhance the deposition of fine-grained particles by their filter feeding activities.

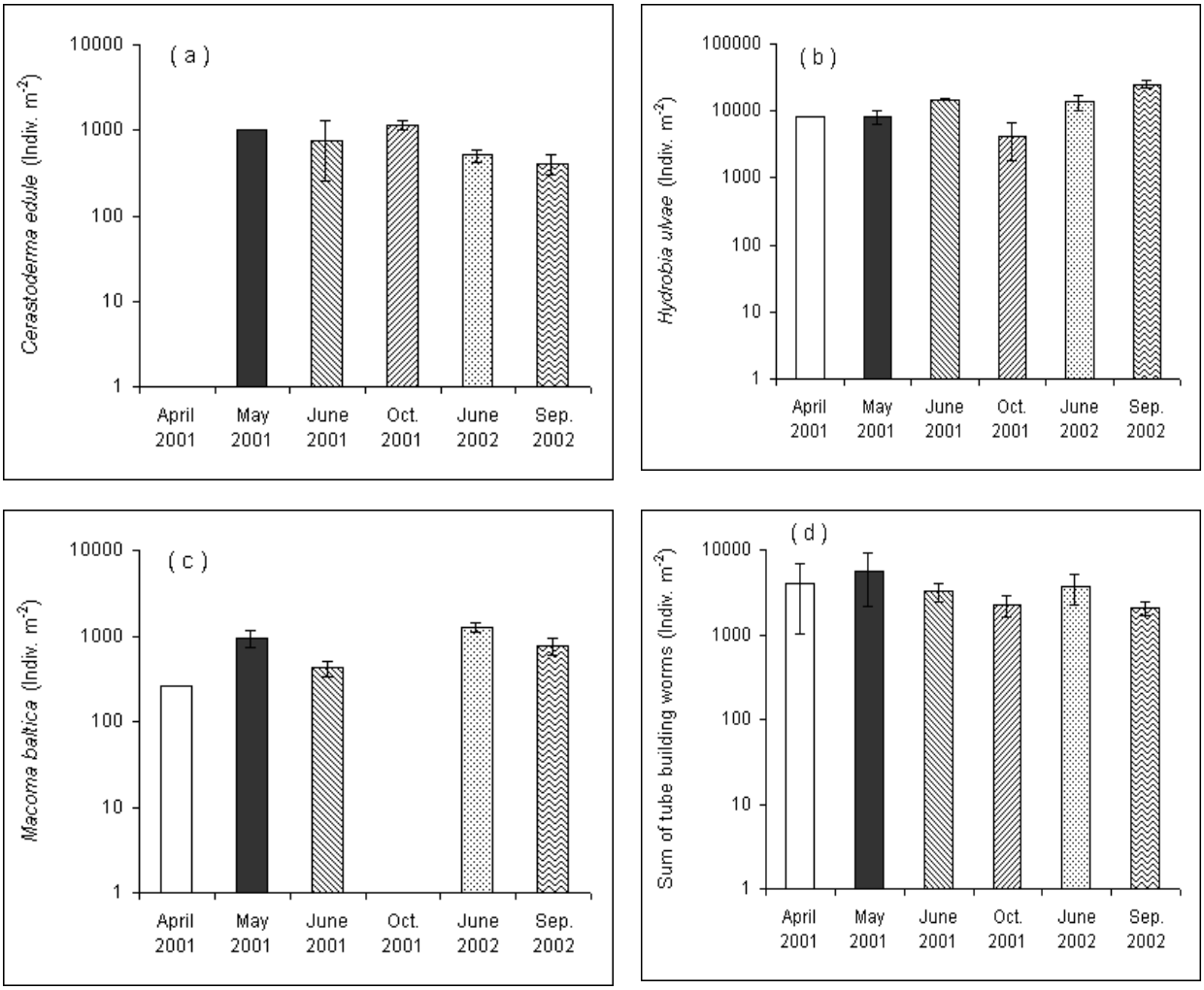

Figure 5.9. Seasonal variation of the (a) *Cerastoderma edule*, (b) *Hydrobia ulvae*, (c) *Macoma baltica*, and (d) sum of tube building worms at the study site (mean ± SE, n = 1– 30).

Colijn and Dijkema (1981) observed higher chlorophyll-a concentration in muddy sediments and attributed the relationship to reduced hydrodynamic energy. Similarly, Lelieveld et al. (2003) also observed higher chlorophyll-a concentration in the muddy site but they attributed this to higher organic compound associated with muddy sediment that can stimulate diatom growth. In the present study the concentration of chlorophyll-a was relatively low at the most muddy station (A) and low and high concentrations were observed at the sandy mud to muddy stations (B– F) indicating that the spatial distribution of chlorophyll-a concentration can not be attributed to the mud content. High

grazing pressure could be one explanation for lower chlorophyll-a concentration at the station A. The densities of diatom grazers including *Hydrobia ulvae*, *Macoma baltica*, and *Pygospio elegans* (Lopez and Kofoed 1986, Widdows et al. 2000a) were relatively high here (Table 3.3) and it is likely that the growth of diatoms was prevented by grazing. In addition, desiccation during long exposure is also a possible cause of reduced diatom biomass at station A.

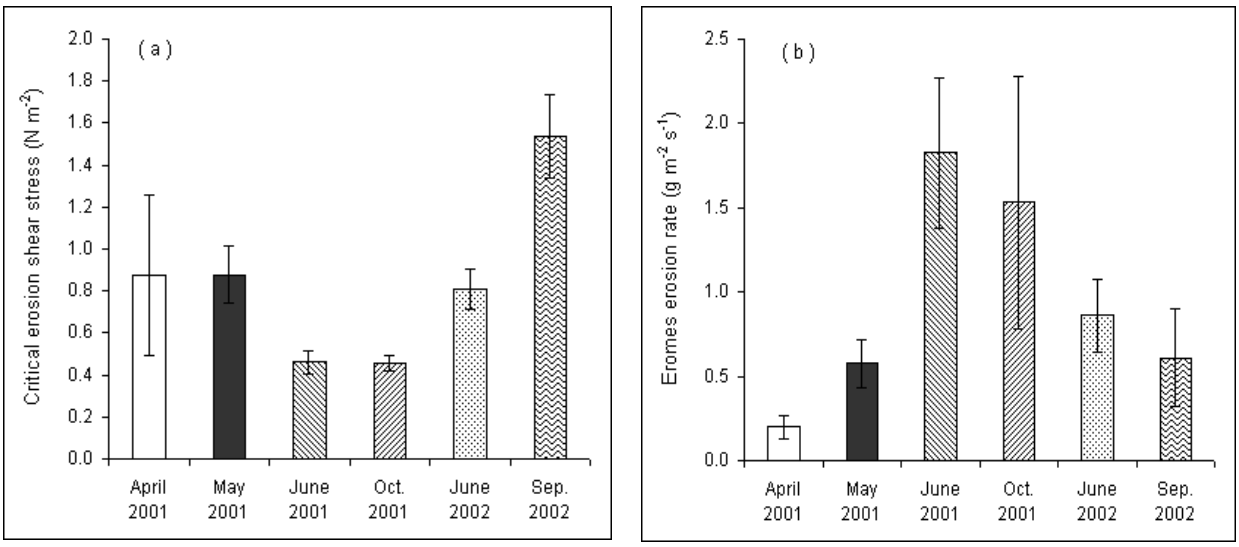

Figure 5.10. Seasonal variation of the (a) critical erosion shear stress and (b) erosion rate at the study site (mean ± SE, n = 4– 31).

The microphytobenthos is known to be variable both spatially and temporarily (Colijn and Dijkema 1981) but generally a peak has been observed in spring and early autumn in the Danish Wadden Sea (Andersen 2001a) and on Dutch tidal flats (Cadee and Hageman 1977). Guarini et al. (1998) observed high summer values and low winter values for the macrotidal Marennes-Oleron Bay in France. The temporal variation of chlorophyll-a with high concentration in early autumn (September) is consistent with the results in this study. Whilst observed lower biomass in early summer (June) could be due to a range of factors, such as nutrient limitation and grazing by macro- or meiofauna (Gerdol and Hughes 1994). The relatively low or lack of temporal variability in chlorophyll-a concentration at station B appears to be related with the high numbers of mud snail *Hydrobia ulvae* at this station, which reduced the microphytobenthos biomass by grazing.

Yallop et al. (1994) observed higher carbohydrate concentrations at the muddy site than concentrations at the sandy sites. Similarly, de Brouwer et al. (2003) observed an increase in carbohydrate concentration with decreasing median grain-size. Contrasting with these findings, no correlation was observed between median grain-size and carbohydrate concentration in this study. The presence of microphytobenthos appears to be more important in determining the spatial as well as temporal variation of carbohydrate concentration at the study site.

Variation in erodibility

Spatial differences (between station) in mean critical erosion shear stress and erosion rate were significant both in June and September 2002 but no consistent spatial pattern across the tidal flat was observed. This is in contrast to other studies which have identified clear and consistent spatial variation in critical erosion shear stress (e.g. Paterson et al. 1990, Austen et al. 1999, Lelieveld et al. 2003). Studies by Paterson et al. (1990) at Tamar and Severn estuaries (UK) showed that the highest sediment stability occurred at the high shore stations (landward stations), where a dense population of epipelic diatoms was present. In the present study, the more stable sediments (i.e. higher critical erosion shear stresses and lower erosion rates) were observed both at stations A and F.

Station A has longest emersion periods among the investigated stations. Thus drying during prolonged air exposure may have increased the sediment stability at this station (Amos et al. 1988, Paterson et al. 1990). Moreover, drying of sediment would enhance the stabilizing effect of mucilage (EPS) produced by benthic diatoms (Paterson 1988). It is also possible that the high density of tube building worms (Figure 5.5) increased the stability of surface sediment at this station as these worms have been shown to increase sediment stability by binding particles with secretions to construct their tubes (Yingst and Rhoads 1978). The increase of critical erosion shear stresses with EPS concentrations was similar to stations D and parts of F which exhibit now sign of drying but together with A share an increased level of tube building worms compared to the other stations.

Chlorophyll-a, colloidal carbohydrate and EPS were generally higher at station F than at other stations, reflecting on the average higher diatom biomass and mucous production. The high diatom biomass and mucous production at station F can be explained by the fact that this station has comparable long emersion time due to its position at the edge of the central depression and therefore at many patches very good conditions for biofilm development (diatom growth). Accumulation of mucilage (biofilm) at the sediment surface reduce sediment susceptibility to erosion by reducing bottom roughness as well as by increasing intergrain-adhesion (Paterson 1989), so higher stability at station F was most likely due to the higher biostabilization effect of benthic diatoms.

Moreover, physical disturbance (by waves or currents) of the surficial sediment structure at station F was probably minimized by the presence of mussel beds. Mussel beds may physically protect sediment from erosion and resuspension by reducing the water flow and bed shear stress (Widdows and Brinsley 2002). Infrequent disturbance would not only minimize susceptibility to particle entrainment but also facilitate the accumulation of mucilage in surface sediments (Lelieveld et al. 2003), which is consistent with the high colloidal carbohydrate and EPS concentrations at station F.

The lowest critical erosion shear stress was observed at station D in June. Low diatom biomass and hence low biostabilizing effect in June at station D was the main explanation for this. The reasons for lower diatom biomass at this station compared with other stations are unclear, but may be related to the presence of high density of *Cerastoderma edule*. These cockles may locally remove diatoms from the surface by movement of their siphons, which in turn would reduce the diatom biomass.

The erosion rate was higher in September than in June at station D. This was unexpected because the rate of erosion should be lower due to increased critical shear stress. Reasons for this are unclear, but may be related to the increased in cockle *Cerastoderma edule* density and hence bioturbation activity in September. Visual observations during the erosion experiments show that the cockles sometimes moved through sediment in response to the increase of turbulence. These moving activities would loosen the sediment and hence increase the erosion rate. Therefore, higher erosion rate in

September at this station can be partly attributed to the higher bioturbation activity of the cockles.

Station B had low erosion shear stresses and high erosion rates and the values were relatively constant throughout the sampling periods. Mud snails *Hydrobia ulvae* were very abundant at this station both in June and September and it was likely that high density of *Hydrobia ulvae* increase the erodibility through grazing on diatoms, surface tracking and pellet production (Gerdol and Hughes 1994, Andersen 2001a). It is also possible that high erodibility at station caused by the bioturbation activity of cockle *Cerastoderma edule* because of the very high density of *Cerastoderma edule* at this station both in June and September.

The seasonal pattern of erodibility of the study transect as a whole

The stability of surface sediment at the study transect was high in September 2002 (early autumn) and lowest in June (early summer) and October 2001 (late autumn). This pattern can not be explained by the relatively small changes in mud content, normalized water content, and organic content of the sediment over the study period.

At the same time the observed seasonal pattern is best reflected by those parameters describing the amount of biofilm present on the sediment surface. The higher sediment stability during September 2002 coincided with higher biomass of benthic diatoms (measured by chlorophyll-a concentrations) and high concentrations of carbohydrate in the sediment. In contrast, during June and October 2001 when lower numbers of diatom were present, the sediments were more easily eroded. This pattern also strongly suggests that temporal variation in sediment erodibility at the study site was closely linked to the presence of benthic diatoms as already observed in the inner station variability and in many other previous studies (e.g. Kornman and de Deckere 1998).

Benthic macrofauna do not seem to have any bearing on the seasonal variation of erodibility. As an example, the highest critical erosion shear stress was in September 2002, and also the highest density of *Hydrobia ulvae*, which is opposite to the trend one would expect if destabilization by *Hydrobia ulvae* was significant.

Low erosion rate observed in April 2001 was probably related to the very high mud content together with the lowest observed normalized water contents present in this period. For mixed sediments the mud/sand ratio is an important parameter determining the strength development of the bed. Mitchener and Torfs (1996) concluded from their laboratory experiment that with increasing mud/sand ratios both the strength of a sediment bed increases and reduction in amount of erosion can be found once erosion occurred. Similarly, erosion experiment conducted by Houwing (1999) on an intertidal mudflat sediment (Dutch Wadden Sea) showed that erosion rates decreased by a factor of 6 and 10 at stations where the mud contents of the sediment increased (over 20 % mud by weight).

5.4. Conclusions

This study has shown that the sediment erodibility varied spatially and temporally. The variations were lower compared to the inner station variations. Sediments were more stable (i.e. higher critical erosion shear stress and lower erosion rate) in September 2002 than in June 2002; this was attributed to be the result of biostabilization by benthic diatoms.

Erosion rates were lower at stations A and F over the study periods. The lower erosion rates at station A were attributed to the either drying or biostabilization of tube building worms or to the combination of both. Bio-stabilization of the benthic diatoms and infrequent disturbance of surface sediment due to the presence of mussel beds were the main cause of lower erosion rate at station F. Erosion rate was highest at the station dominated by mud snails *Hydrobia ulvae*. This is probably explained by the fact that *H. ulvae* feeds mainly on diatoms, thus large number of *H. ulvae* reduce the amount of diatoms, hence their stabilizing effect. Additionally, *H. ulvae* loosens the sediment via surface tracking and pelletization of the surface material and hence enhances erosion rate.

The seasonal patterns of erodibility of the study transect as a whole with low erodibility in September 2002 and high erodibility in June and October 2001 can be attributed exclusively to the presence of benthic diatoms.

CHAPTER 6

PREDICTING CRITICAL EROSION SHEAR STRESS FROM PROXIES

6.1. Introduction

The critical erosion shear stress or erosion threshold of intertidal sediments is a measure of sediment stability, and an important parameter to model the morphodynamic evolution of estuaries. Presently, this erosion parameter is measured only on contact areas up to the order of 1 m^{-2}, depending on the size of the erosion device (Cornelisse et al. 1994, Black and Paterson 1997). Each individual measurement is demanding so that the number of data points is limited. A strategy to generate large scale maps of surface sediment stability parameters is to establish a relationship to proxy parameters which can be mapped either by field surveys or by remote sensing techniques (Riethmüller et al. 2000).

As long as surface disturbance by benthic macrofauna is negligible, chlorophyll-a concentration of surface sediment is one promising candidate as proxy parameter for critical erosion shear stress. This is because chlorophyll-a in the uppermost sediment surface can be detected and quantitatively estimated by means of optical remote sensing techniques (Hakvoort et al., 1998; Paterson et al., 1998). A number of studies have reported a significant increase of critical erosion shear stress with increased chlorophyll-a concentration both on intertidal (Paterson et al. 1994, Riethmüller et al. 1998, Austen et al. 1999) and subtidal flats (Madsen et al. 1993, Sutherland et al. 1998). On the other hand, it was observed that the rise of critical erosion shear stress with increased chlorophyll-a was highly site-specific and depends on the sediment type, the macrofaunal assemblage present and on the exposure to hydrodynamic energy input (Paterson et al. 1994, Riethmüller et al. 2000, Defew et al. 2002). These results show that chlorophyll-a alone is not sufficient as a proxy parameter for critical erosion shear stress.

In this chapter, it is investigated whether other proxies alone or combinations of more than one can predict critical erosion shear stresses more generally and to what extent critical erosion shear stress can be predicted from optically quantifiable parameters. The following study is

arranged in two steps. Firstly, it is investigated whether the variation of critical erosion shear stress can be explained to a high degree by a limited set of parameters. Secondly, several options to predict critical erosion shear stress from a proxy are proposed and discussed and the pros and cons of each option (model) are assessed.

In this study, the full data set ranging from April 2001 to September 2002 is included. The site-specific dependence of critical erosion shear stress on chlorophyll-a, colloidal carbohydrate and EPS was already introduced in chapters 3 and 4 (e.g. Figure 3.3a). Colloidal carbohydrate was not discussed further since it is highly correlated with EPS and EPS has been regarded as a functionally closer proxy to biofilm stability (Paterson 1994).

6.2. Results

Model 1: Chlorophyll-a as only proxy with global calibration

The relationship between chlorophyll-a concentrations and critical erosion shear stresses was quantified using a simple linear regression analysis. A functional relationship between critical erosion shear stress, as the dependent variable, and chlorophyll-a, as independent variable, is suggested. When all data (from the different stations and sampling periods) were pooled, a statistically significant positive relationship was found between chlorophyll-a concentrations and critical erosion shear stresses (Table 6.1). However, the coefficient of determination (r^2) is low: the linear model explained 35 % of the observed variability when the outliers are excluded. Thus, when the location of the samples was not taken into account, it appeared that chlorophyll-a was a weak but still significant predictor of the critical erosion shear stress. As shown in Figure 6.1, the model does not fit the data very well and the variability of the residual values is high with standard deviation of 0.48. The predicted values derived from the model never exceed 2.3 N m^{-2}.

Model 2: Chlorophyll-a as only proxy with site-specific calibration

To consider the obviously site-specific relationships, the model was modified with respect to the different stations of the samples that were likely to

Table 6.1. Regression equations, coefficients of determination, and significance levels of relationship between chlorophyll-a (X) and critical erosion shear stress (Y) [ns: not significant (p > 0.01)] (compare Figure 3.3a).

Type of relationship	Regression equation	coefficient of determination	Significance level
All stations	Y = 0.0104X + 0.3012	$r^2 = 0.35$	p < 0.01
Station A only	Y = 0.0278X - 0.1647	$r^2 = 0.24$	ns
Station B only	Y = 0.0048X + 0.3800	$r^2 = 0.26$	ns
Station C only	Y = 0.0086X + 0.1036	$r^2 = 0.77$	p < 0.01
Station D only	Y = 0.0226X + 0.0431	$r^2 = 0.69$	p < 0.01
Station E only	Y = 0.0082X + 0.0295	$r^2 = 0.42$	p < 0.01
Station F only	Y = 0.0143X - 0.0581	$r^2 = 0.35$	p < 0.01

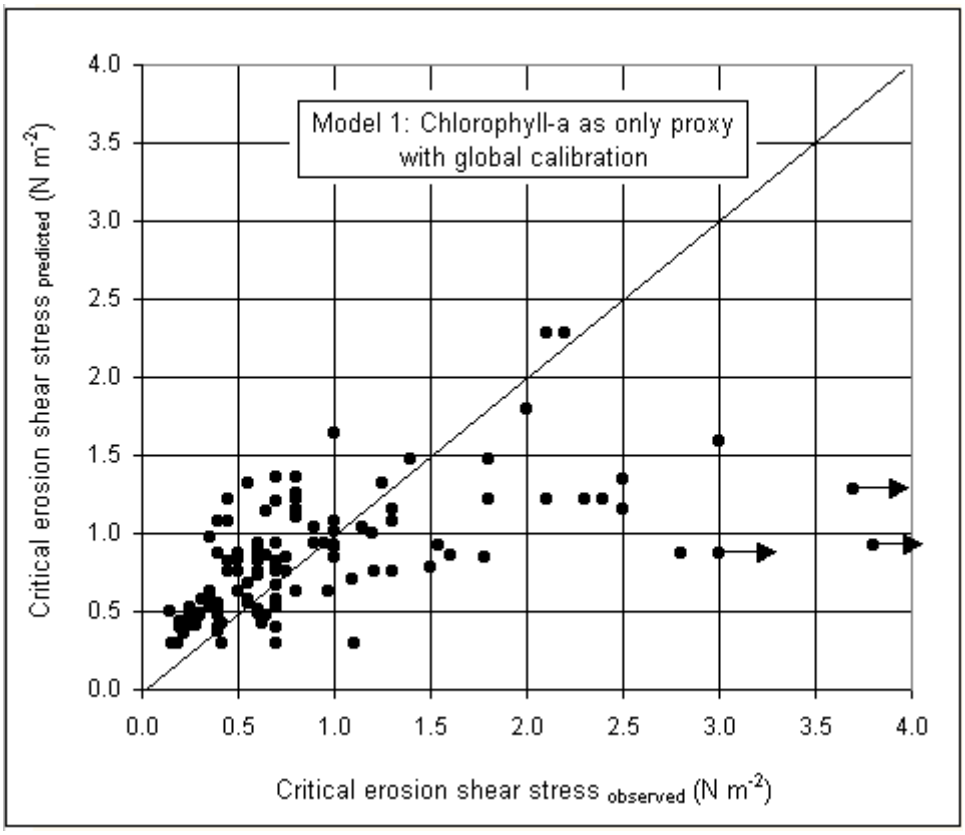

Figure 6.1. Comparison of measured and predicted critical erosion shear stress derived from chlorophyll-a with global calibration. The data with arrows (outliers) were omitted in the linear regression analysis because the upper limit of the erosion device was reached.

affect the relationship. When analyzing the data separately for each sampling station, significant positive relationships between chlorophyll-a and critical erosion shear stress were found for all stations except stations A and B (Table 6.1). However, the slopes of the regression lines and the coefficients of determination differed from station to station. The slopes differed by a factor of up to 3 (see stations C and D). The highest coefficients of determination was observed at station C ($r^2 = 0.77$) and the lowest was observed at station A ($r^2 = 0.24$).

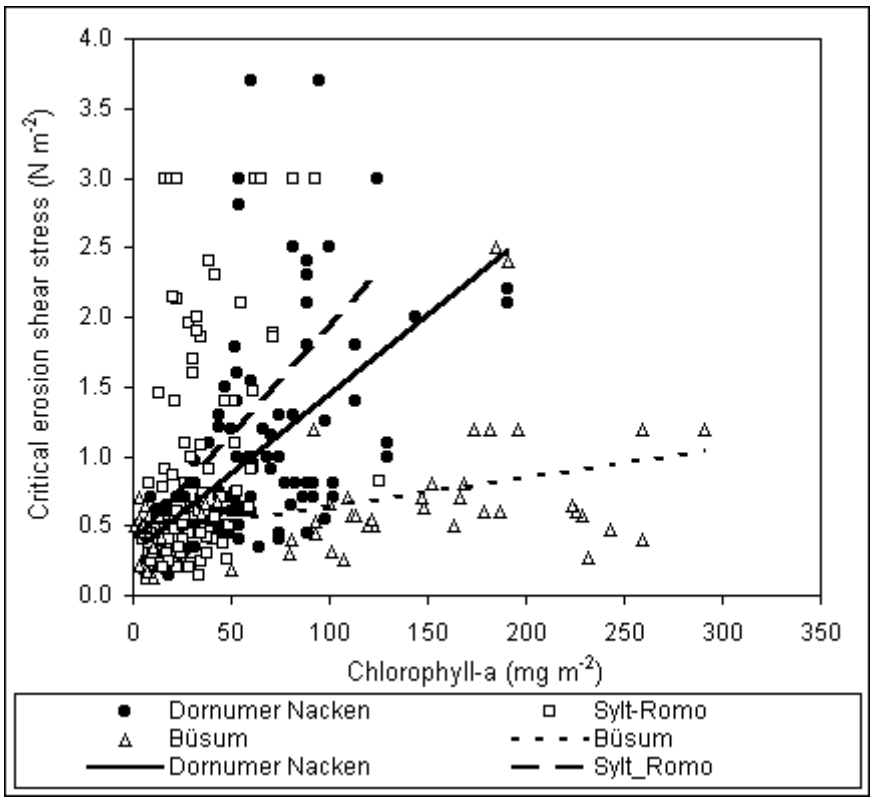

Figure 6.2. The relationships between critical erosion shear stress and chlorophyll-a concentration at the study site (Dornumer Nacken), Sylt-Rømø bight, and Büsum area.

This site-specific behaviour is in line with data obtained in the inner Sylt-Rømø Bight and intertidal flats close to Büsum, both located in the North Frisian Wadden Sea (Riethmüller et al. 2000). The slopes obtained in this study area are on the average lower than those from the Sylt-Rømø bight but the increase is much steeper than in the Büsum area (see Figure 6.2). As a consequence, site specific calibrations are required when using chlorophyll-a as a meaningful proxy parameter to predict critical erosion shear stress.

Therefore, critical erosion shear stress was calibrated separately for each station using the corresponding regression equations listed in table 6.1. A comparison of observed and predicted critical erosion shear stresses derived from chlorophyll-a with site specific calibration is shown in Figure 6.3. The model fits the data reasonably well, at least up to critical shear stress of 1.5 N m^{-2}. The variability of the residual values is relatively low with standard deviation of 0.43. At higher critical erosion shear stresses, the predictions become biased towards the low predicted values which never exceed 2.2 N m^{-2}.

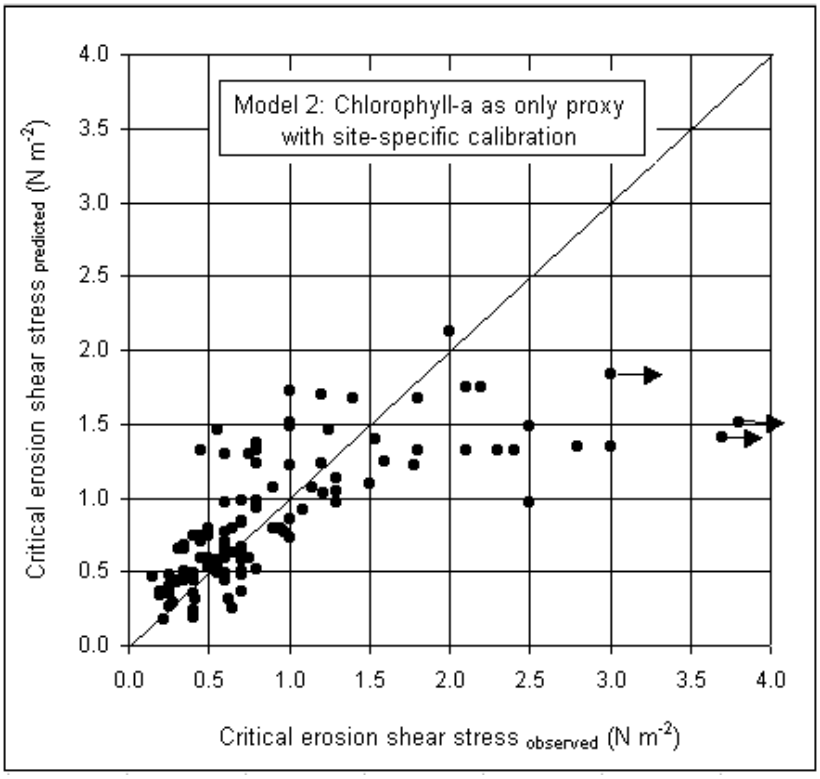

Figure 6.3. Comparison of measured and predicted critical erosion shear stress derived from chlorophyll-a with site-specific calibrations. The data with arrows (outliers) were omitted in the linear regression analysis because the upper limit of the erosion device was reached.

Model 3: Multiple regression analyses of critical erosion shear stress

The stepwise multiple regression analyses showed that with exclusion or inclusion of macrofauna density data, sediment EPS concentration and mud content were found to be the only significant predictors of critical erosion shear stress, which explained 38 % of the variation in the data (r^2 = 0.38,

P < 0.001 when the outliers are excluded). The predictive model generated from the multiple regression analyses was

log (A + 1) = 0.099 [log (B + 1)] + 0.080 [log (C + 1)] - 0.076, where A = critical erosion shear stress, B = EPS concentration, and C = mud content.

The multiple regression coefficient of each variable included in the model was used in an equation to predict the magnitude of critical erosion shear stress by multiplying the magnitude of the variable with the corresponding coefficient that the model yielded. Since the obtained critical erosion shear stresses are still in the logarithmic scale, back transformations are required to obtain the actual magnitude of the predicted critical erosion shear stress. A comparison of observed and predicted critical erosion shear stress derived from the stepwise multiple regression models are shown in Figure 6.4.

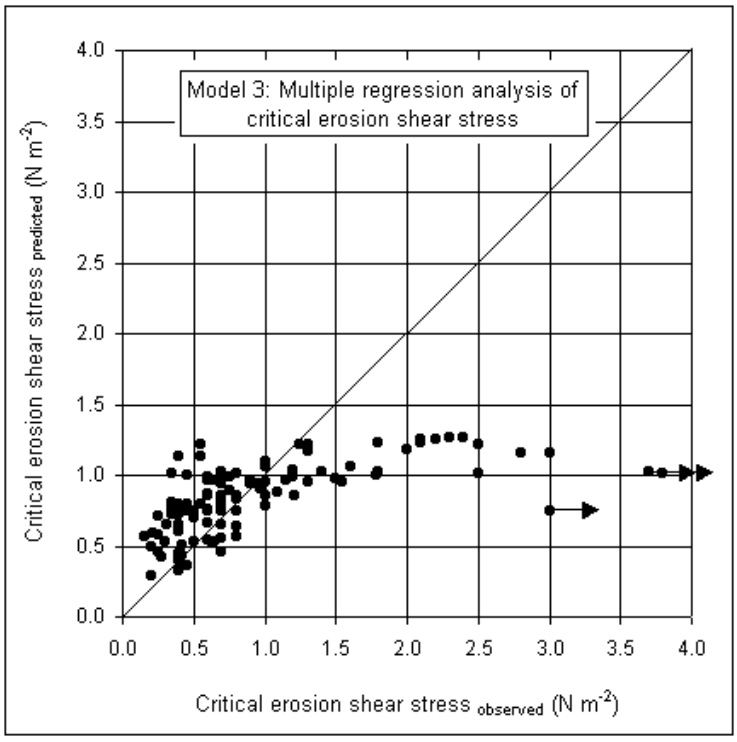

Figure 6.4. Comparison of measured and predicted critical erosion shear stress derived from the multiple linear regression analysis. The data with arrows (outliers) were omitted in the multiple linear regression analysis because the upper limit of the erosion device was reached.

As shown in Figure 6.4, the agreement between prediction and observation was good enough for critical erosion shear stresses lower than 1 N m^{-2}. However, at higher critical erosion shear stresses the prediction becomes systematically biased towards the low predictive values which never exceed

1.3 N m^{-2}. Moreover, the variability of residuals values derived from model 3 is high with standard deviation of 0.47.

Model 4: Combination of EPS and tube building worms as a proxy

To examine the dependence of critical erosion shear stress on EPS concentration, EPS data from all stations except station B was firstly regressed on critical erosion shear stress values. Station B was excluded from the regression analysis because it had high densities of mud snail *Hydrobia ulvae*, which are known to excrete significant amount of mucilage. On first appearance, the relationship between EPS and critical erosion shear stress showed station-specific characteristics with a pronounced bifurcation in the data (Figure 3.3b and Table 6.2). Stations A and D showed a high rise of critical erosion shear stress with increased EPS, while station C and E showed a low rise of critical erosion shear stress with increased EPS. Both low and high rise of critical erosion shear stress with increased EPS was evident at station F.

Table 6.2. Regression equations, coefficients of determination, and significance levels of relationship between EPS (X) and critical erosion shear stress (Y) (compare Figure 3.3b).

Type of relationship	Regression equation	coefficient of determination	Significance level
All stations	Y = 0.0015X + 0.4456	$r^2 = 0.54$	$p < 0.01$
Station A only	Y = 0.0043X + 0.0254	$r^2 = 0.85$	$p < 0.01$
Station C only	Y = 0.0013X + 0.3175	$r^2 = 0.95$	$p < 0.01$
Station D only	Y = 0.0035X + 0.3423	$r^2 = 0.65$	$p < 0.01$
Station E only	Y = 0.0014X + 0.4171	$r^2 = 0.66$	$p < 0.01$
Station F only	Y = 0.0015X + 0.5194	$r^2 = 0.58$	$p < 0.01$

The bifurcation in the data suggests that the structure is non-linear and therefore cannot be detected by statistical methods based on linear regression models. One approach to disentangle the station pattern

(bifurcation) of the relationship between EPS concentrations and critical erosion shear stresses is to look at other potential parameters that may have a direct or indirect influence on critical erosion shear stress. These parameters include drying of sediment surface (normalized water content), mud content, microphytobenthos assemblage, *Macoma baltica* as a documented sediment destabilizer which was present at nearly all stations, and individuals and the sum of species of tube building worms. Since the separation between the two branches observed in Figure 3.3b is evident only for critical erosion shear stresses above 1 N m^{-2} and EPS concentrations above 400 mg m^{-2} only results from those samples fulfilling these conditions are considered. Among the above listed parameters only the sum of the tube building worms showed the above described station pattern. As shown in Figure 6.5, stations A and D belong to group with high densities (> 2000 individuals m^{-2}) of tube building worms, while stations C and E belong to the low density group (< 2000 individuals m^{-2}). Station F falls within both the high and low density group. *Macoma baltica* on the other hand shows no distinctive station pattern.

As the sum of tube building worms showed the station pattern of the two branches observed when critical erosion shear stresses are plotted versus EPS concentrations, it is expected that the different densities of tube building worms present in the sediments to some extent may explain the bifurcation of the relationship between EPS and critical erosion shear stress. To test this hypothesis, the data were split according to the sum of tube building worms density. As shown in Figure 6.6, much clearer dependencies of critical erosion shear stress on EPS emerge after the data were split into density < 2000 and > 2000 indiv. m^{-2}. Regression analysis of both data sets showed a statistically significant linear relationship between EPS and critical erosion shear stress ($P < 0.01$ for both cases). For the data set of densities < 2000 indiv. m^{-2}, the linear model explained 85 % of the variation in the critical erosion shear stress, and for the data set of densities > 2000 indiv. m^{-2} the model explained 81 % of the observed variability. For comparison, the same grouping applied to chlorophyll-a concentrations but no improvement of the critical erosion shear stress and chlorophyll-a relationships emerge (see Figure 6.7).

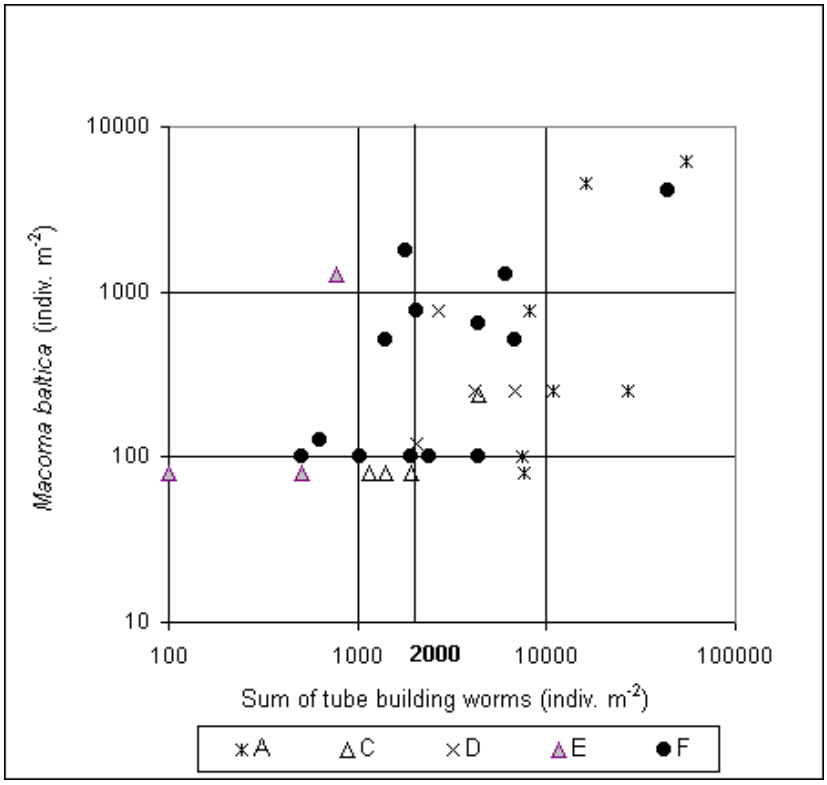

Figure 6.5. Density of *Macoma baltica* versus the sum of tube building worms. Note that only samples with critical erosion shear stresses higher than 1 N m^{-2} and EPS concentrations higher than 400 mg m^{-2} were used.

The density of 2000 indiv. m^{-2} was used to separate the data because here the separation looks clearest in Figure 6.5. Since to use this density value for the separation looks somewhat arbitrary, the sensitivity of this model was investigated by varying the separation density between 1000 and 4500 indiv. m^{-2}. Figure 6.8 shows the relationship between the coefficient of determination (r^2) and the sum of tube building worms separation density. The polynomial fit yields a maximum of r^2 around 3000 indiv. m^{-2}, but the maximal r^2 is indeed at 2000 indiv. m^{-2}. The slow decrease of r^2 with increasing separation density is due to the fact that there are only few samples in this region.

It should be noted that at low EPS concentrations (i.e. low micro-phytobenthos biomass and weak biofilm) there is still relatively high scatter in the data (between 0.2 and 1.0 N m^{-2}). This was probably due to the spatial patchiness of EPS concentrations (i.e. difference between inside and outside erosion core), small-scale patchiness of biofilm strength, cracks, and holes

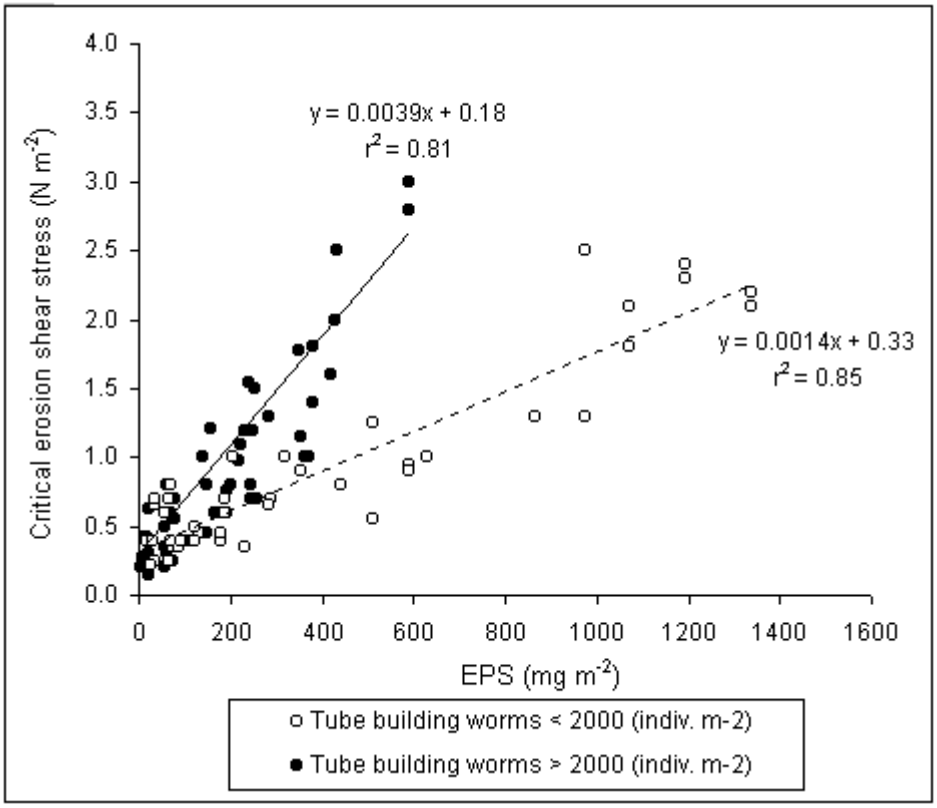

Figure 6.6. Relationships between EPS concentrations and critical erosion shear stresses for low and high tube building worms densities.

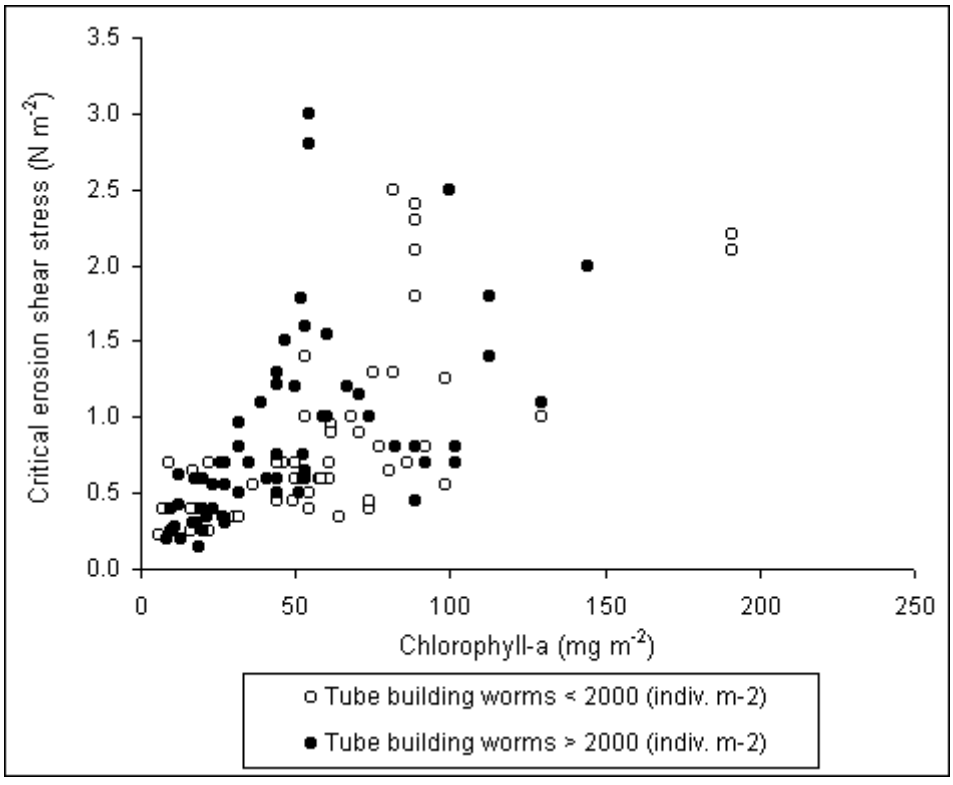

Figure 6.7. Relationships between chlorophyll-a concentrations and critical erosion shear stresses for low and high tube building worms densities.

inside the erosion core. Moreover, with absence or lack biological influence, physical sediment properties may better explain the variability of critical erosion shear stress. For example, Riethmüller et al. (2000) found that for chlorophyll-a less than 20 mg m^{-2} the variation of the data could be better explained by wet bulk density as was found also by Williamson and Ockenden (1996) and Amos et al. (1998). In contrast to these studies, the dependence of critical erosion shear stress on wet bulk density for low chlorophyll-a (less than 20 mg m^{-2}) and EPS (less than 100 mg m^{-2}) samples was not observed in the present study.

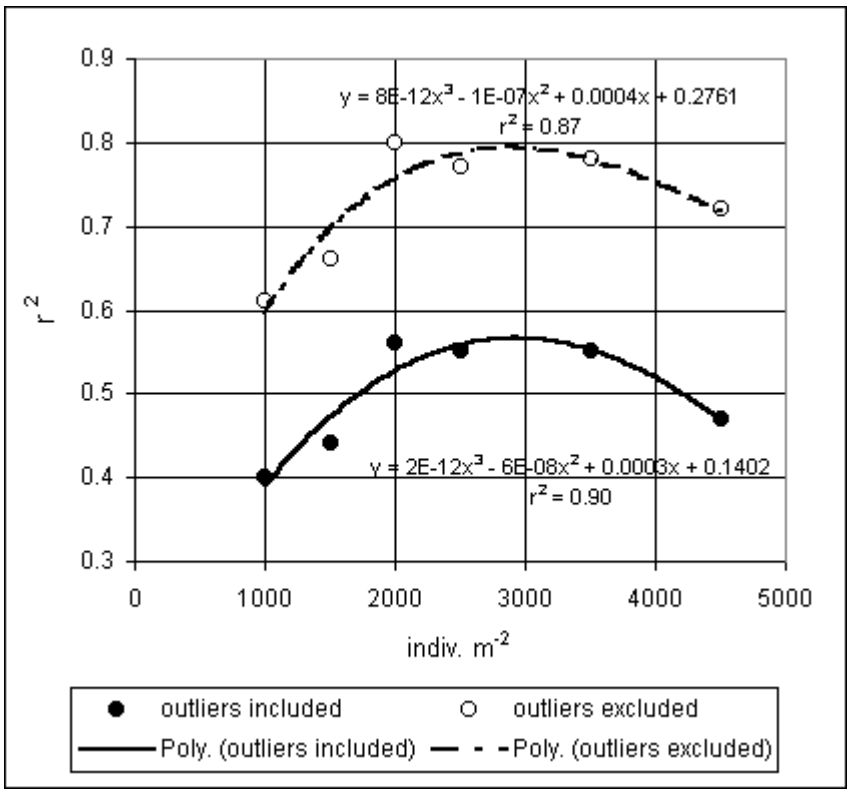

Figure 6.8. The polynomial relationship between coefficient of determination (r^2) and the sum of tube building worms separation density. Outliers are those samples where the erosion experiment was stopped without reaching the critical shear stress.

In the model 4, the critical erosion shear stresses were predicted separately for densities of tube building worms lower and higher than 2000 indiv. m^{-2} using the corresponding regression equations shown in Figure 6.6 and then compared with the observed values. As shown in Figure 6.9, this model explains 80 % of the variances when the outliers are excluded. In addition, the bias of predicted values relative to the measured values is very

low and the saturation of prediction nearly not observed. Noted that two of the three outliers belong to the samples with extremely high density of worms.

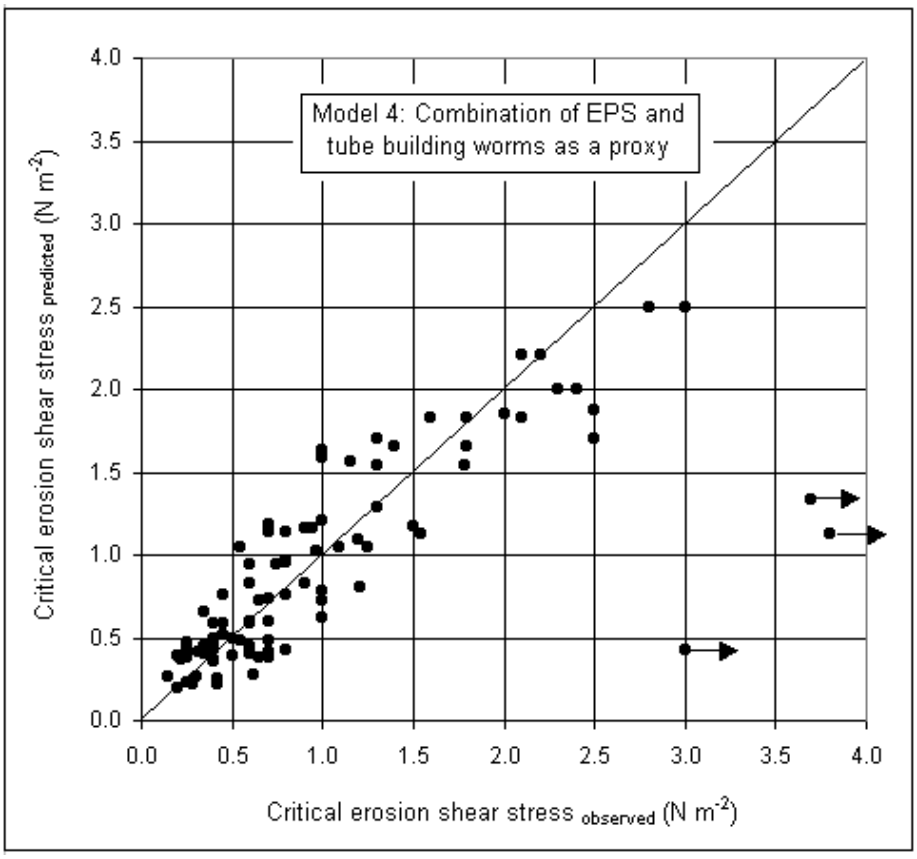

Figure 6.9. Comparison of observed and predicted critical erosion shear stress derived from calibrations with EPS and sum of tube building worms density. The data with arrows (outliers) were omitted in the regression analysis because the upper limit of the erosion device was reached.

6.3. Discussion and conclusions

The advantages and disadvantages of predicting critical erosion shear stress from chlorophyll-a with global calibration (model 1), chlorophyll-a with site specific calibration (model 2), a combination of EPS and mud content (model 3), and a combination of EPS and tube building worms (model 4) are listed in Table 6.3.

Predicting critical erosion shear from chlorophyll-a by a global calibration (model 1) is technically relatively straightforward. Moreover, chlorophyll-a can be detected and quantitatively estimated from sediment surface reflectance spectra in the optically observable spectral range (e.g. Hakvoort et al. 1998, Paterson et al. 1998). Hence chlorophyll-a is apparently a potential proxy para-

Table 6.3. The pros and cons of each predictive model. The expression “high”, “medium” and “low” are used to simplify the assessment and are explained in the text in more detail.

	Type	Optically detectable	Demand of methodology	Power of prediction (r^2) (excl. outlier)	Bias	Standard deviation of residual value
Model 1	Only chlorophyll-a, global calibration	Yes	Low	0.35	High	0.48
Model 2	Only chlorophyll-a Site specific calibrations	Yes	Low	0.51	mediu m	0.43
Model 3	Stepwise multiple linear regression	No	High	0.38	High	0.47
Model 4	EPS and tube building worms	No	High	0.80	Low	0.29

meter for the purpose of large scale mapping of sediment surface erosion parameters. However, the results of this study showed that chlorophyll-a alone is a poor predictor of critical erosion shear stresses: the relationships are either highly site-specific or poor at all (stations A and B). This results in large variability of the residuals between predicted and observed values. Additionally, the predicted values are highly biased from the observed one and saturate at critical erosion shear stresses of 2.3 N m^{-2}. In addition, the use of chlorophyll-a as a proxy of critical erosion shear stress in remote sensing technique is only suitable for bare intertidal areas, as substrata lying beneath plant canopies are not available for assessment by remote sensing (Friend et al. 2003a).

In model 2, chlorophyll-a was used as a predictor of critical erosion shear stress, but with a site-specific calibration. Model 2 gives a better prediction than model 1. This is indicated by higher r^2 and lower variability of the residual values. In addition, the predicted values derived from this model are somewhat less biased, at least up to a critical shear stress of 1.5 N m^{-2}. Therefore, model 2 is a better option when using chlorophyll-a to predict

critical erosion shear stress. However, a disadvantage of this model is that field surveys are required to establish the site-specific calibrations and to define the habitat boundaries of each site.

Similar to model 1, model 3 (a combination of EPS and mud content) gives a bad prediction. The model does not fit the data very well, it produces relatively high variability of the residual values and the predictions saturate already at 1.3 N m^{-2}. Other disadvantages of this model are that parameters involved in the model are only partly detectable by optical remote sensing techniques. In addition the determination of EPS concentrations is methodologically demanding and time consuming. Therefore, a combination EPS and mud content is by no means a good set of proxy parameters for the purpose of large scale mapping of sediment surface erosion parameters.

A combination of EPS concentration and tube building worms yields a quite nice prediction of critical erosion shear stresses. It explains more than 80 % of the observed variability, has very little bias and does not show significant bias. In addition, it explains qualitatively two of the three outliers as cases for extreme high worm densities present. However, for the large-scale mapping by optical remote sensing, these two parameters cannot be directly used as proxy parameters. This is because the remote sensing of EPS and macrofauna is not possible. In addition, predicting critical erosion shear stress by taking measurements of EPS concentration and worm density is methodologically demanding and more time consuming than conducting erosion experiments directly.

CHAPTER 7
GENERAL DISCUSSION AND CONCLUDING REMARKS

7.1. The variation of sediment erodibility

The variation of sediment erodibility at each station was more correlated with chlorophyll-a, colloidal carbohydrate, and EPS than other measured sediment parameters. This indicated that benthic diatom was the main parameters determine the variation of sediment erodibility. Other factors, on other hand, may amplify or reduce the stabilizing effect of benthic diatoms. For example, high density of *Hydrobia ulvae* at station B reduced the amount of benthic diatoms through grazing and hence lowers the stabilizing effect of benthic diatoms. In contrast, the stabilizing effect of benthic diatom at station A was amplified by the physical process of drying and by the presence of high density of tube building worms.

The direct effect of benthic macrofauna on the sediment erodibility was only locally detectable and less dominant compared to the effect of benthic diatom. There was a direct relationship between *Hydrobia ulvae* and erosion rate at station A which the erosion rate increased with increasing the density of *Hydrobia ulvae*. These snails can enhance erosion directly by moving trough the surface sediment and by loosening the sediment through pelletization of the surface material (Andersen 2001a). As erosion rate at station A was relatively low compared to other stations (except station F), the destabilizing effect of *Hydrobia ulvae* appears to be overridden by the stabilizing effects of other factors such as biostabilization by benthic diatom and tube building worms and physical process of drying.

The results from study of erosion potential over bedforms suggest that presence of bedforms may introduce different modes of erosion. The sediments deposited on the crests were more stable than those in the troughs. Crests are completely emerged during low tide and progressively dry out, whereas troughs are often covered with a thin layer of trapped or slowly running water. Reduced water content on the crest results in sediment with increased strength and hence greater resistance to erosion. This drying effect on sediment stability on the crests was particularly important at most lanward

station (station A) where the emersion period is long enough to allow significant drying. The higher benthic diatom biomass on the crests is also likely to stabilize the sediment surface of these features. This process was more important at seaward stations (B–F). The small-scale variability in the sediment erodibility due to the presence of bedforms suggests that the occurrence of bedforms should not be ignored when modeling mudflat development.

Sediments were generally more stable in September 2002 compared to other sampling periods, and this was associated with the presence of visible benthic diatom biofilms, as supported by the markedly higher chlorophyll-a, colloidal carbohydrate, and EPS in the period. The temporal pattern of sediment erodibility at the study site can not be explained by median grain-size, mud content, water content, and organic content of the sediment since these parameters did not vary much during the study. Instead, the temporal (seasonal) variation of sediment erodibility was controlled mainly by the temporal (seasonal) variation of benthic diatom abundance (measured as chlorophyll-a) and carbohydrate concentration of the sediment. Higher chlorophyll-a concentration that observed in September 2002 (early autumn) was probably due to higher light availability and nutrient level during the period. In contrast, lower values observed in June 2001 (summer) may be caused by several factors such as nutrient limitation and grazing by macro- or meiofauna.

Spatial analysis of sediment erodibility showed that the sediments were more stable at station A (close to the salt marsh) and station F (middle tidal flat). The higher stability at station A was attributed to be the results of physical process of drying and biostabilization by tube building worms. Higher level of biostabilization by benthic diatoms was the main cause of the higher stability at station F. Moreover, the presence of mussel beds probably minimized the physical disturbance (waves or currents) of the surficial sediment structure at station F. Minimal disturbance would not only facilitate the accumulation of mucilage in surface sediment but also minimized susceptibility to particle entrainment (Kornman and de Deckere, 1998). By contrast, the erosion rates were highest at the site dominated by *Hydrobia*

ulvae (station B) and this was attributed to the destabilizing effect of *Hydrobia ulvae*.

A strategy to obtain the large-scale distribution of critical erosion shear stress is to establish relationship to proxy parameter that can be mapped either by field surveys or by remote sensing techniques. Ideally, the proxy should be easily sampled and measured and can be optically detected by remote sensing techniques. Chlorophyll-a is one of the potential proxies that meet this criterion. Although this study showed that chlorophyll-a alone is a poor predictor of critical erosion shear stress, the use of chlorophyll-a to predict critical erosion shear stress will provide more realistic threshold values for natural sediments of a given grain-size than the values obtained from criteria develop for abiotic sediments. Moreover, predicting critical erosion shear stress from chlorophyll-a can be further improved by making a site-specific calibration. A combination of EPS concentration and tube building worms yields a quite nice prediction of critical erosion shear stresses. However, for the large-scale mapping by optical remote sensing, these two parameters cannot be directly used as proxy parameters since they are not optically detectable. In addition, predicting critical erosion shear stress by taking measurements of EPS concentration and worm density is methodologically demanding and more time consuming than conducting erosion experiments directly.

From this study one can conclude that spatial and temporal pattern of sediment erodibility at the study site was closely linked to the spatial and temporal variation of benthic diatoms. Moreover, this study showed that the physical factors like drying of sediment due to prolonged air exposure may be just as significant for sediment erodibility variation as biological factors.

7.2. Recommendation for further work

The present study was conducted with several limitations, so that we are still unable to answer all questions concerning the spatial and temporal variation of sediment erodibility at the intertidal flat. However, fundamental information was achieved, enabling the improvement our understanding on erosion characteristics of intertidal flat sediment.

In the present study, the samplings were restricted only to the inner and middle zones of Dornumer Nacken intertidal flat. In order to have a complete picture of the erosion parameter variability of the site, there is a need to extend the erosion study to the outer zone (sandy area) of the site.

The information on variability of erosion parameters in the winter situation is still missing in the present study. Therefore, it is recommended to conduct erosion experiments during winter in order to have a complete temporal pattern of the erodibility at the study site.

Our results showed that the relationships between chlorophyll-a and critical erosion shear stress are generally strong and are not the function of season. So, it should be possible to generate a map of critical erosion shear stress from chlorophyll-a distribution with a site-specific calibration. Mapping of critical erosion shear stress at the site using chlorophyll-a as proxy would be the next challenge.

REFERENCES

Amos, C.L., 1995. Siliciclastic tidal flats. In: Perillo (ed.). *Geomorphology and Sedimentology of Estuaries. Development in Sedimentology*. Elsevier, Amsterdam. Vol. 53, 273–306.

Amos, C.L., Brylinsky, T.F., Sutherland, T.F., O'Brien, D., Lee, S., and Cramp, A., 1998. The stability of a mudflat in the Humber estuary, South Yorkshire, UK. In: Black, K.S., Paterson, D.M. and Cramp, A. (eds). *Sedimentary Processes in the Intertidal Zone*. Geological Society London, Special Publications 139, 231–241.

Amos, C.L., Daborn, G.R., Christian, H.A., Atkinson, A., and Robertson, A., 1992. In situ erosion measurements on fine-grained sediments from the Bay of Fundy. Marine Geology 108, 175–196.

Amos, C.L., Feeney, T., Sutherland, T.F., and Luternauer, J.L., 1997. The stability of fine-grained sediments from the Fraser River Delta. Estuarine, Coastal and Shelf Science 45, 507–524.

Amos, C.L., Van Wagoner, N.A., and Daborn, G.R., 1988. The influence of subaerial exposure on the bulk properties of fine-grained intertidal sediment from Minas Basin, Bay of Fundy. Estuarine, Coastal, and Shelf Science 27, 1–12.

Andersen, T.J., 2001 (a). Seasonal variation in erodibility of two temperate, microtidal mudflats. Estuarine, Coastal, and Shelf Science 53, 1–12.

Andersen, T.J., 2001 (b). Cohesive sediment transport in coastal lagoons with special emphasis on the biological influence on the erosion and deposition of fine-grained material. Phd thesis. Uneversity of Copenhagen.

Andersen, T.J., Jensen, K.T., Lund-Hansen, L., Mouritsen, K.N., and Pejrup, M., 2002. Enhanced erodibility of fine-grained marine sediments by *Hydrobia ulvae*. Journal of Sea Research 48, 51–58.

Andersen, T.J., Lanuru, M, van Bernem, C., Pejrup, M., and Riethmüller, R. (in review). Erodibility of a mixed mudflat inhabited by *Cardium edule* and *Heteromastus filiformis*, East Frisian Wadden Sea, Germany.

Andersen, T.J., and Pejrup, M., 2002. Biological mediation of the settling velocity of bed material eroded from an intertidal mudflat, the Danish Wadden Sea. Estuarine, Coastal and Shelf Science 54, 737–745.

Anderson, F.E., and Howell, B.A., 1984. Dewatering of an unvegetated muddy tidal flat during exposure--Desiccation or drainage? Estuaries 7, 225 –232.

Augustinus, P.G.E.F., 2002. Biochemical factors influencing deposition and erosion of fine grained sediment. In: Healy, T., Wang, Y., and Healy, J.A. (eds.). *Muddy Coasts of the World: Processes, Deposits, and Function*. Proceeding in Marine Science 4, 203–228.

Austen, I., 1997. Temporal and spatial variations of biodeposits – a preliminary investigation of the role of fecal pellets in the Sylt-Rømø tidal area. Helgolander Meeresuntersuchungen 51, 281–294.

Austen, I.,Andersen,T.J. and Edelvang, K., 1999. The influence of benthic diatoms and invertebrates on the erodability of an intertidal mudflat, the Danish Wadden Sea. Estuarine, Coastal, and Shelf Science 49, 99–111.

Black, K.S. and Paterson, D.M., 1997. Measurement of the erosion potential of cohesive, marine sediments: a review of current in situ technology. Journal of Marine Enviromental Engineering 4, 43–84.

Black, K.S., Tolhurst, T.J., Paterson, D.M., Hagerthey, S.E., 2002. Working with natural cohesive sediments. Journal of Hydraulic Engineering 128, 1–7.

Blanchard, G.F., Paterson, D.M., Stal, L.J., Richard, P., Galois, R., Huet, V., Kelly, J., Honeywill, C., de Brouwer, J., Dyer, K.R., Christie, M., and Seguignes, M., 2000. The effect of geomorphological structures on potential biostabilisation by microphytobenthos on intertidal mudflats. Continental Shelf Research 20, 1243–1256.

Blanchard, G.F., Sauriau, P.G., Cariou-Le Gall, V., Gouleau, D., Garet, M.J., and Oliver, F., 1997. Kinetics of tidal resuspension of microbiota: testing the effect of sediment cohesiveness and bioturbation using flume experiment. Marine Ecology Progress Series 151, 17–25.

Cadée, G.C., 1979. Sediment reworking by the polychaete Heteromastus filiformis on a tidal flat in the Dutch Wadden Sea. Netherlands Journal of Sea Research 13, 441–456.

Cadée, G.C., 2001. Sediment dynamics by bioturbating organisms. In: Ecological studies, vol. 151. K. Reise (ed.). Ecological Comparisons of sedimentary shores. Springer-Verlag Berlin Heidelberg. pp. 127–148.

Cadée, G.C., and Hegeman, J. 1977. Distribution of primary production of the benthic microflora and accumulation of organic matter on a tidal flat area, Balgzand, Dutch Wadden Sea. Netherlands Journal of Sea Research 11, 24–41.

Christie, M.C., Dyer, K.R., Blanchard, G., Cramp, A., Mitchener, H.J., and Paterson, D.M., 2000. Temporal and spatial distributions of moisture and organic contents across a macro-tidal mudflat. Continental Shelf Research 20, 1219–1241.

Colijn, F and Dijkema, K.S., 1981. Species composition of benthic diatoms and distribution of chlorophyll a on an intertidal flat in the Dutch Wadden Sea. Marine Ecology Progress Series 4, 9–21.

Cornelisse, J.M., Mulder, H.P.J., Williamson, H.Y., Witte, G. and Houwing, E.J., 1994. On the development of instruments for *in situ* erosion measurement. *Fourth Nearshore and Estuarine Cohesive Sediment Transport Conference*, Wallingford. pp. 175–186.

Dade, W.B., Nowell, A.R.M., and Jumars, P.A., 1992. Predicting erosion resistance of mud. Marine geology 105, 285–297.

Dauer, D.M., Maybury, C.A., and Ewing, R.M., 1981. Feeding behavior and general ecology of several spionids polychates from the Chesapeake Bay. Journal of Experimental Marine Biology and Ecology 54, 2–38.

de Brouwer, J.F.C., Bjelic, S., de Deckere, E.M.G.T., and Stal, L.J., 2000. Interplay between biology and sedimentology in a mudflat (Biezelingse Ham, Westerschelde, The Netherlands). Continental Shelf research 20, 1159–1177.

de Brouwer, J.F.C., de Deckere, E.M.G.T., and Stal, l.J., 2003. Distribution of extracellular carbohydrates in three intertidal mudflats in Western Europe. . Estuarine, Coastal, and Shelf Science *56*, 313–324.

de Deckere, E.M.G.T., Tolhurst, T.J., and de Brouwer, J.F.C., 2001. Destabilization of cohesive intertidal sediments by infauna. Estuarine, Coastal and Shelf Science 53, 665–669.

de Deckere, E.M.G.T., van de Koppel, J., and Heip, C.H.R., 2000. The influence of Corophium volutator abundance on resuspension. Hydrobiologia 426, 37–42.

Defew, E.C., Tolhurst, T.J., and Paterson, D.M., 2002. Site-specific features influence sediment stability of intertidal sediments. Hydrology and Earth System Sciences 6, 971–982.

Dubois, M., Giles, K.A., Hamilton, J.K. Rebers, P.A., and Smith, F., 1956. Colorimetric methods for determination of sugars and related substances. Analytical Chemistry 28, 350–356.

Dyer, K.R., 1986. *Coastal and Estuarine Sediment Dynamics* (337 pp.). Chichester: Wiley.

Eckman, J.E., Nowell, A.R. and Jumars, P.A., 1981. Sediment destabilization by animal tubes. Journal of Marine Research 39, 361–374.

Flemming, B. W., 2000. A revised textural classification of gravel-free muddy sediments on the basis of ternary diagrams. Continental Shelf Research 20, 1125–1137.

Flemming, B. W., and Delafontaine, M.T., 2000. Mass physical properties of muddy intertidal sediments: some applications, misapplications, and non-applications. Continental Shelf Research 20, 1179–1197.

Fowler, J., and Cohen, L., 1997. *Practical statistics for field biology* (227 pp.). Chichester: Wiley.

Friend, P.L., 2001. Biological influences on the stability of intertidal flat sediments. PhD thesis. University of Southhampton. pp. 223.

Friend, P.L., Ciavola, P., Cappucci, S., and Santos, R., 2003 (a). Bio-dependent bed parameters as a proxy tool for sediment stability in intertidal areas. Continental Shelf Research 23, 1899–1917.

Friend, P.L., Collins, M.B., and Holligan, P.M., 2003 (b). Day-night variation of intertidal flat sediment properties in relation to sediment stability. Estuarine, Coastal, and Shelf Science 58, 663–675.

Gerdol, V., and Hughes, R.G., 1994. Effect of Corophium volutator on the abundance of benthic diatoms, bacteria and sediment stability in two estuatries in southeastern England. Marine Ecology Progress Series 114, 109–115.

Graf, G. and Rosenberg, R., 1997. Bioresuspension and biodeposition. Journal of Marine Systems 11, 269–278.

Grant, J., Bathmann, U.V., and Mills, E.L., 1986. The interaction between benthic diatom films and sediment transport. Estuarine, Coastal, and Shelf Science 23, 225–238.

Grant, J., and Gust, G., 1987. Prediction of coastal sediment stability from photopigment content from mats of purple sulphur bacteria. Nature 330, 244–246.

Grant, W.D., Boyer, L.F., and Sanford, L.P., 1982. The effects of bioturbation on the initiation of motion of intertidal sands. Journal of Marine Research 40, 659–677.

Guarini, J., Blanchard, G.F., Bacher, C., Gros, P., Riera, P., Richard, P., Gouleau, D., Galois, R., Prou, J., and Sauriau, P.G., 1998. Dynamics of spatial patterns of microphytobenthic biomass:inferences from a geostatistical analysis of two comprehensive surveys in Marennes-Oleron Bay (France). Marine Ecology Progress Series 166, 131–141.

Gust, G. and Müller, V., 1997. Interfacial dynamics and entrainment functions of currently used erosion devices. In: Burt, N., Parker, R., Watt, J. (eds) : Cohesive Sediments. Wiley, New York. pp. 149–174.

Hakvoort, J.H.M., Heineke, M., Heymann, K., Kühl, H., Riethmüller, R., and Witte, G., 1998. A basis for mapping erodibility of tidal flats by optical remote sensing. Marine and Freshwater Research 49, 867–873.

Hartley, B., 1996. In: An Atlas of British Diatoms. Biopress Ltd, Bristol, England, pp. 601.

Haven, D.S., and Morales-Alamo, R., 1966. Aspects of biodeposition by oysters and other invertebrate filter feeders. Limnology and Oceanography 11, 487–498.

Hay, S.J., Maitland, T.C., and Paterson, D.M., 1993. The speed of diatom locomotion through natural and artificial substrata. Diatom Research 8, 371–384.

Heinzelmann, C. H. and Wallisch, S., 1991. Benthic settlement and bed erosion. A review. Journal of Hydraulic Research 29, 355–371.

Holland, A.F., Zingmark, R.G., and J.M, Dean., 1974. Quantitative evidence concerning the stabilization of sediments by marine benthic diatoms. Marine Biology 27, 191–196.

Houwing, E.J., 1999. Determination of the critical erosion threshold of cohesive sediments on intertidal mudflats along the Dutch Wadden Sea coast. Estuarine, Coastal, and Shelf Science 49, 545–555.

Houwing, E. J., and Van Rijn, L. C., 1998. In Situ Erosion Flume (ISEF); determination of bed shear stress and erosion of a kaolinite bed. Journal of Sea Research 39, 243–253.

Hustedt, F., 1930. Die Kieselalgen Deutschlands, Österreichs und der Schweiz. 1.Teil. Akademische Verlagsgesellschaft mbH, Leipzig (in German).

Hustedt, F., 1959. Die Kieselalgen Deutschlands, Österreichs und der Schweiz. 2. Teil. Reprint Otto Koeltz Science Publishers, Königsstein 1977 (in German).

Jumars, P.A., and Nowell, A.R.M., 1984. Effect of benthos of sediment transport : difficulties with functional grouping. Continental Shelf Research 3, 115–130.

Kocum, E., Nedwell, D.B., and Underwood, G.J.C., 2002. Regulation of phytoplankton primary production along a hypernutrified estuary. Marine Ecology Progress Series 231, 13–22.

Kornman, B.A. and de Deckere, E.M.G.T., 1998. Temporal variation in sediment erodibility and suspended sediment dynamics in the Dollard estuary. In: Black, K.S., Paterson, D.M. and Cramp, A. (eds). *Sedimentary Processes in the Intertidal Zone*. Geological Society London, Special Publications 139, 231–241.

Krögel, F. and Flemming, B.W., 1998. Evidence for temperature-adjusted sediment distribution in the back barrier tidal fltas of the East Frisian Wadden Sea (Southern North Sea). In C.R. Alexander, R.A. Davis, and V.J. Henry (Eds.), *Tidalites: Processes and products*. *SEPM special publication*, *61* (pp. 31–41).

Lelieveld, S.D., Pilditch, C.A., and Grenn, M.O., 2003. Variation in sediment stability and relation to indicators of microbial abundance in the Okura Estuary, New Zealand. Estuarine, Coastal and Shelf Science 57, 123–136.

Lopez, G.R. and Kofoed, L.H., 1980. Episammic browsing and deposit feeding in mud snails (Hydrobiidae). Journal of Marine Research 38, 585–599.

Lund-Hansen, L.C., Laima, M., Mouritsen, K., Lam, N.N., and Hai, D.N., 2002. Effects of benthic diatoms, fluff layer, and sediment condition on critical shear stress in a non-tidal coastal environment. Journal of the Marine Biological Association United Kingdom 82, 3855.2–3855.8.

Maa, J.P.Y., Sanford; L., and Halka, J.P., 1998. Sediment resuspension characteristics in Baltimore Harbour, Maryland. Marine Geology 146,137–145.

Maa, J. P.Y., Wright, L. D., Lee, C.H., and Shannon T. W., 1993. VIMS Sea Carousel: A field instrument for studying sediment transport. Marine Geology 115, 271–287.

Madsen, K.N., Nilsson, P., and Sundbäck, K., 1993. The influence of benthic micro algae on the stability of a subtidal seiment. Journal of Experimental Marine Biology and Ecology 170, 159–177.

Manzenrieder, H. 1983. Retardation of initial erosion under biological effects in sandy tidal flats, Leichtweiss, Inst. Tech. Univ. Braunschweig, 469–479.

Meadows, P.S. and Tait, J., 1989. Modification of sediment permeability and shear strength by two burrowing invertebrates. Marine Biology 101, 75–82.

Mehta, A.J., 1988. Laboratory studies of cohesive sediment deposition and erosion. In: Dronker, J., and van Leussen, W. (eds.). *Physical Processes in Estuaries*. Springer, Berlin, pp. 427–445.

Mehta, A.J., Parchure, T.M., Dixit, J.G., and Ariathurai, R., 1982. Resuspension potential of deposited cohesive sediment beds: In V.S. Kennedy (ed.), Estuarine Comparisons. Academic Press, pp.591–609.

Mitchener, H., and Torfs, H., 1996. Erosion of mud/sand mixtures. Coastal Engineering 29, 1–25.

Mouritsen, K.N., Mouritsen, L.T., and Jensen, K.T., 1998. Change of topography and sediment characteristics on an intertidal mud-flat following mass-mortality of the amphipod Corophium volutator. Journal of the Marine Biological Association United Kingdom 78, 1167–1180.

Newel, R.I.E., Cornwell, J.C., and Owens, M.S., 2002. Influence of simulated bivalve biodeposition and microphytobenthos on sediment nitrogen dynamics: A laboratory study. Limnology and Oceanography 47, 1367–1379.

Nowel, A.R.M. and Church, M., 1979. Tubulent flow in a depth-limited boundary layer. Journal of Geophysical Research 84, 4816–4824.

Nowell, A.R.M., Jumars, P.A., and Eckman, J.E., 1981. Effects of biological activity on the entrainment of marine sediments. Marine Geology 42, 133–153.

Open university course team, 1989. Waves, tides, and shallow-water processes. Butterworth-Heinemann, Oxford. pp. 187.

Pankow, H., 1990. In: Ostsee- Algenflora. G. Fischer Verlag, Jena, pp. 648 (in German).

Paterson, D.M., 1988. The influence of epipelic diatoms on the erodibility of an artificial sediment. *Proceeding of the 10th International Symposium on Living and Fossil Diatoms*, 345–355.

Paterson, D.M., 1989. Short term changes in the erodibility of intertidal cohesive sediments related to the migratory behaviour of epipelic diatoms. Limnology and Oceanography 34, 223–234.

Paterson, D.M., 1994. Microbial mediation of sediment structure and behaviour. In: Stal, L.J., and Caumette, P. (eds.) NATO ASI Series, vol G35, Microbial Mats. Springer Verlag, Berlin, pp. 97–109.

Paterson, D.M., 1997. Biological mediation of sediment erodibility: ecology and physical dynamics. In: Burt, N., Parker, R., and Watts, J. (Eds), Cohesive sediments. John Wiley & Sons, London, pp. 215–229.

Paterson, D.M., and Black, K.S., 1999. Water flow, sediment dynamics and benthic biology. Advances in Ecological Research 29, 155–193.

Paterson, D.M., Crawford, R.M., and Little, C., 1990. Subaerial exposure and changes in the stability of intertidal estuarine sediment. Estuarine, Coastal, and Shelf Science 30, 541–556.

Paterson, D.M., Tolhurst, T.J., Kelly, J.A., Honeywill, C., de Deckere, E.M.G.T., Huet, V., Shaylor, S.A., Black, K.S., de Brouwer, J., and Davidson, I., 2000. Variation in sediment stability and sediment properties across the skeffling mudflat, Humber Estuary, U.K. Continental Shelf Research 20, 1373–1396.

Paterson, D.M., Wiltshire, K.H., Miles, A., Blackburn, J., Davidson, I., Yates, M.G., McGrorty, S., and Eastwood, J.A., 1998. Microbiological mediation of spectral reflectance from intertidal cohesive sediments. Limnology and Oceanography 43, 1207–1221.

Postma, H., 1961. Transport and accumulation of suspended matter in the Dutch Wadden Sea. Netherlands Journal of Sea Research 1, 148–190.

Postma, H., 1967. Sediment transport and sedimentation in the estuarine environment. In Lauff, G.H. (ed.). *Estuaries*. American Association for the Advancement of Science Publ., pp. 158–184.

Raudkivi, A.J., 1998. Loose boundary hydraulics. 3rd Edition. Balkema, Rotterdam.

Rhoads, D.C., 1974. Organism-sediment relations on the muddy sea floor. Oceanography and Marine Biology Annual Review 12, 263–300.

Rhoads, D.C., Yingst, J.Y. and Ullmann, W. J., 1978. Seafloor stability in Central Long Island Sound: Part I Temporal changes in erodibility of fine-grained sediment. In Wiley, M. L. (ed.). *Estuarine Interactions*. pp. 221–244.

Riethmueller, Heineke, M., Kuehl, H. and Keuker-Rüdiger, R., 2000. Chlorophyll a concentration as an index of sediment surface stabilisation by microphytobenthos? Continental Shelf Research 20, 1351–1372.

Riethmueller, R., Haakvoort, J.H., Heineke, M., Heymann, K., Kuehl, H. and Witte, G., 1998. Relating shear stress to tidal flat surface color. In K.S. Black, D.M. Paterson, and A. Cramp (Eds.), *Sedimentary processes in the intertidal zone*. *Special publication*, 139 (pp. 283–293). London: Geological Society.

Rissgård, H.U. and Kamermsn, P., 2001. Switching between deposit and suspension feeding in coastal zoobenthos. In: Ecological studies, vol. 151. K. Reise (ed.). Ecological Comparisons of sedimentary shores. Springer-Verlag Berlin Heidelberg. pp. 73–101.

Rowden, A.A., Jago, C.F., and Jones,S.E., 1998. Influence of benthic macrofauna on the geotechnical and geophysical properties of surficial sediment, North Sea. Continental Shelf Research 18, 1347–1363.

Sanford, L.P. and Halka, J.P., 1993. Assessing the paradigm of mutually exclussive erosion and deposition of mud, with examples from upper Chesapeake Bay. Marine Geology 114, 37–57.

Sanford, L.P. and Maa, J.P.Y. 2001. A unified erosion formulation for fine sediments. Marine Geology 179, 9–23.

Schunemann, M., and Kuhl, H., 1991. *A device for erosion measurement on naturally formed, muddy sediments : the EROMES system* (28 pp). Report of GKSS Research Centre GKSS 91/E/18.

Smaal, A.C:, Verhagen, J.H.G, Coosen, J., and Haas, H.A., 1986. Interaction between sestom Quantity and quality and benthic suspension feeders in the Oosterschelde, the Netherlands. Ophelia 26, 385–399.

Soulsby, R.L., and Whitehouse, R., 1997. Thereshold of sediment motion in coastal environment. In: Proc Pacific Coast and Ports Conf 1, University of canterbury, Christchurch, New Zealand, pp 149–154.

Sündback, K., 1984. Distribution of microbenthic chlorophyll a and diatom species related to sediment characteristics. Ophelia, suppl. 3, 229–246.

Sutherland, T.F., Amos, C.L., and Grant, J., 1998. The effect of buoyant biofilms on the erodibility of sublittoral sediments of a temperate microtidal estuary. Limnology and Oceanography 43, 225–235.

Swanberg, I.L., 1991. The influence of filter-feeding bivalve *Cerastoderma edule* L. on microphytobenthos: a laboratory study. Journal of Experimentally Marine Biology and Ecology 151, 93–111.

Taghon, G.L., Nowell, A.R.M., and Jumars, P.A., 1984. Transport and breakdown of fecal pellets: Biological and sedimentological consequences. Limnology and Oceanography 29, 64–72.

Tolhurst, T.J., Gust, G., and Paterson, D.M., 2002. The influence of an extracellular polymeric substance (EPS) on cohesive sediment stability. In: Winterwerp, J.C., and Kranenburg, C (eds), *Fine Sediment Dynamics in the Marine Environment* (pp 409–425). Amsterdam: Elsevier Science.

Tolhurst, T.J., Black, K.S., Paterson, D.M., Mitchener, H., Termaat, R. and Shayler, S.A., 2000 (a). A comparison and measurement standardisation of four in situ devices for determining the erosion shear stress of intertidal sediments. Continental Shelf Research 20, 1397–1418.

Tolhurst, T.J., Riethmüller, R., and Paterson, D.M., 2000 (b). In situ versus laboratory analysis of sediment stability from intertidal mudflats. Continental Shelf Research 20, 1317–1334.

Tolhurst, T.J., Black., K.S., Shayler, S.A., Mather, S., Black, I., Baker, K., and Paterson, D.M., 1999. Measuring the *in situ* erosion shear stress of intertidal sediments with the cohesive strength meter (CSM). Estuarine, Coastal, and Shelf Science 49, 281–294.

Tomas, C.R., 1997. Identifying Marine Phytoplankton. Academic Press, San Diego, USA, 858 pp.

Torfs, H., Jiang, J., and Mehta, A.J., 2001. Assessment of the erodibility of fine/coarse sediment mixtures. In: McAnally, W.H and Mehta, A.J. (eds), *Coastal and Estuarine Fine Sediment Processes* (pp 109–123). Amsterdam: Elsevier Science.

Underwood, G.J.C. and Paterson, D.M., 1993 (a). Recovery of intertidal benthic diatoms after biocide treatment and associated sediment dynamics. Journal of the Marine Biological Association United Kingdom 73, 25–45.

Underwood, G.J.C. and Paterson, D.M. 1993 (b). Seasonal changes in diatom biomass, sediment stability and biogenic stabilization in the Severn estuary. Journal of the Marine Biological Association of the United Kingdom 73, 871–887.

Underwood, G.J.C., Paterson, D.M., and Parkers, R.J., 1995. The measurement of the microbial carbohydrate exopolymers from intertidal sediments. Limnology and Oceanography 40, 1243–1253.

van Bernem, K.H., 1999. Auswirkungen einer Pipeline-Verlegung auf das marine Benthos im Tidebecken von Baltrum-Langeoog. German Journal of Hydrography, Supplement 10, 45–64.

Van Rijn, L.C., 1993. Principles of sediment transports in Rivers, Estuaries, and Coastal Seas. Aqua Publications, Amsterdam.

Van Straaten, L.M.N.U., and Kuenen., 1957. Accumulation of fine-grained sediments in the Dutch Wadden Sea. Geologie end Mijnbouw 19, 329–354.

Verwey, J., 1952. On the ecology of distribution of cockle and mussel in the Dutch Wadden Sea, their role in sedimentation and the source of their food supply. Archives Neerlandaises de Zoologie 10, 171–239.

Vos, P.C., de Boer, P.L., and Misdorp, R., 1988. Sediment stabilization by benthic diatoms in intertidal sandy shoals; qualitative and quantitative observations. In P.L., de Boer, A.V., Gelder., and S.D., Nio (eds.), *Tide-influenced sedimentary environments and facies* (pp. 511–526). Dordrecht: D. Reidel Publishing Company.

Whitehouse, R.J.S, Soulsby, R.L, Roberts, W., and Mitchener, H.J., 2000 (a). Dynamics of estuarine muds. Thomas Telford, London, pp. 210.

Whitehouse, R.J.S., Bassoullet, P., Dyer, K.R., Mitchener, H.J., and Roberts, W., 2000 (b). The influence of bedforms on flow and sediment transport over intertidal mudflats. Continental Shelf Research 20, 1099–1124.

Widdows, J., Brinsley, M.D., Bowley, N. and Barrett, C., 1998 (a). A benthic annular flume for in situ measurement of suspension feeding/biodeposition rates and erosion potential of intertidal cohesive sediments. Estuarine, Coastal and Shelf Science 46, 27–38.

Widdows, J., Brinsley, M.D, and Elliott, M., 1998 (b). Use of *in situ* flume to quantify particle flux (biodeposition rates and sediment erosion) for an intertidal mudflat in relation to changes in current velocity and benthic macrofauna. In K.S. Black, D.M. Paterson, & A. Cramp (Eds.), *Sedimentary processes in the intertidal zone*. *Special publication*, 139 (pp. 85–97). London: Geological Society.

Widdows, J., Brinsley, M.D., Salked, P.N., and Elliott, M., 1998 (c). Use of an annular flumes to determine the influence of current velocity and bivalves on material flux at the sediment-water interface. Estuaries 21, 552–559.

Widdows, J., Brinsley, M.D, Salkeld, P.N., and Lucas, C.H., 2000 (a). Influence of biota on spatial and temporal variation in sediment erodability and material flux on a tidal flat (Westerschelde, The Netherlands). Marine Ecology-Progress Series 194, 23–37.

Widdows, J., Brown, S., Brinsley, M.D., Salkeld, P.N., and Elliott, M., 2000 (b). Temporal changes in intertidal sediment erodability: influence of biological and climatic factors. Continental Shelf research 20, 1275–1289.

Widdows, J., and Brinsley. M.D., 2002. Impact of biotic and abiotic processes on sediment dynamics and the consequences to the structure and functioning of the intertidal zone. Journal of Sea Research 48, 143–156.

Williamson, H.J., and Ockenden, M.C., 1996. ISIS: an instrument for measuring erosion shear stress *in situ*. Estuarine, Coastal, and Shelf Science 42, 1–18.

Wright, S., Jeffery, S.W., Mantoura, R.F.C., Llewellyn, C.A., Bjorland, T., Rapeta, D., and Welschmeyer, N., 1991. Improved HPLC method for analyses of chlorophyll and carotenoids from marine phytoplankton. Marine Ecology Progress Series 77, 183–196.

Yallop, M.L., de Winder, B., Paterson, D.M., and Stal, L.J., 1994. Comparative structure, primary production and biogenic stabilization of cohesive and non-cohesive marine sediments inhabited by microphytobenthos. Estuarine, Coastal and Shelf Science 39, 565–582.

Yingst, J.Y. and Rhoads, D.C., 1978. Seafloor stability in Central Long Island Sound: Part II. Biological interaction and their potential importance for seafloor erodibility. In: Wiley, M.L. (ed.) Estuarine interaction. Academic Press, New York. pp. 245–260.

Young, R.A. and Southard, J.B., 1978. Erosion of fine-grained marine sediments: sea-floor and laboratory experiments. Geol. Soc. America. Bull. 89, 663–672.

Ziervogel, K., and Bohling, B., 2003. Sedimentological parameters and erosion behaviour of submarine coastal sediments in the south-western. Baltic Sea. Geo-Marine Letters 23, 43–52.

Appendix 1. Critical erosion shear stress, erosion rate and determined physical and biological properties of surface sediment at stations B, C, E and F in 2001

Sample name	Station	Sampling date	Erosion shear stress ($N\ m^{-2}$)	Erosion rate ($g\ m^{-2}\ s^{-1}$)	Wet bulk density ($g\ cm^{-3}$)	Mud content (%)	Median particle size (μm)	water content (%)	Normalised water (%)	Organic content (%)	Chl. a concentration ($mg\ m^{-2}$)	Colloidal carbohydrate ($mg\ m^{-2}$)	EPS ($mg\ m^{-2}$)
Ero-374	B	10-Apr-01	0.35	0.25	1.51	63	41	46	106	6.0	27	532	239
Ero-388	B	17-May-01	0.70	0.70	1.82	17	128	33	102	2.2	26	414	88
Ero-390	B	17-May-01	0.50	0.55	1.80	25	109	34	103	2.9	31	377	90
Ero-409	B	14-Jun-01	0.50	4.21	1.78	19	112	33	103	3.0	44	521	140
Ero-410	B	14-Jun-01	0.60	2.02	1.78	19	112	33	103	3.0	44	521	140
Ero-423	B	24-Oct-01	0.55	0.09	1.52	62	43	49	107	7.3	23	1140	440
Ero-424	B	24-Oct-01	0.40	0.20	1.52	62	43	49	107	7.3	23	1140	440
Ero-371	C	10-Apr-01	0.70	0.24	1.46	52	59	52	107	6.8	86	1114	290
Ero-383	C	16-May-01	0.65	0.45	1.58	36	91	47	105	5.0	81	1946	283
Ero-386	C	16-May-01	0.60	0.61	1.60	31	99	44	104	3.9	58	1088	188
Ero-399	C	13-Jun-01	0.40	0.53	1.82	15	125	31	102	2.4	16	155	18
Ero-400	C	13-Jun-01	0.40	0.79	1.82	15	125	31	102	2.4	16	155	18
Ero-402	C	13-Jun-01	0.65	1.11	1.82	22	121	31	102	2.4	17	195	33
Ero-419	C	24-Oct-01	0.40	5.42	1.72	23	114	33	103	2.6	10	102	68
Ero-420	C	24-Oct-01	0.40	0.31	1.72	23	114	33	103	2.6	10	102	68
Ero-377	E	11-Apr-01	0.45	0.31	1.88	—	—	27	102	2.3	49	317	133
Ero-381	E	15-May-01	1.40	0.14	1.59	29	105	44	105	5.0	53	1700	321
Ero-382	E	15-May-01	1.00	1.12	1.59	29	105	44	105	5.0	53	1700	321
Ero-396	E	12-Jun-01	0.20	4.04	1.89	8	139	25	101	1.3	9	134	55
Ero-412	E	14-Jun-01	0.40	2.96	1.79	11	144	32	103	2.6	18	392	93
Ero-417	E	23-Oct-01	0.40	0.58	1.79	11	149	31	102	2.3	7	82	30
Ero-418	E	23-Oct-01	0.40	0.59	1.79	11	149	31	102	2.3	7	82	30
Ero-425	E	25-Oct-01	0.70	4.40	1.89	12	142	27	102	1.6	9	172	63
Ero-375	F	11-Apr-01	2.00	0.00	1.56	86	37	46	106	6.0	144	1464	428
Ero-380	F	15-May-01	1.30	0.03	1.48	33	102	51	106	6.3	75	2540	864
Ero-392	F	12-Jun-01	0.25	0.99	1.74	12	143	32	102	2.2	20	193	74
Ero-394	F	12-Jun-01	0.40	0.92	1.94	—	—	26	102	1.7	20	341	103
Ero-411	F	14-Jun-01	0.80	0.70	1.78	24	117	35	103	3.0	32	156	62
Ero-414	F	23-Oct-01	0.50	22.41	1.84	12	151	27	102	2.4	51	789	55
Ero-426	F	25-Oct-01	0.35	0.67	1.48	31	118	50	105	5.4	32	555	88

Appendix 2. The average density (individual m^{-2}) of dominant macrofauna species during the sampling period in 2001 at the study site.

Species	Station B	Station C	Station E	Station F
Capitella capitata	18	223	382	291
Cerastoderma edule	692	0	32	0
Eteone longa	36	16	0	18
Heteromastus filiformis	55	557	255	528
Hydrobia ulvae	8935	16	16	0
Macoma baltica	400	127	191	0
Pygospio elegans	5914	191	287	764
Tharyx killariensis	4968	1274	812	2147
Tubificoides benedeni	3421	175	175	1838

Appendix 3. Pearson correlation coefficient (r) between critical erosion shear stress and physical and biological sediment properties for the combined data set. Den. = wet bulk density, Mud = mud content, Median = median grain-size, Water = water content, N. water = normalised water content, Org. = organic content, Chl-a = chlorophyll-a, Coll. Car. = colloidal carbohydrate concentration, EPS = EPS concentration, τ_{cr} = critical erosion shear stress, and E. rate = erosion rate.

	Den.	Mud	Median	Water	N. water	Org.	Chl-a	Coll. car.	EPS	τ_{cr}
Mud	**-0.70**									
Median	**0.63**	**-0.95**								
Water	**-0.98**	**0.71**	**-0.64**							
N. water	**-0.36**	**-0.32**	**0.37**	**0.38**						
Org.	**-0.89**	**0.73**	**-0.67**	**0.89**	0.22					
Chl-a	**-0.27**	0.15	-0.09	0.22	-0.02	**0.37**				
Coll.car.	**-0.48**	0.14	-0.15	**0.44**	0.19	**0.53**	**0.77**			
EPS	**-0.55**	0.20	-0.18	**0.51**	0.24	**0.59**	**0.70**	**0.92**		
τ_{cr}	**-0.38**	**0.25**	-0.19	**0.36**	0.16	**0.48**	**0.59**	**0.71**	**0.73**	
E. rate	**0.37**	**-0.44**	**0.36**	**-0.37**	0.08	**-0.41**	**-0.38**	**-0.34**	**-0.31**	**-0.33**

Numbers in bold: significant at P < 0.01

Appendix 4. Pearson correlation coefficient (r) between critical erosion shear stress and physical and biological sediment properties for station A and B only. Den. = wet bulk density, Mud = mud content, Median = median grain-size, Water = water content, N. water = normalised water content, Org. = organic content, Chl-a = chlorophyll-a, Coll. Car. = colloidal carbohydrate concentration, EPS = EPS concentration, τ_{cr} = critical erosion shear stress, and E. rate = erosion rate (Numbers in bold: significant at P < 0.01).

	Den.	Mud	Median	Water	N. water	Org.	Chl-a	Coll. car.	EPS	τ_{cr}
Station A										
Mud	**-0.89**									
Median	**0.92**	**-0.98**								
Water	**-0.98**	**0.91**	**-0.95**							
N. Water	**-0.83**	0.55	-0.64	**0.85**						
Org.	-0.33	0.37	-0.31	0.25	-0.02					
Chl-a	0.25	-0.11	0.22	-0.26	-0.41	0.53				
Coll.car.	**0.73**	-0.51	0.60	**-0.76**	**-0.89**	0.23	0.53			
EPS	**0.73**	-0.57	0.63	**-0.73**	**-0.77**	0.25	0.68	**0.93**		
τ_{cr}	**0.73**	-0.61	0.68	**-0.78**	**-0.83**	0.20	0.49	**0.96**	**0.92**	
E. rate	-0.42	0.13	-0.22	0.38	0.61	-0.30	-0.66	-0.57	-0.59	-0.42
Station B										
Mud	**-0.92**									
Median	**0.91**	**-0.98**								
Water	**-0.97**	**0.96**	**-0.93**							
N. water	0.34	**-0.65**	**0.65**	-0.40						
Org.	**-0.92**	**0.95**	**-0.93**	**0.97**	-0.46					
Chl-a	**0.61**	-0.59	0.44	**-0.68**	0.04	-0.58				
Coll.car.	-0.22	-0.01	-0.08	0.10	0.21	0.12	0.35			
EPS	**-0.71**	0.50	-0.56	**0.64**	0.05	**0.66**	-0.17	**0.72**		
τ_{cr}	0.57	**-0.64**	0.58	-0.57	0.51	-0.54	0.51	0.27	-0.14	
E.rate	0.41	-0.53	0.44	-0.43	0.58	-0.40	0.31	-0.18	-0.20	0.32

Appendix 5. Pearson correlation coefficient (r) between critical erosion shear stress and physical and biological sediment properties for station C and D only. Den. = wet bulk density, Mud = mud content, Median = median grain-size, Water = water content, N. water = normalised water content, Org. = organic content, Chl-a = chlorophyll-a, Coll. Car. = colloidal carbohydrate concentration, EPS = EPS concentration, τ_{cr} = critical erosion shear stress, and E. rate = erosion rate (Numbers in bold: significant at P < 0.01).

	Den.	Mud	Median	Water	N. water	Org.	Chl-a	Coll. car.	EPS	τ_{cr}
Station C										
Mud	**-0.93**									
Median	**0.93**	**-0.99**								
Water	**-0.96**	**0.93**	**-0.91**							
N. water	**-0.84**	**0.68**	**-0.65**	**0.90**						
Org.	**-0.95**	**0.94**	**-0.96**	**0.92**	**0.74**					
Chl-a	-0.40	0.36	-0.46	0.25	0.09	0.55				
Coll.car.	-0.39	0.31	-0.41	0.24	0.12	0.50	**0.98**			
EPS	-0.47	0.35	-0.43	0.31	0.23	0.55	**0.92**	**0.95**		
τ_{cr}	-0.46	0.34	-0.39	0.30	0.23	0.54	**0.88**	**0.89**	**0.97**	
E. rate	0.16	-0.19	0.25	-0.18	-0.13	-0.30	-0.47	-0.44	-0.37	-0.34
Station D										
Mud	-0.28									
Median	0.29	**-0.96**								
Water	**-0.98**	0.23	-0.22							
N. water	**-0.89**	-0.15	0.13	**0.93**						
Org.	**-0.95**	0.18	-0.20	**0.98**	**0.93**					
Chl-a	**-0.92**	-0.02	-0.05	**0.89**	0.40	**0.91**				
Coll.car.	**-0.94**	0.00	0.00	**0.96**	0.39	**0.97**	**0.91**			
EPS	**-0.48**	-0.38	0.27	0.47	0.37	**0.50**	**0.79**	**0.72**		
τ_{cr}	**-0.73**	-0.07	-0.06	**0.72**	0.45	**0.77**	**0.83**	**0.72**	**0.81**	
E. rate	0.05	**-0.55**	0.46	-0.03	0.20	-0.01	0.23	0.26	-0.17	-0.16

Appendix 6. Pearson correlation coefficient (r) between critical erosion shear stress and physical and biological sediment properties for station E and F only. Den. = wet bulk density, Mud = mud content, Median = median grain-size, Water = water content, N. water = normalised water content, Org. = organic content, Chl-a = chlorophyll-a, Coll. Car. = colloidal carbohydrate concentration, EPS = EPS concentration, τ_{cr} = critical erosion shear stress, and E. rate = erosion rate (Numbers in bold: significant at P < 0.01).

	Den.	Mud	Median	Water	N. water	Org.	Chl-a	Coll. car.	EPS	τ_{cr}
Station E										
Mud	**-0.86**									
Median	**0.73**	**-0.93**								
Water	**-0.97**	**0.91**	**-0.79**							
N. water	**-0.82**	**0.61**	-0.44	**0.82**						
Org.	**-0.96**	**0.92**	**-0.82**	**0.98**	**0.80**					
Chl-a	-0.46	**0.61**	**-0.75**	0.46	0.21	**0.55**				
Coll.car.	**-0.72**	**0.72**	**-0.80**	**0.71**	0.47	**0.75**	**0.85**			
EPS	**-0.81**	**0.75**	**-0.72**	**0.83**	**0.69**	**0.83**	**0.67**	**0.88**		
τ_{cr}	**-0.76**	**0.78**	**-0.73**	**0.79**	**0.55**	**0.81**	**0.65**	**0.75**	**0.81**	
E.rate	0.28	-0.43	0.41	-0.29	-0.17	-0.40	**-0.54**	-0.43	-0.30	-0.37
Station F										
Mud	**-0.55**									
Median	**0.56**	**-0.97**								
Water	**-0.99**	**0.57**	**-0.59**							
N. water	-0.43	-0.43	0.39	0.44						
Org.	**-0.89**	**0.77**	**-0.82**	**0.91**	0.13					
Chl-a	-0.30	**0.60**	**-0.56**	0.30	-0.44	0.44				
Coll.car.	**-0.66**	0.26	-0.35	**0.70**	0.40	**0.67**	0.47			
EPS	**-0.71**	0.27	-0.35	**0.74**	0.47	**0.70**	0.41	**0.97**		
τ_{cr}	-0.40	0.29	-0.36	0.45	0.08	0.49	**0.59**	**0.76**	**0.76**	
E.rate	0.40	-0.42	0.43	-0.42	0.20	**-0.54**	**-0.87**	**-0.64**	**-0.58**	**-0.68**